

UNCLASSIFIED

AD NUMBER	
AD077127	
CLASSIFICATION CHANGES	
TO:	unclassified
FROM:	confidential
LIMITATION CHANGES	
TO:	Approved for public release, distribution unlimited
FROM:	Distribution authorized to U.S. Gov't. agencies and their contractors; Administrative/Operational Use; DEC 1954. Other requests shall be referred to Army Materiel Command, Alexandria, VA.
AUTHORITY	
31 Dec 1966, DoDD 5200.10; USMAC ltr, 15 Dec 1972	

THIS PAGE IS UNCLASSIFIED

# UNCLASSIFIED

---

## AD \_\_\_\_\_

*Reproduced  
by the*

ARMED SERVICES TECHNICAL INFORMATION AGENCY  
ARLINGTON HALL STATION  
ARLINGTON 12, VIRGINIA



DOWNGRADED AT 3 YEAR INTERVALS:  
DECLASSIFIED AFTER 12 YEARS  
DOD DIR 5200.10

---

# UNCLASSIFIED

**77127**

# **Armed Services Technical Information Agency**

**Reproduced by  
DOCUMENT SERVICE CENTER  
KNOTT BUILDING, DAYTON 2, OHIO**

This document is the property of the United States Government. It is furnished for the duration of the contract and shall be returned when no longer required, or upon recall by ASTIA to the following address:  
Armed Services Technical Information Agency, Document Service Center,  
Knott Building, Dayton 2, Ohio.

**NOTICE: WHEN GOVERNMENT OR OTHER DRAWINGS, SPECIFICATIONS OR OTHER DATA ARE USED FOR ANY PURPOSE OTHER THAN IN CONNECTION WITH A DEFINITELY RELATED GOVERNMENT PROCUREMENT OPERATION, THE U. S. GOVERNMENT THEREBY INCURS NO RESPONSIBILITY, NOR ANY OBLIGATION WHATSOEVER; AND THE FACT THAT THE GOVERNMENT MAY HAVE FORMULATED, FURNISHED, OR IN ANY WAY SUPPLIED THE SAID DRAWINGS, SPECIFICATIONS, OR OTHER DATA IS NOT TO BE REGARDED BY IMPLICATION OR OTHERWISE AS IN ANY MANNER LICENSING THE HOLDER OR ANY OTHER PERSON OR CORPORATION, OR CONVEYING ANY RIGHTS OR PERMISSION TO MANUFACTURE, USE OR SELL ANY PATENTED INVENTION THAT MAY IN ANY WAY BE RELATED THERETO.**

**UNCLASSIFIED**

**CONFIDENTIAL**

This document contains information affecting the national defense of the United States, within the meaning of the Espionage Laws, Title 18, U.S.C., Sections 793 and 794, the transmission or revelation of which in any manner to an unauthorized person is prohibited by law.

**REPORT NO. 20-77**

**BASIC FACTORS INVOLVED  
IN THE DESIGN AND OPERATION OF CATALYTIC  
MONOPROPELLANT-HYDRAZINE REACTION CHAMBERS**

**A. F. GRANT, JR.**

**JET PROPULSION LABORATORY  
CALIFORNIA INSTITUTE OF TECHNOLOGY**

**PASADENA 3, CALIFORNIA**

**DECEMBER 31, 1954**

**55AA**

**55460**

**CONFIDENTIAL**

**DEC 3 1955**

AD No 77/27  
ACTA FILE COPY

CONFIDENTIAL


ORDCIT Project  
Contract No. DA-04-495-Ord 18  
Department of the Army  
ORDNANCE CORPS

Report No. 20-77

BASIC FACTORS INVOLVED IN THE DESIGN AND OPERATION  
OF CATALYTIC MONOPROPELLANT-HYDRAZINE REACTION CHAMBERS

A. F. Grant, Jr.

Copy No. A 79

  
David Altman, Chief  
Chemistry Section

  
Arthur J. Stasick, Chief  
Rockets and Materials Division

  
W. H. Pickering, Director  
Jet Propulsion Laboratory

JET PROPULSION LABORATORY  
California Institute of Technology  
Pasadena 3, California  
December 31, 1954

CONFIDENTIAL

55AA

5546

---

THIS REPORT HAS BEEN DISTRIBUTED ACCORDING TO SECTION A,  
WITH ABSTRACTS TO SECTIONS C AND DP, OF THE SUBCOMMITTEE,  
ON ANAF/GM MAILING LIST, OFFICE OF THE ASSISTANT SECRETARY  
OF DEFENSE (RESEARCH AND DEVELOPMENT), GUIDED MISSILE  
TECHNICAL INFORMATION DISTRIBUTION LIST, MML 200/7, LIST  
NO. 7, DATED 1 JUNE 1955.

---

## TABLE OF CONTENTS

	Page
I. Introduction . . . . .	1
II. Thermochemistry . . . . .	2
A. Concentrated Hydrazine . . . . .	2
B. Mixtures of Hydrazine, Hydrazine Nitrate, and Water . . . . .	3
1. Advantages . . . . .	3
2. Preparation . . . . .	3
3. Storage and Handling . . . . .	4
4. Thermodynamic-Performance Calculations . . . . .	5
III. Optimum Performance of Hydrazine . . . . .	5
IV. Chemical Equilibrium and Kinetics . . . . .	6
V. Catalyst Development . . . . .	7
A. Catalysts for the Primary Decomposition of Hydrazine . . . . .	7
B. Catalysts for the Dissociation of Ammonia . . . . .	8
C. Catalysts Which Cause Spontaneous Ignition of Hydrazine . . . . .	9
VI. Reaction-Chamber Design and Operation . . . . .	10
A. Reaction-Chamber Assembly . . . . .	10
B. Ignition . . . . .	11
1. Electrical Ignition System . . . . .	11
2. Bipropellant Ignition System . . . . .	12
C. Injection and Feed-System Arrangement . . . . .	13
1. Pressure Instability . . . . .	13
a. Caused by improper injection . . . . .	13
b. Caused by improper arrangement of feed system . . . . .	14
2. Injection Requirements for Bipropellant Ignition Systems . . . . .	14
3. Injector Arrangement . . . . .	15
VII. Test Equipment and Operating Procedures . . . . .	15
A. Reaction-Chamber Test Installation . . . . .	15
B. Gas-Analysis Apparatus . . . . .	16
1. Continuous Gas Analysis . . . . .	16
2. Intermittent Gas Analysis . . . . .	18
C. Summary of Operating Procedures . . . . .	19
1. Preparation of Reaction Chamber . . . . .	19
a. Injector . . . . .	19

## TABLE OF CONTENTS (Cont'd)

	Page
b. Catalyst bed . . . . .	19
2. Firing Procedure . . . . .	19
VIII. Engineering Data . . . . .	20
A. Catalytic Decomposition of Hydrazine . . . . .	20
1. Factors Involved in Ideal Reaction Chambers . . . . .	20
a. Factors which influence the depth of zone A . . . . .	20
b. Factors which influence the depth of zone B . . . . .	21
c. Minimum bed depth required for the complete decomposition of hydrazine . . . . .	21
2. Factors Involved in Actual Reaction Chambers . . . . .	22
3. Experimental Evaluation of Catalysts . . . . .	22
a. Estimation of the depth of type H-7 catalyst required for the complete decomposition of hydrazine . . . . .	22
b. Estimation of the depth of type H-A-3 catalyst required for the complete decomposition of hydrazine . . . . .	24
B. Catalytic Dissociation of Ammonia . . . . .	25
1. Factors Which Govern the Catalytic Dissociation of Ammonia . . . . .	25
2. Experimental Evaluation of Catalysts . . . . .	26
a. Dissociation of ammonia over type H-7 catalyst . . . . .	26
(1) Experimental procedures . . . . .	26
(2) Interpretation of data . . . . .	26
b. Dissociation of ammonia over type H-A-3 catalyst . . . . .	30
C. Estimation of Pressure Drop Across Catalyst Beds . . . . .	31
1. Basic Factors . . . . .	31
2. Experimental Determination . . . . .	33
D. Equations for Predicting the Performance of Monopropellant- Hydrazine Reaction Chambers . . . . .	36
1. Conditions Required for the Attainment of Predicted Performance . . . . .	36
2. Equations for Type H-7 Catalyst . . . . .	37
3. Equations for Type H-A-3 Catalyst . . . . .	38
E. Influence of Additives on the Performance of Monopropellant Hydrazine . . . . .	39



## TABLE OF CONTENTS (Cont'd)

	Page
1. Water . . . . .	39
2. Aniline . . . . .	39
3. Hydrazine Nitrate . . . . .	39
F. Influence of Operating Time and Repeated Use on Catalyst Performance . . . . .	40
IX. Explosion Hazard Involved in the Use of Hydrazine Decomposition Gases to Pressurize the Oxidizer (RFNA) Storage Tank of the <u>Corporal</u> Flight Vehicle . . . . .	41
X. Conclusions . . . . .	43
Tables . . . . .	45
Figures . . . . .	52
References . . . . .	70
Appendix	
Sample Calculations . . . . .	72

## LIST OF TABLES

I. Nomenclature . . . . .	45
II. Calculated Performance As a Monopropellant of Concentrated Hydrazine . . . . .	48
III. Calculated Performance As a Monopropellant of a Mixture Consisting of 74 Wt % $N_2H_4$ , 20 Wt % $HNO_3$ , and 6 Wt % $H_2O$ . . . . .	49
IV. Calculated Performance As a Monopropellant of a Mixture Consisting of 70 Wt % $N_2H_4$ , 20 Wt % $HNO_3$ , and 10 Wt % $H_2O$ . . . . .	50
V. Calculated Performance As a Monopropellant of a Mixture Consisting of 74 Wt % $N_2H_4$ , 16 Wt % $HNO_3$ , and 10 Wt % $H_2O$ . . . . .	51

## LIST OF FIGURES

1. Calculated Performance of Hydrazine . . . . .	52
2. Change in Enthalpy Associated with Cooling of Hydrazine Decomposition Gases . . . . .	53
3. Variation of Exhaust Temperature with Pressure Ratio (Concen- trated Hydrazine) . . . . .	53

## LIST OF FIGURES (Cont'd)

	Page
4. Reaction Chamber of 1-Inch Diameter . . . . .	54
5. Reaction Chamber of 2-Inch Diameter . . . . .	54
6. Reaction Chamber of 3 1/2-Inch Diameter . . . . .	55
7. Reaction Chamber of 4 7/8-Inch Diameter . . . . .	55
8. Reaction Chamber of 6-Inch Diameter, Showing Catalyst-Bed Arrangement Used to Generate Gases for Pressurization of Tanks Containing RFNA . . . . .	56
9. Reaction Chamber with Electrical Ignition System . . . . .	56
10. Bipropellant Ignition System . . . . .	57
11. Typical Pressure Record Obtained During Ignition Period Using Bipropellant Starting Technique . . . . .	57
12. Typical Pressure Record Obtained with Proper Injection and Feed- System Arrangement . . . . .	58
13. Pressure Instability Caused by Improper Atomization and/or Nonuniform Cross-Sectional Distribution of Injected Hydrazine . . . . .	58
14. Pressure Instability Caused by Harmonic Coupling Between Reaction Chamber and Hydrazine Feed System . . . . .	58
15. Arrangement of Apparatus Used in Testing of Hydrazine-Monopro- pellant Reaction Chambers . . . . .	59
16. Apparatus Used for Continuous Analysis of Hydrazine Decomposition Gases . . . . .	59
17. Apparatus Used for Intermittent Analysis of Hydrazine Decomposition Gases . . . . .	60
18. Variation of Porosity $F_v$ and Specific Area $a_v$ (in. <sup>2</sup> /in. <sup>3</sup> ) with Chamber Diameter . . . . .	60
19. Influence of Chamber Pressure on Dissociation of Ammonia over Type H-7 Catalyst (1/4-In. Spheres) . . . . .	61
20. Influence of Bed Depth on the Dissociation of Ammonia over Type H-7 Catalyst . . . . .	62
21. Influence of Chamber Pressure on Depth of Type H-7 Catalyst Required to Dissociate Various Fractions of Ammonia . . . . .	62
22. Influence of Chamber Pressure on Incremental Bed Depth $\Delta L_x$ Required with Type H-7 Catalyst to Dissociate Various Fractions of the Ammonia . . . . .	63

## LIST OF FIGURES (Cont'd)

	Page
23. Curves Used in the Determination of Equation (38) . . . . .	63
24. Influence of Chamber Pressure on Dissociation of Ammonia over Type H-A-3 Catalyst (1/8- by 1/8-In. Cylinders) . . . . .	64
25. Influence of Bed Depth on Dissociation of Ammonia over Type H-A-3 Catalyst . . . . .	65
26. Influence of Residence Time $\theta$ on the Extent of Ammonia Dissociation over Type H-A-3 Catalyst . . . . .	65
27. Variation of Pressure Drop with Hydrazine Feed Rate . . . . .	66
28. Variation of Pressure Drop with Hydrazine Feed Rate . . . . .	67
29. Variation of Pressure Drop with Bed Depth in Type H-7 Catalyst (1/4-In. Spheres) . . . . .	68
30. Variation of Pressure Drop with Bed Depth in Type H-A-3 Catalyst (1/8- by 1/8-In. Cylinders) . . . . .	68
31. Variation of Apparent Wetted Depth $L'_w$ With Flow Rate . . . . .	69
32. Curves Used in Evaluation of Constants in Equation (50) . . . . .	69

## ABSTRACT

This report summarizes the factors which must be considered in the design and operation of catalytic monopropellant-hydrazine reaction chambers. The influences of feed-system arrangement, ignition, injection, and catalyst-bed geometry on the performance of reaction chambers are described. The performances of two catalysts are discussed: one containing iron, nickel, and cobalt on fused (inactive) alumina particles (type H-7), and the other containing iron, nickel, and cobalt on compressed (active) alumina pellets (type H-A-3). The effects of chamber pressure and hydrazine feed rate on the performance of these catalysts are evaluated. Relationships for estimating the volumes of the catalysts required to decompose hydrazine completely and to dissociate various fractions of the ammonia formed in the decomposition of hydrazine are derived. Equations for determining the pressure drop across catalyst beds have also been derived. The explosion hazards associated with the use of hydrazine decomposition gases to pressurize the oxidizer (RFNA) tank of the Corporal flight vehicle are described.

## I. INTRODUCTION

During the past 4 years, the Jet Propulsion Laboratory has been engaged in programs directed toward the development of monopropellant-hydrazine, gas-generating systems for two principal applications: (1) to pressurize the propellant-storage tanks of the Corporal flight vehicle and (2) to drive gas turbines in both the electrical power-supply and the hydraulic control systems of rocket vehicles. The specific details of these two programs will be discussed in separate reports. The purpose of this report is to summarize the experience gained in these programs as related to the design and operation of catalytic monopropellant-hydrazine reaction chambers. This information should be useful in connection with applications other than those investigated at this Laboratory.

When hydrazine is decomposed adiabatically, a large volume of low-molecular-weight gases consisting of ammonia, nitrogen, and hydrogen is evolved at moderate temperatures. Because of the heat released and the large volume of gases evolved relative to the volume of the liquid (sp gr of liquid hydrazine is approx 1.01 at 80°F), hydrazine may be used as a monopropellant and gas-generating fluid in applications where low weight and small volume are required and/or in which it is necessary to limit the temperature for mechanical or other reasons. Among the applications for which monopropellant hydrazine appears to be well suited are the following:

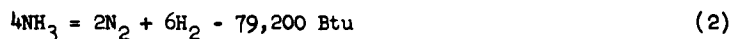
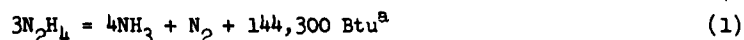
1. As a source of thrust in rocket propulsion systems.

2. As a source of energy to drive gas turbines in the power-supply and propellant-transfer systems of rocket vehicles.
3. As a source of gases for the pressurization of the fuel-storage tanks of rocket vehicles.
4. As a source of energy in jet-engine ignition systems.
5. As a source of gases for use in catapults and similar high-pressure displacement systems.
6. As a compact and convenient source of high-pressure gases for use in the field with a number of different types of military equipment.

## II. THERMOCHEMISTRY

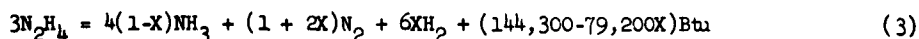
### A. CONCENTRATED HYDRAZINE

Hydrazine is thermochemically unstable; hence under suitable conditions it undergoes exothermic decomposition, forming ammonia, nitrogen, and hydrogen. This thermal decomposition of hydrazine at low temperatures apparently proceeds in a stepwise manner (Cf. Ref. 1), which may be represented by two consecutive equations, as follows:



The reaction represented by Equation (2) is generally slower than the reaction represented by Equation (1); hence, in practical systems where the reaction time is limited by considerations of weight and space, only part of the ammonia can be dissociated.

In certain systems, such as flames maintained by the decomposition of pure hydrazine vapor, the reaction products for 2 moles of decomposed hydrazine are  $2\text{NH}_3 + \text{N}_2 + \text{H}_2$  (Cf. Refs. 5, 6, and 7), whereas, when hydrazine in dilute aqueous solutions is decomposed on metal surfaces (e.g., Raney nickel) at room temperature (Cf. Ref. 8), the products of reaction are predominately  $\text{H}_2$  and  $\text{N}_2$ , with only traces of ammonia. Because of the variation of the hydrazine decomposition reaction with catalysts and temperature, it is difficult to specify the exact stoichiometry in any given system. For this reason, Equations (1) and (2) have been combined to give the following expression, where X represents the fraction of the ammonia which is dissociated:



<sup>a</sup>The standard heat of formation of hydrazine is 21,700 Btu/lb mol (Cf. Ref. 2), and that of ammonia is 19,800 Btu/lb mol (Cf. Ref. 3). The thermodynamic properties of the gases were taken from Ref. 4.

Using Equation (3), the parameters<sup>a</sup>  $M_g$ ,  $T_c$ ,  $C^*$ ,  $I_{sp}$ ,  $\eta_a$ ,  $\eta_n$ , and  $\eta_H$  were computed (Cf. Ref. 9). The variation of these parameters with  $X$  is shown in Table II and in Figure 1. From Figure 1 it can be seen that the characteristic velocity  $C^*$  and the specific impulse  $I_{sp}$  are virtually constant until about 50% of the ammonia has been dissociated. Beyond this point both parameters fall quite rapidly as  $X$  increases. Both the adiabatic reaction temperature  $T_c$  and the average molecular weight of the decomposition gases  $M_g$  decrease steadily as  $X$  increases.

Most applications of hydrazine involve cooling of the decomposition gases from the adiabatic reaction temperature  $T_c$  to some temperature  $T_e$  through heat exchange or adiabatic expansion of the gases. To assist in the calculation of the heat transfer or conversion of enthalpy to kinetic energy involved in such applications, the parameter  $\Delta H_{T_e}^{T_c}$  has been computed. The variation of this parameter with  $X$  and  $T_e$  is shown in Table II and in Figure 2. The exhaust temperature  $T_e$ , obtained through the adiabatic expansion of the decomposition gases from a reaction pressure  $P_c$  to an exhaust pressure  $P_e$ , is plotted in Figure 3 as a function of  $X$  and the pressure ratio  $P_c/P_e$ .

The influence of water (generally present as an impurity in commercial concentrated hydrazine) on the parameters  $T_c$ ,  $M_g$ ,  $C^*$ , and  $I_{sp}$  is shown<sup>b</sup> in Table II.

## B. MIXTURES OF HYDRAZINE, HYDRAZINE NITRATE, AND WATER

### 1. Advantages

The general use of concentrated hydrazine as a monopropellant and as a gas generant is limited by its high freezing point (34°F). Further, it has not been found practicable with presently developed catalysts to reduce the ammonia concentration in the decomposition gases of concentrated hydrazine below 15 mol % (Cf. Section VIII). For this reason, the decomposition gases of concentrated hydrazine cannot be used in certain applications (Cf. Section IX).

Through the addition of hydrazine nitrate and water to hydrazine, it is possible to produce mixtures which freeze below -40°F (max acceptable freezing point for most military applications) and to reduce the concentration of ammonia in the gases produced through the use of a given catalyst and reaction time. Thus, for example, using hydrazine which contains 20 wt % nitric acid (present as hydrazine nitrate) and 6 wt % water, it is possible to produce gases which contain less than 5 mol % ammonia (Cf. Section IX).

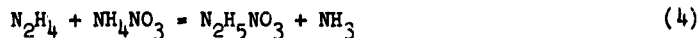
### 2. Preparation

Mixtures of hydrazine and hydrazine nitrate can be conveniently prepared through the addition of ammonium nitrate to concentrated hydrazine (Cf. Ref. 10). Hydrazine nitrate is formed, and the ammonia in excess of that required to saturate the solution (up to 5 wt % ammonia remains in the solution at room temperatures)

<sup>a</sup>The nomenclature used in this report is given in Table I.

<sup>b</sup>The heat of solution of water in hydrazine was estimated from data given in Ref. 8.

is evolved, as follows:



The ammonia concentration in the solution may be reduced to less than 1 wt % through evacuation. If water is to be included in the mixture, it should be added after the removal of the ammonia; otherwise, a large fraction of the ammonia cannot be removed because of its greater solubility in aqueous solutions of hydrazine.

### 3. Storage and Handling

Although mixtures of hydrazine and hydrazine nitrate are less stable thermally than concentrated hydrazine (Cf. Ref. 1), they may be safely stored and handled at room temperature. The shock sensitivity of such mixtures, even when a concentration of nitric acid as high as 25 wt % is used, is not greatly different from that of nitromethane (Cf. Ref. 10).

Experience at this Laboratory indicates that mixtures containing as much as 20 wt % nitric acid may be safely stored in aluminum or stainless-steel (type-347) containers for periods as long as 6 months. One stainless-steel drum of hydrazine containing 20 wt % nitric acid and 3 wt % water was stored for 9 months, during which time the ambient temperature varied from a low of about 50°F to a high of about 105°F. Analysis of the mixture at the end of this period showed only a slight change in composition. The solution has assumed a pale pink color, which indicated that some corrosion of the container had occurred. A similar mixture was stored in a type-431 steel bomb for 2 months at 130°F; the maximum pressure developed in the bomb during this period was about 10 psi. This pressure was attained within a week after the bomb had been heated to 130°F. Analysis of the mixture at the end of the 2 months indicated no material change in composition. The mixture contained small concentrations of metals, indicating that some corrosion of the bomb had occurred.

Experience at this Laboratory indicates that the principal precautions which should be taken in the storage and handling of these mixtures are as follows:

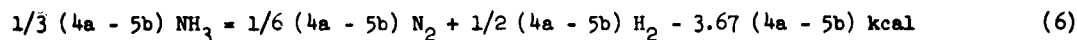
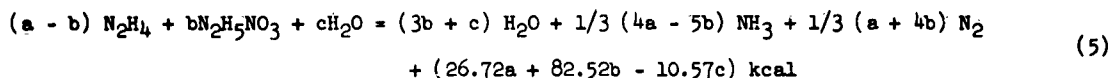
1. Containers which are to be used for the storage of the mixtures should first be freed of all organic materials and metal oxides and then allowed to stand in contact with a dilute solution of hydrazine for about 24 hours.
2. Containers of the mixtures should not be stored in direct sunlight.
3. Since contact with metal oxides, earth, wood, paper, cloth, and similar materials can cause the mixtures to inflame, they should be stored in a fireproof structure, and spillage during transfer from the containers should be carefully avoided.
4. The containers should be capable of withstanding a pressure of at least 25 psig and should be equipped with a burst diaphragm or pressure-relief valve.
5. Containers, pipelines, etc., which have been used with the mixtures should be thoroughly washed out with water. If small quantities of the mixtures are allowed to evaporate to dryness, a

residue of hydrazine nitrate is deposited which is quite sensitive to shock.

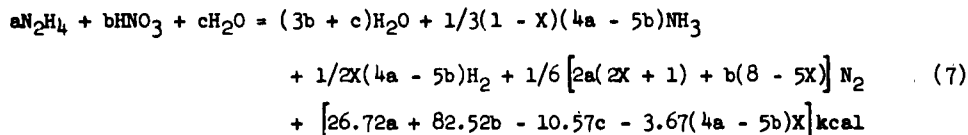
6. Contamination of the mixtures with carbon tetrachloride or other organic halides should be avoided since the presence of these materials greatly accelerates the corrosive action of the mixtures on stainless steels.
7. The mixtures should be pressurized only with nitrogen, helium, or other inert gases. The vapor space in tanks, etc., should be pressurized slowly to prevent adiabatic compression of any hydrazine vapors which may be present.
8. Packings and other seals which come into contact with the mixtures may be made of Teflon, Kel-F, Polyethylene, Silicone Rubber, U. S. Rubber No. 20995, or Butyl rubber.

#### 4. Thermodynamic-Performance Calculations

The thermal decomposition of a mixture consisting of a moles of hydrazine, b moles of nitric acid, and c moles of water may be represented by the following equations:



These two equations can be combined to give the following expression, in which X represents the fraction of the ammonia which has been dissociated:



Using Equation (7), the performance parameters  $T_c$ ,  $C^*$ ,  $M_g$ ,  $I_{sp}$ ,  $n_a$ ,  $n_N$ ,  $n_H$ ,  $n_w$ ,  $\Delta H_{T_e}^{T_c}$ , and  $T_e$  have been computed for several low-freezing mixtures of hydrazine, hydrazine nitrate, and water. The variation of these parameters with X is shown in Tables III, IV, and V. The standard heat of formation of hydrazine nitrate (109,000 Btu/lb mol) and the heats of solution of hydrazine nitrate in hydrazine and in mixtures of hydrazine and water were taken from Reference 11. The freezing points of the mixtures were taken from the same source.

### III. OPTIMUM PERFORMANCE OF HYDRAZINE

The efficient use of hydrazine in any application requires the completion of the reaction represented by Equation (1), whereas the extent of the completion of the reaction represented by Equation (2), i.e., the



value of  $X$  in Equation (3), which is required for the optimum performance of hydrazine in a given application, is dependent on the nature of the application. When hydrazine is used as a monopropellant in a rocket motor, it is desirable to operate at as low a chamber temperature as possible and, at the same time, to obtain near-maximum  $I_{sp}$ . For this type of application, therefore, it is desirable to dissociate from 30 to 50% of the ammonia (Cf. Fig. 1). When hydrazine is to be used as a source of energy for gas turbines, it is generally necessary, for mechanical reasons, to reduce the temperature of the gases to 1800°F or less. For such applications, therefore, it is usually necessary to dissociate at least 52% of the ammonia. For high-temperature isobaric pressure-displacement systems, e.g., catapults, optimum performance is achieved when  $T_c/M_g$  is at a maximum. For pure hydrazine this optimum performance is achieved when about 43% of the ammonia is dissociated. In low-temperature isobaric pressure-displacement systems (i.e., systems in which the gas temperature must be less than 1100°F, as, e.g., in propellant-tank pressurizing systems in rockets), the maximum efficiency of hydrazine as a gas generant is achieved when all the ammonia has been dissociated so that gases of minimum molecular weight are produced.

#### IV. CHEMICAL EQUILIBRIUM AND KINETICS

Under adiabatic conditions, chemical equilibrium favors the complete decomposition of hydrazine to the elements (Cf. Ref. 9); however, the extent to which the reactions represented by Equations (1) and (2) can be completed in a given reaction chamber is dependent on the rates of the reactions and the residence time  $\theta_c$  provided by the reaction chamber, where  $\theta_c$  may be arbitrarily defined<sup>a</sup> as follows:

$$\theta_c = (P_c/\dot{w})(M_g/RT)V_c = (P_c/G)(M_g/RT_c)L_c \quad (8)$$

In a specific application,  $P_c$  and  $\dot{w}$  are fixed by factors related to the particular application, whereas the value of the ratio  $M_g/T_c$  required for optimum performance is determined by the use which is to be made of the decomposition gases. As a result, the residence time generally can be varied only by varying the volume of the reaction chamber.

In most practical systems, the volume of the reaction chamber must be limited in order to conserve weight and space. Therefore, the practical attainment of the efficient use of hydrazine as a gas generant or as a monopropellant requires that the reactions represented by Equations (1) and (2) proceed rapidly.

When the thermal decomposition of hydrazine is carried out adiabatically in the absence of catalysts, a residence time of approximately 35 milliseconds is required to produce decomposition gases which are free of

---

<sup>a</sup>Eq. (8) is based on conditions at the outlet of the catalyst bed and on the total volume of the reaction chamber or catalyst bed. However, there are wide variations in  $T_c$ ,  $M_g$ , and to a lesser extent in  $P_c$  throughout the reaction chamber; when a catalyst is used, the true gas volume is the volume of the chamber less the volume occupied by the catalyst particles. As a result, Eq. (8) gives only an approximation of the true residence time.

detectable concentrations of hydrazine. With this residence time in reaction chambers similar to those shown in Figures 4, 5, and 6, it was found that approximately 29% of the ammonia was dissociated; i.e., X in Equation (3) was about 0.29. It was also found that the extent of ammonia dissociation obtained in the absence of a catalyst was virtually independent of pressure over the range studied (200 to 800 psia). Increasing the residence time from 35 milliseconds to about 50 milliseconds had no measurable effect on the amount of ammonia which was dissociated.

Based on the experimental value of X of 0.29 and its apparent independence of residence time, it has been concluded that, although Equation (1) describes the primary decomposition of hydrazine at low temperatures (about 400 to 500°F) in a closed system (Cf. Ref. 1), it does not apply to the adiabatic decomposition of hydrazine in a steady-state flow system. It appears that a more correct expression for the primary decomposition of hydrazine in adiabatic flow systems is (Cf. Refs. 5, 6, and 7)



This equation is obtained when X in Equation (3) is 0.25. The experimentally measured value of X of 0.29 has been attributed to wall-catalyzed dissociation of ammonia which accompanies the reaction represented by Equation (9).

Because of the large residence time required for the complete decomposition of hydrazine and because of the extremely slow rate of dissociation of ammonia, it can be seen that the efficient use of hydrazine as a monopropellant or gas generant in reaction chambers of moderate size requires the use of catalysts which increase the rates of the primary hydrazine-decomposition and secondary ammonia-dissociation reactions.

## V. CATALYST DEVELOPMENT

### A. CATALYSTS FOR THE PRIMARY DECOMPOSITION OF HYDRAZINE

Previous studies (Cf. Ref. 1) indicated that the thermal decomposition of hydrazine is a heterogeneous reaction which apparently proceeds for the most part in the vapor phase. The rate of decomposition reaction was found to be markedly increased by a large variety of surfaces, the extent of the increase in the rate of the reaction produced by a given surface being directly proportional to its area in contact with the hydrazine. Among the materials which were tested, it was found that iron, nickel, and cobalt gave the highest specific surface activities.

Based on these studies, it was concluded that in order to be effective a catalyst would have to meet the following criteria:

1. Have a high unit-surface activity.
2. Expose a large surface per unit volume in order to permit the development of a large surface in a reaction chamber of moderate size.

3. Have a high thermal conductivity so that the rate of the vaporization process could be increased by the transfer of heat through the solid catalyst from the high-temperature regions to the low-temperature inlet regions of the catalyst bed and thence to the incoming hydrazine.
4. Have a sufficiently high melting point to prevent fusion at all temperatures encountered in the adiabatic decomposition of hydrazine.
5. Have sufficiently high mechanical strength to prevent powdering and packing during use.

In order to satisfy the last four criteria, it was found necessary to use a porous refractory material as the catalyst support. For this purpose three forms of porous fused (inactive) aluminum-oxide particles were tested: (1) 3/16- by 3/16-inch cylinders, (2) 3- by 8-mesh polysurface granules, and (3) 1/4-inch spheres. In order to produce high unit-surface activity, the aluminum oxide particles were impregnated with concentrated aqueous solutions of the nitrates of iron, nickel, and cobalt, either separately or in various combinations. After the saturated particles were dried in an oven at about 150 to 200°C, they were tested in a reaction chamber similar to that shown in Figure 5. Seventeen catalysts of this type were tested. Of these seventeen, the most satisfactory catalyst was found to be that which consisted of an equimolar concentration of metallic iron, nickel, and cobalt on the alumina support, the reduced catalyst containing a total of approximately 11 wt % free metals. Using this catalyst (Cf. Ref. 12), which has been designated type H-7, it was found possible to bring the reaction represented by Equation (1) to completion with a residence time of about 2 milliseconds. The performance of this catalyst is discussed in Section VIII.

#### B. CATALYSTS FOR THE DISSOCIATION OF AMMONIA

Although the iron, cobalt, nickel, and fused alumina catalyst (type H-7) previously described is capable of greatly accelerating the rate of the reaction represented by Equation (1), it is not particularly active in the dissociation of ammonia. Therefore, this catalyst is not suitable for use in those applications where low temperatures and/or low molecular weights and concentrations of ammonia are required (Cf. Section IX). Consequently, an investigation of catalysts for the acceleration of the reaction represented by Equation (2) was undertaken. This study was divided into two phases.

In the first phase, an attempt was made to develop a catalyst which would increase the rates of the reactions represented by Equations (1) and (2) to the same extent or would cause the decomposition of hydrazine to nitrogen and hydrogen to occur directly, without the intermediate formation of ammonia. For this purpose, more than seventy catalysts were tested. These catalysts, which were prepared in a number of different ways, incorporated the oxides and other compounds of the following elements: aluminum, barium, calcium, cerium, chromium, cobalt, copper, iron, magnesium, manganese, molybdenum, nickel, platinum, potassium, silver, sodium, tungsten, and vanadium. These materials were supported on carriers of alumina, charcoal, filtrol, fuller's earth, kieselguhr, silicon carbide, and zirconium oxide. For the most part, these catalysts were inferior in activity to the H-7 catalyst. With one exception, those catalysts which were superior in activity to the H-7 catalyst had physical properties which made them unsuitable for use in monopropellant reaction chambers.

The catalyst which was found to be superior to the H-7 catalyst in catalytic activity consisted of only

a slight modification of the H-7 catalyst. This modification consisted of substituting porous 1/8- by 1/8-cylinders of compressed activated alumina for the fused aluminum-oxide support used with the H-7 catalyst. The method of preparation of the catalyst and the concentration of the metals in the catalyst were identical to those used with the H-7 catalyst (Cf. Ref. 12). However, the activity of this catalyst in the dissociation of ammonia was far greater than that of the H-7 catalyst (Cf. Section VIII-B). Although measurements of the minimum residence time required over this catalyst for the complete decomposition of hydrazine have not been made, it is believed that it would be equal to or slightly less than that required over H-7. The physical strength of this catalyst, which has been designated type H-A-3, is somewhat inferior to that of type H-7. However, a large number of tests have been made with this catalyst in which, with two exceptions, no difficulties were encountered with powdering or packing of the catalyst. In the two exceptions noted, the reaction chambers had been operated in such a manner that the pressure drop across the catalyst bed exceeded 50 psi, which was sufficient to cause crushing of the particles and consequent plugging of the bed, which in turn caused a rapid rise in pressure drop. The performance of the H-A-3 catalyst is discussed in Section VIII.

In the second phase of this study, which was completed prior to the development of the H-A-3 catalyst, an attempt was made to develop a catalyst which would be active in the dissociation of the ammonia formed in the decomposition of hydrazine over the H-7 catalyst. For this purpose, many of the catalysts developed in the first phase of this study were tested in series with the type H-7 catalyst. However, with the best of the catalysts, H-A-3 excepted, only a slight increase in the amount of ammonia which could be dissociated in a given residence time was observed. Therefore, several industrial ammonia-synthesis catalysts were tested. Of these, the most satisfactory from the standpoint of activity and physical properties was Aero-catalyst, type-FM, produced by the Chemical Construction Company. This catalyst consists of  $\text{Fe}_3\text{O}_4$  promoted and stabilized with  $\text{K}_2\text{O}$  and  $\text{Al}_2\text{O}_3$  and is supplied in the form of 3- by 6-mesh grains. Using this catalyst it was possible to dissociate up to 75% of the ammonia with a residence time of approximately 21 milliseconds (an additional residence time of about 10 millisecond in H-7 catalyst was used to insure the completion of the reaction represented by Eq. 1). The performance of this catalyst is discussed in Reference 13. Because of the superior physical properties and equal activity of the H-A-3 catalyst, no further study of the performance of FM catalyst has been made.

#### C. CATALYSTS WHICH CAUSE SPONTANEOUS IGNITION OF HYDRAZINE

An attempt was made to develop catalysts which would be sufficiently active to initiate the thermal decomposition of hydrazine at room temperatures, thereby eliminating the need for a special ignition system. For this purpose, eleven catalysts were prepared and tested. These catalysts consisted of alumina, silicon carbide, or coconut-charcoal pellets impregnated and/or coated with one or more of the following compounds: cobaltic, ferric, mercuric, nickelous, and silver oxides; ammonium, potassium, and sodium dichromates; potassium and sodium permanganates; and potassium chloroplatinate. Of these catalysts, two were found which caused spontaneous ignition of hydrazine. The first was a modification of the H-7 catalyst in which a concentrated

solution of the metal nitrates saturated with ammonium dichromate was used to impregnate 3- by 8-mesh polysurface aluminum oxide granules. The granules were then dried at 250°F for 4 hours. When hydrazine was brought into contact with this catalyst in a reaction chamber similar to that shown in Figure 5, ignition occurred within 10 milliseconds after the introduction of hydrazine into the chamber. Twenty-three tests were made with this catalyst in which smooth ignition and efficient performance were attained. However, in tests made with catalyst which had been stored in airtight containers for several weeks, it was found that the activity of the catalyst had declined to a point where over 50 milliseconds was required to initiate reaction. As a result, when ignition occurred, the reaction was extremely violent because of the large accumulation of hydrazine in the reaction chamber. On one occasion the reaction was so violent that the reaction chamber was seriously damaged. Because of the evident deterioration of the activity of this catalyst with time, further study was abandoned. The second spontaneously igniting catalyst consisted of metallic cobalt deposited on coconut-charcoal pellets and promoted with potassium chloroplatinate. This catalyst was extremely reactive with hydrazine at room temperatures. However, its ignition properties were erratic and its physical properties were not found suitable for prolonged use since the catalyst tended to pack in the catalyst chamber, thereby causing excessive pressure loss. Neither of these two catalysts was found to be spontaneous on re-use, although the platinum-cobalt catalyst could be regenerated by heating for several hours at about 150°F in air. When either catalyst was used, it was evident that the ignition properties resulted from an oxidation reaction rather than from true catalysis.

On the basis of these studies and because of the simplicity and reliability of electrical and bipropellant ignition systems (Cf. Section VI-B), further work on the development of spontaneously igniting catalysts was abandoned.

## VI. REACTION-CHAMBER DESIGN AND OPERATION

### A. REACTION-CHAMBER ASSEMBLY

The arrangement and dimensions of the principal parts of the reaction chambers used in this study are shown schematically in Figures 4, 5, 6, 7, and 8. The ranges of hydrazine flow rates and pressures used in the chambers are indicated in the Figures. The reaction chambers consisted of the following principal parts:

1. A stainless-steel (type- 347 or 304) injector containing jets for the injection of the hydrazine and the introduction of the oxidizer required for ignition.
2. A stainless-steel reaction-chamber body.
3. A catalyst bed consisting of one or more types of catalyst.
4. A stainless-steel catalyst-retainer plate and a nickel-wire retainer screen.
5. An alundum liner. (Used only when the hydrazine contained large concentrations of hydrazine nitrate and low concentrations of water, e.g., with mixture No. 1).

## B. IGNITION

With the exception of the two spontaneous catalysts described in Section V-C, all catalysts developed in this program required preheating in order to permit the initiation of monopropellant operation. With the H-7 and H-A-3 catalysts, it was necessary to preheat the catalyst beds to about 700°F in order to obtain smooth and rapid ignition. Two methods of preheating catalyst beds have been developed: (1) an electrical ignition system and (2) a bipropellant ignition system (Cf. Ref. 12).

## 1. Electrical Ignition System

In earlier studies (Cf. Refs. 9 and 12), electrical heaters either internally or externally located were used to preheat reaction chambers. Metal-shielded commercial heaters similar to Calrod units were used for this purpose. These heaters were of heavy and bulky construction. Because the heating elements in these units were thermally as well as electrically insulated from the catalyst bed, an excessively large time (up to 30 min.) was required to achieve ignition temperatures. In this study, the electrical heater was formed by inserting a coil of Nichrome-V wire directly into the catalyst bed, with the wire in direct contact with the catalyst particles. When unused, i.e., when in an unreduced state, the catalysts served as electrical insulators which prevented short-circuiting of the coils on each other or on the wall of the chamber. With the H-A-3 catalyst, this method of ignition could be used with reduced catalyst since the particles did not become electrical conductors after the catalyst had been reduced by hydrazine. However, using reduced H-7 catalyst, this method of ignition could not be used because when reduced with hydrazine this catalyst became a conductor of electricity, thereby tending to short-circuit the coils of the heater.

Figure 9 shows a typical reaction chamber designed for use with an electrical ignition system. In addition to the normal components of a reaction chamber (Cf. Section VI-A), this chamber incorporated two 10-mm spark plugs for introducing electrical power, a 1 1/4-inch-diameter coil of 18-gage Nichrome-V wire, wound with seven coils per inch of coil length, and a liner made of "Lava" Grade A, a thermal and electrical insulating grade of natural magnesium-aluminum-silicate stone produced and sold by the American Lava Corporation. With units similar to that shown in Figure 9, using the H-A-3 catalyst and a current of 15 amperes through the coil of 18-gage wire, it was found possible with heating periods of less than 3 minutes to obtain smooth and rapid ignition. A total of twenty-five tests, each test lasting for periods of at least 10 minutes, was made using a single reaction chamber, heater coil, and liner. At the end of this period of testing, all components of the reaction chamber were in good working condition.

The power input and heating time required for the attainment of ignition temperatures are dependent on the volume and geometric arrangement of the catalyst bed. Based on data obtained in reaction chambers similar to that shown in Figure 9, it appears that the minimum heat input required for proper ignition is about 30 Btu per cubic inch of catalyst bed. The maximum rate of heat input is determined by the size of the heating wire and its arrangement in the catalyst bed. With a ratio of coil diameter to catalyst bed diameter of 0.7 and with seven coils per inch of bed depth, it has been found possible to use amperages in the coil equal to about 80 % of the current capacity of the wire in air. At higher amperages the life of the coil was materially reduced,

and, when amperages in excess of the air rating of the wire were used, the coils burned out in less than 3 minutes.<sup>a</sup>

Because of the power requirements and the time required for ignition, the electrical ignition system is not suited for all applications of the monopropellant. The use of this method of ignition is recommended only for small units or for those systems where it is not possible or desirable to provide the oxidizer required with a bipropellant ignition system.

## 2. Bipropellant Ignition System

The principal parts of the bipropellant ignition system are shown schematically in Figure 10. The system consisted of a dual-acting pneumatically actuated valve (a) which was used to control the admission of both the oxidizer and the hydrazine into the reaction chamber, a pneumatically operated piston (b) used to force the requisite quantity of oxidizer into the reaction chamber simultaneously with the hydrazine, and the hydrazine (c) and oxidizer (d) jets. The oxidizer jets were designed to give a mixture ratio ( $W_{OX}/W_F$ ) of from 0.20 to 0.30 when a pressure equal to that in the hydrazine feed system was applied to the upstream surface of the piston. The length of travel of the piston was adjusted to permit the injection of the oxidizer for a period of about 0.5 second.

In this study, RFNA was used as the oxidizer. However, it should be possible to use any oxidizer which spontaneously ignites with hydrazine (Cf. Ref. 12). Because of the extremely short ignition delay which is obtained with RFNA and hydrazine, ignition occurred within 10 milliseconds after the opening of the propellant control valve. The heat liberated by the combustion reaction between the RFNA and hydrazine was sufficient to raise the temperature of the catalyst bed well above the minimum required for the initiation of monopropellant operation. Figure 11 shows a typical oscillograph record of the injection and chamber pressures obtained during the ignition period.

When the hydrazine and RFNA feed systems were properly filled, simultaneous injection of the propellants was insured by a positive linkage between the oxidizer and fuel pintles of the dual-acting control valve. The hydrazine and RFNA jets were so located that reasonably complete mixture of the two propellants at the surface of the catalyst bed was attained. Under these conditions of over-all mixture ratio and uniform mixing, the temperatures which were obtained during the ignition period were well below the melting point of the catalyst bed, and no damage to the catalyst was encountered.

The bipropellant starting technique has been found to be simple to use and extremely reliable. Over 1,500 successful tests have been made using this method of ignition. It is believed that this method of ignition is suitable for nearly all potential applications of the hydrazine monopropellant, the exceptions being those applications where from the standpoint of logistics it is undesirable to provide an oxidizer for the ignition system.

The principal difficulties which were encountered with the bipropellant ignition system resulted from

---

<sup>a</sup>Data relative to the ratings of various gages of Nichrome-V wire may be obtained from catalogues prepared by the Driver-Harns Co., Harrison, N. J.

the use of separate hydrazine and RFNA control valves. On several occasions the oxidizer valve failed to open; hence hydrazine alone was injected into the chamber. With pure hydrazine, no difficulties were encountered when the oxidizer valve failed to operate. However, when this failure occurred using mixtures of hydrazine and hydrazine nitrate and the chamber was not promptly flushed with water, a detonation resulted within 30 seconds after the initial injection of the mixture into the chamber.<sup>a</sup> Although the flow of the mixture into the chamber was shut off within 0.5 second after the initial injection, a sufficient quantity of the mixture was present in the chamber to cause the destruction of the chamber and severe damage to the test installation. The use of the dual-acting control valve eliminated this form of failure. The positive linkage between the oxidizer and fuel-valve pintles prevented the opening of only one side of the valve. No difficulties in sticking or other malfunctioning of the acid piston were encountered. The periodic replacement of the O-ring seals in the piston and the filtering of the acid through a 200-mesh wire screen before its introduction to the piston prevented leakage around the acid piston and plugging of the acid jets.

### C. INJECTION AND FEED SYSTEM ARRANGEMENT

The performance of a hydrazine monopropellant reaction chamber is dependent to a large extent on the arrangement of the hydrazine feed system and the manner in which the hydrazine is introduced into the chamber. When the feed system is properly proportioned and the hydrazine is introduced as a highly atomized stream which is uniformly distributed across the upstream surface of the catalyst bed, smooth and efficient performance is obtained (Cf. Fig. 12). When the feed system is improperly proportioned or the hydrazine atomization and distribution is inadequate, large and rapid fluctuations in the chamber pressure occur, and/or the performance of the catalyst is materially reduced (Cf. Section VIII).

#### 1. Pressure Instability

a. Caused by improper injection. Improper injection was the most frequent cause of the pressure instability which was encountered on several occasions during this investigation. When the hydrazine was inadequately atomized, large and erratic fluctuations in the pressures in the reaction chambers were often observed. Figure 13 shows the form of the pressure instability which resulted when the hydrazine was not properly atomized. The same form of instability was obtained when the hydrazine stream was permitted to impinge on the chamber wall upstream from the catalyst bed, thus permitting coalescence of the atomized particles before they entered the catalyst bed. On several occasions, the pressure fluctuations were sufficiently severe to cause the breakup of some of the catalyst particles. Because of this disintegration of the catalyst, the resistance to the passage of the gases through the bed was markedly increased, and a large pressure drop and consequent reduction in the pressure at the outlet of the catalyst bed resulted. In several other tests in which poor distribution of the hydrazine across the upstream surface of the catalyst bed was

---

<sup>a</sup>Explosive reaction may be prevented by flushing the catalyst bed with water. In the two explosions encountered in this study, the water flush system failed to operate.



provided, undecomposed hydrazine and excessive concentrations of ammonia were detected in the exhaust gases, thus indicating channeling of the hydrazine and decomposition gases through the catalyst bed. In these tests the pressure drop across the catalyst bed was much lower than normal.<sup>a</sup>

b. Caused by improper arrangement of feed system. On two occasions during this investigation, a large and uniformly rapid fluctuation in the pressure in hydrazine reaction units was observed. This pressure instability (Cf. Fig. 14), which persisted through a number of tests, could not be attributed to improper injection. In both instances, the instability was found to be related to the arrangement of the hydrazine feed system.

Under normal operating conditions, there is a slight ( $\pm 1$  to  $2\%$ ) variation in the pressure in a reaction chamber. The frequency of this variation in chamber pressure is related to the dimensions of the reaction chamber and the volume and arrangement of the catalyst bed. In the two installations wherein major pressure instability was caused by the feed system, it was found that the vibrational period of the feed system (determined from oscillograph records of the shock waves developed in the system when the control valve was rapidly closed) was very nearly the same as that of the normal chamber-pressure fluctuation. Altering the length of the feed system eliminated this form of instability. From these observations it has been concluded that a complex coupling between the feed system and reaction chamber can occur, which causes reinforcement of the normal variations in the chamber pressure. No information is available at this time to assist in predicting the proper arrangement of the feed system. It should be noted, however, that the use of a hydrazine-injector pressure drop of 100 psi or 30% of the upstream chamber pressure is generally sufficient to prevent this form of instability. In those instances in which proper atomization, distribution, and injector pressure drop are used and a pressure instability still persists, it is then necessary by trial-and-error methods to alter the length of the feed system until harmonic coupling between the feed system and reaction chamber no longer occurs.

## 2. Injection Requirements for Bipropellant Ignition Systems

In order to avoid the occurrence of local overoxidation during the ignition period, it is necessary that the oxidizer be uniformly mixed with hydrazine. Under these conditions, fusion of the catalyst bed is avoided. Further, uniform heating of the catalyst bed during the ignition period permits the rapid attainment of equilibrium monopropellant operation. If improper mixing and distribution of the oxidizer is used, the catalyst bed may be damaged, and severe channeling of the hydrazine through the bed for the first 10 to 20 seconds of operation may result. In several tests made during this investigation, when improper acid injection was used, the hydrazine-monopropellant reaction stabilized out at a point several inches below the upstream surface of the catalyst bed, and only part of the catalyst was effective in these tests. (The location of the hydrazine decomposition reaction in the catalyst chamber was determined by the color of the outside of the reaction-chamber

---

<sup>a</sup>It is believed that a large part of the scatter in the pressure-loss and catalyst-performance data was caused by variations in the degree of atomization and/or distribution of the hydrazine.

walls during operation. The unlined reaction chambers turned red from the heat of the reaction, and the upper boundary of the red zone marked very closely the point at which the monopropellant reaction was occurring.)

### 3. Injector Arrangement

The following injector arrangements were used in this investigation:

1. A single axially located full-cone spray jet for the injection of the hydrazine and a pair of impinging jets for the introduction of the RFNA during ignition. (With this injector arrangement it was necessary to adjust the position of the acid jets carefully to insure proper impingement and mixing with the hydrazine.)
2. A single axially located, full-cone spray jet for the injection of hydrazine and two full-cone spray jets for the introduction of RFNA. (The acid jets were located in such a manner that the finely atomized acid spray was uniformly distributed across the upstream surface of the catalyst bed. When this arrangement was used, a large part of the mixing of the acid and hydrazine occurred at the upstream surface of the catalyst bed. The advantage of this system relative to that described in 1 was that repeated adjustment of the relative positions of the acid and hydrazine sprays was not necessary.)
3. Four full-cone spray jets with their axes parallel to the axis of the chamber for the introduction of the hydrazine, and an equal number of full-cone spray jets for the introduction of the oxidizer. Both the oxidizer and hydrazine spray jets were located to give uniform distribution across the upstream surface of the catalyst bed. This arrangement was used in reaction chambers having large diameters (Cf. Fig. 8).

## VII. TEST EQUIPMENT AND OPERATING PROCEDURES

### A. REACTION-CHAMBER TEST INSTALLATION

Figure 15 is a flow diagram of the test installation used in this investigation. The hydrazine storage tank (a) and flush tank (b) were pressurized with nitrogen. The hydrazine tank was equipped with an emergency shutdown valve (c), which was used to stop the flow of hydrazine in the event of a failure in the hydrazine feed system or in the operation of the dual-control valve (d). The RFNA required for ignition was supplied by a piston (e) which was actuated by nitrogen supplied from the nitrogen flush line. Three hand valves, (f), (g), and (h), were installed to permit refilling of the piston from the RFNA storage tank (Cf. Fig. 10). A nitrogen flush valve (i) was connected to the RFNA injector lines between the dual-acting valve and the reaction chamber (j); a water flush valve (k) was similarly connected into the hydrazine injector lines. The gases from the reaction chamber were cooled by means of a water-cooled tube-in-tube heat exchanger (l). The cooled decomposition gases were discharged through a contoured nozzle (m). A throttling valve (n) was used to vary the flow rate of hydrazine into the chamber.

## B. GAS-ANALYSIS APPARATUS

## 1. Continuous Gas Analysis

The method developed for the continuous analysis of hydrazine decomposition gases is based on the use of two adjacent critical nozzles which continuously divide the flow of hydrazine decomposition gases into two known fractions. The smaller of the two fractions is then passed through a dilute solution of sulfuric acid for the purpose of removing the ammonia formed in the reaction system. The ammonia-free gases, consisting of  $N_2$  and  $H_2$  saturated with water, are then dried over activated alumina and passed through an orifice meter. From the stoichiometry of the hydrazine decomposition reaction (Cf. Eq. 3) and by comparison of the ratio of the mass flow into the analysis system through the critical nozzle with that leaving through the orifice meter, it is possible to compute the fraction of ammonia dissociated in the reaction system.

The apparatus used for the continuous analysis of hydrazine decomposition gases is shown schematically in Figure 16. The apparatus consisted of a small critical-flow nozzle (a) which was located just upstream from the main discharge nozzle (b). The gases which entered the sampling system through nozzle (a) passed into a scrubber (c) which contained dilute sulfuric acid for the removal of ammonia, hydrazine, water, and any small quantity of soluble or condensable impurities which were present in the hydrazine feed. The gases which left the scrubber passed into an entrainment separator (d), followed by a water-cooled dryer (e) which contained activated alumina. The dry-gas stream leaving the dryer then passed through a back-pressure nozzle (f) into a calibrated gas-metering orifice (g). The purpose of nozzle (f) was to maintain a sufficiently high pressure in the scrubber to prevent entrainment of dilute acid into the dryer and metering section. In order to permit rapid response of the sampling system to changes in conditions in the reaction system, the free volume in the sampling system upstream from nozzle (f) was maintained as small as possible, and the throat area of nozzle (f) was about eighteen times larger than that of nozzle (a). The throat diameter of nozzle (a) was about 0.050 inch.

Using this system of analysis, the values of X in Equations (3) and (7) were computed as follows: Because nozzles (a) and (b) are adjacent to each other, gases of the same temperature and composition pass through both nozzles; as a result, the flow of gases through the nozzles is directly proportional to the area of their throats, and

$$\dot{\omega}_s = \frac{\dot{\omega}}{\left[ 1 + \left( \frac{D_m}{D_s} \right)^2 \right]} \quad (10)$$

where  $\dot{\omega}_s$  equals the flow rate of gases entering the sample system (lb/sec);  $\dot{\omega}$ , the total flow rate of propellant into the reaction system (lb/sec);  $D_m$ , the throat diameter of nozzle (b)(in.); and  $D_s$ , the throat diameter of nozzle (a)(in.).

The flow rate of nitrogen and hydrogen through the metering orifice (g) is given by the following equation:

$$\dot{w}_o = K_o \sqrt{\frac{P_o \Delta P_o M_o}{RT_o}} \quad (11)$$

where  $\dot{w}_o$  is the flow rate of gas through the metering orifice (lb/sec);  $K_o$ , the orifice coefficient determined by calibration (in. ft  $^{3/2}$ /sec) ( $K_o$  is a function of  $P_o$  and  $\Delta P_o$ , but is independent of gas composition when  $T_o$  is low);  $\Delta P_o$ , the pressure drop across the orifice (psi);  $M_o$ , the average molecular weight of gases passing through the orifice (lb/mol);  $R$ , the perfect gas constant, 10.73 (psi)(cu ft)/(lb/mol)(°R);  $T_o$ , the temperature of gases entering the orifice (°R); and  $P_o$ , the pressure upstream from the orifice (psia).  $P_o$  was measured by means of a differential strain gage installed with the low-pressure side of the gage exposed to atmospheric pressure. Atmospheric pressure was measured before each test.

From Equation (7)

$$\frac{\dot{w}_s}{\dot{w}_o} = \frac{6(32.05a + 63.02b + 18.02c)}{6.06(4a - 5b)X + 28.02[2a(1 + 2X) + (8 - 5X)b]} \quad (12)$$

and

$$M_o = \frac{6.06(4a - 5b)X + 28.02[2a(1 + 2X) + (8 - 5X)b]}{3(4a - 5b)X + 2a(1 + 2X)X + (8 - 5X)b} \quad (13)$$

Combining Equations (10), (11), (12), and (13) and solving the resulting quadratic for  $X$  yields the following expression:

$$X = \frac{(a + 4b)}{(4a - 5b)} \left\{ 0.572 \sqrt{1 + 0.0752K_o^2 \left[ 1 + \frac{D_m^2}{D_s} \right]^2 \left[ \frac{32.05a + 63.02b + 18.02c}{(a + 4b)} \right]^2 \frac{P_o \Delta P_o}{T_o \dot{w}_o^2} - 1.071} \right\} \quad (14)$$

Let  $Y$  equal the weight fraction of  $N_2H_4$  in the feed to the reaction system, and let  $Z$  equal the weight fraction of  $HNO_3$  in the feed to the reaction system; then

$$(a + 4b) = \frac{Y}{32.05} \left( 1 + 2.0343 \frac{Z}{Y} \right) \quad (15)$$

$$(4a - 5b) = \frac{4Y}{32.05} \left( 1 - 0.6357 \frac{Z}{Y} \right) \quad (16)$$

Defining,

$$A = 1 + 2.034 \frac{Z}{Y} \quad (17)$$

$$B = 1 - 0.6357 \frac{Z}{Y} \quad (18)$$

$$S = K_o^2 \left[ 1 + \left( \frac{P_m}{D_s} \right)^2 \right]^2 \frac{P_o \Delta P_o}{T_o (Y \omega)^2} \quad (19)$$

Substituting these values into Equation (14) yields

$$\frac{BX}{A} = 0.1431 \sqrt{1 + 77.16 \frac{S}{(A)^2}} - 0.2681 \quad (20)$$

It should be noted that when Z is 0, Equation (20) reduces to

$$X = 0.1431 \sqrt{1 + 77.16 S} - 0.2681 \quad (21)$$

It is assumed that all impurities in the hydrazine are condensed or dissolved out of the sample gas stream in the scrubber.

Based on an analysis of the errors in the measurements of the parameters involved in Equation (14), it is believed that the error in the values of X measured with this system does not exceed 5 %.

## 2. Intermittent Gas Analysis

Before the analysis system described in the preceding section was developed, the values of X in Equations (3) and (7) were determined by means of an analysis system similar to that which is shown schematically in Figure 17. Using this system, a small quantity of gas was withdrawn from the reaction system through a remotely operated valve (a). The gas sample was then passed into a scrubber (b) which contained a dilute solution of sulfuric acid for the removal of hydrazine, ammonia, and water. The scrubbed gases (nitrogen and hydrogen) were then passed through a length of hypodermic tubing (used to reduce the pressure of the gases) into a gas collector (c) which was initially filled with water. The water which was displaced from the gas collector was caught in a receiver (d) and weighed. From the weight of water displaced, the volume of nitrogen and hydrogen which passed through the scrubber was computed. The volume of ammonia which entered the scrubber was determined by weighing and analyzing the liquid in the scrubber. The ratio N of the volume of ammonia to the volume of nitrogen and hydrogen in the gas sample was computed, and the value of X in Equations (3) or (7) was determined by using the following equation:

$$X = \frac{a(4 - N) - b(5 + 4N)}{(4a - 5b)(1 + 2N)} \quad (22)$$

The values of X obtained by means of this method of analysis showed large scatter, which was found to result from random errors in the analytical procedure. These errors were introduced both through inaccuracies involved in determining the end point of the titration of the dilute (less than 1 % by wt) solutions of ammonia from the scrubber and through transfer losses involved in draining the scrubber. These difficulties led to the development of the continuous gas-analysis system described in the preceding section.

### C. SUMMARY OF OPERATING PROCEDURES

This section has been included to indicate the precautions which should be observed in the preparation and operation of hydrazine-monopropellant reaction units.

#### 1. Preparation of Reaction Chamber

a. Injector. The manner in which the hydrazine stream is introduced into a reaction chamber has a marked effect on the stability of operation (Cf. Section VI-C-1) and the amount of catalyst which is required to decompose the hydrazine completely and to dissociate a given fraction of the ammonia (Cf. Sections VIII-B and C). In this report, the following procedure was observed: Before each test, the hydrazine and oxidizer jets were tested with water and adjusted to insure proper atomization, distribution, and mixing. The hydrazine jets were then tested separately to determine the approximate distance from the injector to the point at which the hydrazine stream impinged on the chamber wall. This point of impingement was adjusted to conform with the location of the upstream surface of the catalyst bed in the chamber.

b. Catalyst bed. The arrangement of the catalyst bed in a reaction chamber has a major effect on the pressure drop across the bed (Cf. Section VIII) and on the effectiveness of a given volume of catalyst in the decomposition of hydrazine and the dissociation of ammonia. In this report, an attempt was made to obtain random dense arrangement of the particles in the bed (Cf. Section VIII). For this purpose, the catalyst was added to the reaction chamber at such a rate that each successive layer of catalyst was permitted to fill the cross-section of the chamber completely before the next layer was started. In order to detect major changes in the packing of the bed, the weight of catalyst charged to the chamber was determined before each test. When the weight of catalyst required to obtain a given level in the chamber was markedly different from that determined in previous chargings, the catalyst was emptied from the chamber, and a new bed was formed. When the reaction chamber was to be operated in any position other than with its axis vertical, a nickel screen was placed across the upstream surface of the bed. This screen was held in place by stainless-steel wires which were passed through the bed and fastened to the retainer plate.

#### 2. Firing Procedure

When the reaction chamber was to be operated over a range of pressures in a particular test, the reaction chamber was started at the highest pressure which would be encountered. In this manner, with constant feed pressure, the pressure drops across the hydrazine and oxidizer jets were at their maximum values, and the highest degree of atomization of the propellants was achieved during ignition. When the reaction chamber

was shut down, a small stream of water was turned on the hydrazine injector line in order to prevent heating and consequent decomposition of hydrazine in the feed system.

### VIII. ENGINEERING DATA

The purpose of this Section is to present relationships based on experimental data which will permit with accuracy sufficient for most design purposes the prediction of the performance of hydrazine monopropellant reaction chambers over a wide range of operating conditions.

#### A. CATALYTIC DECOMPOSITION OF HYDRAZINE

##### 1. Factors Involved in Ideal Reaction Chambers

In order to describe the steps which are believed to be necessary in the catalytic decomposition of hydrazine, an ideal reaction chamber is assumed in which the primary decomposition of hydrazine takes place adiabatically in accordance with the reaction represented by Equation (9),  $2\text{N}_2\text{H}_4 = 2\text{HN}_3 + \text{N}_2 + \text{H}_2$ , and in which no dissociation of ammonia occurs until all of the hydrazine is decomposed. In addition, it is assumed that no back flow of hydrazine or decomposition gases occurs and that the flow rates, compositions, temperatures, and reaction rates are uniform across a given cross-section of the catalyst bed. Under these conditions, the catalyst bed may be divided into three longitudinal sections. In the upstream section, zone A, the hydrazine which enters the chamber as a highly atomized liquid at room temperature is evaporated. In zone B, the undecomposed hydrazine vapor in the gases leaving zone A is completely decomposed. In the downstream section of the bed, zone C, the dissociation of ammonia occurs.

a. Factors which influence the depth of zone A. In the absence of back flow, the heat necessary for the evaporation of hydrazine in zone A must be supplied by the following methods:

1. Conduction through the catalyst bed and chamber wall from zone B.
2. Radiation from zone B.
3. Decomposition of hydrazine in zone A.

Because of the low thermal conductivity of the bed, the small cross-sectional area of the chamber wall, and the low temperatures involved, it is likely that only a small part of the heat is supplied to zone A by methods 1 and 2. As a result, it has been concluded that the major portion of the heat necessary for the evaporation of hydrazine is supplied by decomposition in zone A.

If the heat transferred by conduction and radiation is neglected and if the temperature of the stream leaving zone A is assumed to be at the boiling point  $T_B$  of hydrazine at the existing chamber pressure, the following equation based on a heat balance may be written, where  $Y_A$  is the fraction of hydrazine decomposed in zone A and where  $H_v$  and  $H_p$  are the respective enthalpies of hydrazine vapor and the products of the reaction represented by Equation (9) at  $T_B$ :

$$Y_A = \frac{H_V}{41,500 \text{ Btu/lb mol} + H_V - H_P} \quad (23)$$

Calculations based on Equation (23) show that  $Y_A$  increases with chamber pressure. At 500 psia,  $Y_A$  was estimated to be 0.48.

The depth of zone A,  $L_A$ , is given by the following equation, where  $\rho_c$  is the density of the catalyst particles,  $F_V$  is the fraction of voids in the bed, and  $r_A$  is the rate of decomposition of hydrazine in zone A, expressed in moles per pound of catalyst per second:

$$L_A = \frac{G}{\rho_c(1 - F_V)} \int_0^{Y_A} \frac{dy}{r_A} \quad (24)$$

Before Equation (24) may be integrated,  $r_A$  must be expressed in terms of  $Y$ .

If, as other studies indicate (Cf. Ref. 1), the decomposition of hydrazine is predominately a heterogeneous vapor-phase reaction, the over-all rate of decomposition of hydrazine  $r_A$  may be limited by one or more of the following steps:

1. The evaporation of hydrazine.
2. The mass transfer of hydrazine vapor to the catalyst surface.
3. The activated adsorption of hydrazine and the activated desorption of decomposition products on the catalyst.
4. The chemical decomposition of hydrazine on the catalyst.
5. The mass transfer of the decomposition products from the catalyst to the stream.
6. The transfer of heat from the catalyst and decomposition products to the liquid hydrazine.

b. Factors which influence the depth of zone B. Using the same assumptions on which Equation (24) is based, the depth of zone B is given by the following expression, where  $Y_B$  is the equilibrium fraction of hydrazine decomposed under adiabatic conditions:

$$L_B = \frac{G}{\rho_c(1 - F_V)} \int_{Y_A}^{Y_B} \frac{dy}{r_B} \quad (25)$$

The over-all rate of hydrazine decomposition  $r_B$  in zone B may be limited by steps 2, 3, 4, and/or 5, described in the preceding Section.

c. Minimum bed depth required for the complete decomposition of hydrazine. The minimum bed depth  $L_0$  required for the complete decomposition of hydrazine is obtained by combining Equations (24) and (25), as



follows:

$$L_0 = L_A + L_B = \frac{G}{\rho_c(1 - F_V)} \int_0^{Y_A} \frac{dy}{r_A} + \int_{Y_A}^{Y_B} \frac{dy}{r_B} \quad (26)$$

The values of  $r_A$  and  $r_B$  are determined by the slow step or steps in the two zones.

## 2. Factors Involved in Actual Reaction Chambers

The ideal conditions upon which the preceding discussion was based do not prevail in actual reaction chambers. Because of asymmetries in the injection pattern, nonuniform packing of the bed, wall effects, and heat losses, the flow rates, compositions, temperatures, and reaction rates vary widely across a given cross-section of the bed. In addition, it is likely that some liquid-phase and homogeneous gas-phase decomposition of hydrazine occurs and that some secondary dissociation of ammonia takes place in zones A and B. Consequently, some overlapping of zones occurs; hence sharp boundaries cannot be defined and simple rate expressions cannot be applied to those regions of the bed in which hydrazine is present.

In order to evaluate Equation (26), it would be necessary to perform tests under carefully controlled laboratory conditions in which the reactions in zones A and B could be isolated and the rate-controlling mechanism or mechanisms determined. However, because of the influence of other factors such as heat losses, variations in injector performance, channeling of the fluid stream, and nonreproducible packing of the bed, it is not likely that such information could be applied directly to hydrazine-monopropellant reaction chambers.

In an actual reaction chamber, the depth of zone A and, therefore, the value of  $L_0$ , is determined to a large extent by the manner in which the hydrazine is injected. If the hydrazine is injected as a highly atomized stream which is uniformly distributed across the upstream surface of the catalyst bed, all of the catalyst in the inlet regions of the bed should be effective in the decomposition of hydrazine. If, on the other hand, the hydrazine enters the bed in the form of large droplets and/or is nonuniformly distributed, some of the liquid penetrates deeply into the bed, bypassing part of the catalyst in certain regions, thereby increasing  $L_0$ . In this study, the variations of injector performance from test to test were sufficient to obscure the effects of such parameters as  $P_c$ ,  $\omega$ , and  $D_c$  on  $L_0$ .

## 3. Experimental Evaluation of Catalysts

### a. Estimation of the depth of type H-7 catalyst required for the complete decomposition of hydrazine.

For the reasons discussed in the preceding Section, and because of difficulties involved in the direct measurement of  $L_0$ , it has not been found possible to obtain an analytical expression for  $L_0$  in terms of the principal design parameters. In the absence of such an expression it is necessary to specify certain limits of operation, where experience has shown that satisfactory performance can be achieved.

In the course of this study, a large number of tests were made using type H-7 catalyst (1/4-in. spherical, 3/16- by 3/16-in. cylindrical, and 3- by 8-mesh polysurface particles) in reaction chambers having diameters

of 1, 2, 3.5, 4.8, and 6 inches. These reaction chambers were operated over a wide range of mass-flow rates (0.004 to 0.11 lb/in.<sup>2</sup> sec) and chamber pressures (150 to 850 psia). From these tests it was found that in uninsulated chambers the most efficient performance was obtained at mass-flow rates in excess of 0.020 lb/in.<sup>2</sup> sec. At lower flow rates, in uninsulated reaction chambers, unstable operation was obtained, and excessively long catalyst beds were required to insure sustained operation. This effect of low mass-flow rates has been attributed to excessive heat losses and/or channeling in the catalyst beds. In general, it has been found that efficient performance is favored by high mass-flow rates. For this reason it is desirable to design reaction chambers to give as high mass-flow rates as possible. The upper limit of mass-flow rate is determined by the maximum pressure drop (Cf. Section VIII-C) which can be safely withstood by the catalyst bed.

In an earlier study (Cf. Ref. 12), the variation with bed depth  $L_c$  of characteristic velocity  $C^*$  and chamber temperature  $T_c$  was determined using concentrated hydrazine and 3/16- by 3/16-inch cylinders of H-7 catalyst in a 2-inch-diameter reaction chamber which was operated at a pressure of 300 psia with a hydrazine mass-flow rate of about 0.1 lb/in.<sup>2</sup> sec. It was found that  $C^*$  and  $T_c$  increased with  $L_c$  up to a depth of about 2 inches, beyond which bed length these two parameters decreased as  $L_c$  was increased. The attainment of maximum values of  $T_c$  and  $C^*$  at a bed depth of 2 inches was attributed to complete decomposition of hydrazine at that depth. The lower values of  $C^*$  and  $T_c$  obtained with shorter beds was believed to result from incomplete decomposition of hydrazine, whereas in beds longer than 2 inches the lower values of  $C^*$  and  $T_c$  were attributed to an increase in the extent of ammonia dissociation with bed depth. Accordingly, it was concluded that under the conditions of these tests the minimum bed depth  $L_c$  required for the complete decomposition of hydrazine was about 2 inches. This bed depth corresponded to a residence time  $\theta_c$  (Cf. Eq. 8) of about 2 milliseconds.

In this study, an attempt has been made to determine the influence of chamber pressure  $P_c$ , chamber diameter  $D_c$ , and hydrazine mass-flow rate  $G$  on  $L_c$ . For this purpose, a series of tests was made using concentrated hydrazine (95 wt % or better) and 1/4-inch spheres of H-7 catalyst in reaction chambers similar to those shown in Figures 5, 6, and 7. The three reaction chambers were operated at values of  $G/P_c$  which gave residence times insufficient for the complete decomposition of hydrazine in the absence of a catalyst. The values of  $G$  and the total residence times (Cf. Eq. 8) used were as follows:

Reaction-Chamber Diameter (in.)	Hydrazine Mass-Flow Rate $G$ [lb/(in. <sup>2</sup> /sec)]	Total Residence Time $\theta_c$ (sec)
2 (Cf. Fig. 5)	$0.020 < G < 0.08$	0.023
3 1/2 (Cf. Fig. 6)	$0.030 < G < 0.12$	0.021
4 7/8 (Cf. Fig. 7)	$0.027 < G < 0.10$	0.025

Bed depths of 0, 1/2, 1, 1 1/2, 2, and 2 1/2 inches were tested in each chamber. Three tests were made at each bed depth in each chamber. In each test, gas samples were taken at chamber pressures of 200, 400, 600, and 800 psia by means of the intermittent-gas-analysis apparatus described in Section VII-B-2. The acid solution from the gas scrubber was analyzed for hydrazine, and the weight fraction of undecomposed hydrazine

in the decomposition gases was computed. However, because of large errors involved in the analysis of the extremely dilute solutions of hydrazine obtained from the scrubber, it was not found possible to determine the variation with bed depth of the weight fraction of undecomposed hydrazine in the decomposition gases. Therefore, in order to obtain values of  $L_0$ , it was necessary to divide the tests into two groups: (1) those in which undecomposed hydrazine was detected in the scrubber solution, and (2) those in which no hydrazine or only extremely small traces of hydrazine could be detected. From the latter group of tests, the shortest bed depths were taken as the minimum required for the complete decomposition of hydrazine. Based on these data, the following empirical equation was derived, where  $a_v$  is the geometric surface area of the catalyst particles per unit volume of bed ( $\text{in.}^2/\text{in.}^3$ ):

$$L_0 = 1 + 8 \times 10^4 \frac{G}{P_c a_v} \quad (27)$$

Values of  $a_v$  for 1/8- by 1/8-inch and 3/16- by 3/16-inch cylinders and for 1/4-inch spheres are shown in Figure 18. Values of  $a_v$  for particles of other shapes and sizes may be obtained from Reference 16.

With good atomization (injector pressure drop of at least 100 psi) and reasonably uniform cross-sectional distribution of the injected hydrazine, reaction chambers designed in accordance with Equation (27) should give smooth, efficient, and reproducible performance. In tests made in which the depth of the H-7 catalyst was equal to that given by Equation (27), it was found that approximately 40 % of the ammonia was dissociated and that the decomposition gases contained only traces of hydrazine. For this reason, the values of  $L_0$  predicted by Equation (27) may be used to obtain optimum performance (Cf. Section III) of concentrated hydrazine (95% by wt hydrazine or better) in rocket thrust chambers. Equation (27) may also be used to predict the minimum depth required for the complete decomposition of hydrazine in mixtures containing hydrazine nitrate and water, in which the ratio of the weight fraction of hydrazine nitrate to that of water is greater than 1.7.

Larger bed depths than those predicted by Equation (27) are required with hydrazine which contains more than 5 wt % water or with mixtures in which the ratio of the weight fraction of hydrazine nitrate to that of water is less than 1.7 (Cf. Section VIII).

b. Estimation of the depth of type H-A-3 catalyst required for the complete decomposition of hydrazine.

No tests have been made to determine the values of  $L_0$  for H-A-3 catalyst. However, because of the activity of this catalyst in the dissociation of ammonia and because of its similarity to H-7 catalyst, it is reasonable to expect that the depth of bed required to decompose the hydrazine completely should be equal to or less than that predicted by Equation (27).

The physical strength of the H-A-3 catalyst is somewhat inferior to that of the H-7 catalyst. Consequently, in order to obtain satisfactory performance with this catalyst, it is necessary to limit the pressure drop across the bed to considerably lower values (25 psi or less) than can be used with the H-7 catalyst (up to 50 psi). In addition, the degree of pressure instability which can be withstood by this catalyst is considerably less

than that which can be tolerated by the H-7 catalyst. For these reasons, it is recommended that the H-7 catalyst be used in those applications in which it is not necessary to dissociate more than 50 % of the ammonia and that the H-A-3 catalyst be used in other applications in which it is necessary or desirable to dissociate a larger fraction of the ammonia.

## B. CATALYTIC DISSOCIATION OF AMMONIA

### 1. Factors Which Govern the Catalytic Dissociation of Ammonia

The rate of dissociation of ammonia over most iron catalysts is given by the following expression (Cf. Ref. 14) where  $E_a$  is the apparent energy of activation over the particular catalyst:

$$r_c = \frac{4G}{96.15 P_c(1 - F_v)} \left( \frac{dX}{dL} \right) = K_r \frac{P_{NH_3}^d}{P_{H_2}^3} e^{-E_a/RT} \quad (28)$$

It is assumed that this Equation is applicable to the catalysts developed in this study.

If adiabatic conditions are assumed,  $T_c$  may be substituted for  $T$  in Equation (28). From the reaction represented by Equation (3),

$$P_{NH_3} = \frac{4(1 - X)P_c}{5 + 4X} \quad (29)$$

and

$$P_{H_2} = \frac{6XP_c}{5 + 4X} \quad (30)$$

Referring to Figure 1, it can be seen that  $T_c$  varies linearly with  $X$  and may be represented by the following equation:

$$T_c (^{\circ}K) = 782 (2.11 - X) \quad (31)$$

By substituting for  $P_{NH_3}$ ,  $P_{H_2}$ , and  $T_c$  in Equation (28) and solving for  $dL$ , the following expression is obtained in integral form:

$$L_c - L_o = \Delta L_X = \frac{4G}{(1 - F_v)P_c^{d-e}} \int_{X_o}^X \frac{(5 + 4X)^{d-e} X^e e_n^{\frac{\beta}{2.11-X}}}{(1 - X)^d} dX \quad (32)$$

where

$X_0$  = fraction of ammonia dissociated at  $L_0$ ;

$$\alpha = \frac{4 \times 6^e}{96.15 \times 4^d \rho_c K_r}; \text{ and}$$

$$\beta = \frac{E_a}{782R}.$$

An empirical solution of Equation (32) is presented in the following section.

## 2. Experimental Evaluation of Catalysts

a. Dissociation of ammonia over type H-7 catalyst. In order to determine the influence of chamber pressure and bed depth on the extent of ammonia dissociation over the H-7 catalyst, a series of tests was made.

(1) Experimental procedure. In these tests, 1/4-inch spherical particles were used in a reaction chamber similar to that shown in Figure 6. The arrangement of the test apparatus was similar to that shown in Figure 15, and the decomposition gases were analyzed by the method described in Section VII-B-1. Bed depths of 1, 1 3/4, 2 1/4, 2 1/2, 3 1/2, 4 1/2, 5 1/2, 6, and 7 inches were tested. A minimum of 5 tests was made at each bed depth. In each test a new charge of catalyst was used, and the chamber pressure was varied from about 200 to 800 psia in steps of approximately 50 psi.<sup>a</sup> Three tests were also made without catalyst in order to determine the extent of the ammonia dissociation in the empty chamber.

In these tests, the throat area of the discharge nozzle (m in Fig. 15) was maintained constant so that the ratio  $G/\bar{P}_c$  and therefore the total residence time in the reaction chamber would be virtually constant at all chamber pressures and flow rates. The ratio of  $G/\bar{P}_c$  was  $8.6 \times 10^{-5} \pm 2.3\%$  for all tests in the series. The volume of the reaction system upstream from the heat exchanger was 92 cubic inches. Using a value of  $T_c/M_g$  of  $165^\circ R$  mol/lb the residence time was found to be 36 milliseconds (Cf. Eq. 8).

(2) Interpretation of data. The values of  $X$  obtained for each test at a given bed depth were plotted against  $\bar{P}_c$  on rectangular co-ordinate paper, and a smooth curve was drawn through each set of data. From these curves the values of  $X$  at a particular chamber pressure were averaged. The average values of  $X$  obtained in this manner were then plotted against  $\bar{P}_c$ . Typical curves of  $X$  vs  $\bar{P}_c$  are shown in Figure 19.

From the Figure it can be seen that  $X$  changes with  $\bar{P}_c$  at all bed depths. However, the manner in which  $X$  varies with  $\bar{P}_c$  changes progressively with bed depth. In the shorter beds,  $X$  increases uniformly with  $\bar{P}_c$ . In the intermediate bed depths,  $X$  approaches a limit as  $\bar{P}_c$  increases. In the longer beds,  $X$  falls off steadily as the chamber pressure increases.

<sup>a</sup>Approximately 20 sec of operation was used at each pressure to insure equilibrium conditions in the chamber and in the gas-analysis system.

The change in the shapes of the curves suggests the presence of two opposing effects of increasing chamber pressure: (1) to increase  $X_0$  and/or decrease  $L_0$  and (2) to alter the rate of dissociation of the ammonia. For reasons which will be discussed in a subsequent section of this report, it has been concluded that  $L_0$  rather than  $X_0$  varies with chamber pressure, the inverse variation of  $L_0$  with  $\bar{P}_c$  being explained by changes in the performance of the injector.

Equation (32) may be written as follows, where the quantity  $f(X) - f(X_0)$  represents the value of the integral between  $X_0$  and  $X$ :

$$L_c - L_0 = \frac{aG}{(1 - F_v)P_c^{d-e}} [f(X) - f(X_0)] \quad (33)$$

If, as in these tests,  $\frac{aG}{(1 - F_v)P_c} = K$ , a constant, Equation (33) may be written as follows:

$$L_c - L_0 = K [f(X) - f(X_0)] P_c^{1-d+e} \quad (34)$$

or, solving for  $f(X)$ ,

$$f(X) = \frac{L_c - L_0}{KP_c^{1-d+e}} + f(X_0) \quad (35)$$

The exponent  $d-e$  in Equation (33) is generally less than unity for ammonia-dissociation catalysts which contain iron (Cf. Ref. 14). Consequently, the pressure exponent  $1-d+e$  in Equations (34) and (35) should be greater than 0, and, if the values of  $X_0$  and  $L_0$  were independent of pressure,  $f(X)$  and therefore  $X$  would decrease at all values of  $L_c$  as  $\bar{P}_c$  was increased. However, if, as is believed to be true in these tests,  $X_0$  remained constant but  $L_0$  decreased as  $\bar{P}_c$  was increased, the manner in which  $X$  varied with  $\bar{P}_c$  would be dependent on the value of  $L_c$ .

In the shorter beds, it appears that the term  $L_c - L_0$  increased more rapidly with pressure than the term  $P_c^{1-d+e}$ , and  $X$  increased with pressure. In the intermediate bed depths at lower pressures, the increase in  $L_c - L_0$  was greater than that of  $P_c^{1-d+e}$ ; hence  $X$  increased with pressure. However, as the pressure was increased, the change in  $L_c - L_0$  decreased relative to that of  $P_c^{1-d+e}$  until a pressure was reached by which the two terms increased with  $\bar{P}_c$  to the same extent, and  $X$  approached a limiting value. In the larger bed depths, the change in  $L_c - L_0$  was less than that of  $P_c^{1-d+e}$  at all pressures and  $X$  decreased uniformly as the pressure was increased.

The hydrazine storage tank used in these tests could not be pressurized above 1000 psig. As a result, the pressure drop  $\Delta P_1$  across the injector was about 215 psi at a chamber pressure of 800 psia. This pressure drop decreased with  $\bar{P}_c^2$  ( $\dot{\omega}/P_c$  constant and  $\Delta P_1$  proportional to  $\dot{\omega}^2$ ); hence at a chamber pressure of 200 psia  $\Delta P_1$  was only about 15 psi. Because of the low injector pressure drops, it was anticipated that the performance

of the injector would be marginal at the lower chamber pressures. Accordingly, a series of water-flow tests was made<sup>a</sup> in which the cross-sectional distribution of water in the spray was determined at a distance from the injector which corresponded to the normal position of the upstream surface of the catalyst bed in the chamber. These tests, which were made over a range of pressure drops from 20 to 250 psi, showed that the distribution of water in the spray was not particularly influenced by flow rate. However, it was observed that the size of the droplets in the spray increased markedly as the pressure drop was decreased. At a pressure drop of 250 psi, the droplets were very small, and the spray had the appearance of a fine mist. At a pressure drop of 20 psi, the droplets were quite large, and the spray was extremely coarse.

The degree of atomization of the injected hydrazine should have a major influence on the depth of penetration of liquid hydrazine into the catalyst bed and therefore on  $L_0$ . For this reason and because of the observed decrease in injector performance with flow rate, it has been concluded that changes in  $L_0$  rather than in  $X_0$  were responsible for the manner in which  $X$  varied with  $\bar{P}_c$  (Cf. Section VIII-C-2).

Using smoothed data obtained from the curves of  $X$  vs  $\bar{P}_c$  at constant bed depth, cross-plots of  $X$  vs  $L_c$  at constant  $\bar{P}_c$  and  $\omega$  were prepared as shown in Figure 20. From the Figure it can be seen that  $X$  increases with  $L_c$ , the rate of increase becoming smaller as  $L_c$  increases. It should also be noted that  $X$  changes less with  $L_c$  as  $\bar{P}_c$  increases. Although the data are quite consistent at bed depths of 3 1/2 inches or greater, there is considerable scatter in the points obtained with the shorter bed depths. This scatter in the data for the short beds has been attributed to random changes in injector performance. Because of the low values of  $X$  obtained with a bed depth of 1 inch, it has been concluded that this depth was less than  $L_0$  at all values of chamber pressure studied.

It was pointed out in Section VIII-B that when bed depths equal to those given by Equation (27) were used, approximately 40 % of the ammonia and all but traces of the hydrazine were decomposed. Accordingly,  $X_0$  in Equation (32) has been taken as 0.40, and  $L_0$  has been taken as the bed depth required to dissociate this fraction of the ammonia.

From the curves in Figure 20 it can be seen that the bed depth  $L_0$  required to dissociate 40 % of the ammonia decreases as  $\bar{P}_c$  increases. This variation in  $L_0$  with  $\bar{P}_c$  is shown in Figure 21. Curves of  $L_c$  vs  $\bar{P}_c$  at several values of  $X$  greater than 0.40 are also shown in the Figure.

Using the smoothed values of  $L_0$  and  $L_X$  ( $L_c$  at a particular value of  $X$ ), the quantity  $\Delta L_X$  (equal to  $L_c - L_0$ ) was computed for several pressures. These values of  $\Delta L_X$  were plotted against  $\bar{P}_c$  on log-log paper as shown in Figure 22. From the Figure it can be seen that the data may be represented by straight lines. In drawing the lines shown in the Figure, a constant slope was used for all of the data. This slope was determined on the basis of the best apparent fit for all of the data. The deviations of some of the points from these lines resulted from inaccuracies involved in the determination of  $\Delta L_X$ .

Referring to Equation (32), it can be seen that the integral is a function only of  $X$ , which may be designated as  $C_X$ . The following equation may be written, where  $\Delta L_X$  is the bed depth beyond  $L_0$  required to dissociate

<sup>a</sup>Unpublished data prepared by J. H. Rupe of this Laboratory.

a fraction X of the ammonia:

$$C_X = \frac{(1 - F_v) \bar{P}_c^{d-e} \Delta L_X}{G} \quad (36)$$

In these tests,  $G = 8.6 \times 10^{-5} \bar{P}_c$ , and  $F_v = 0.38$ . Substituting these values in Equation (36) and solving for  $\bar{P}_c$ ,

$$\bar{P}_c^{1-d+e} = \bar{P}_c^{1-g} = \frac{7.18 \times 10^3 \Delta L_X}{C_X} \quad (37)$$

Since  $C_X$  is a constant for given limits of X,  $\log \Delta L_X$  should be linear with  $\log \bar{P}_c$ , as was found in the data from these tests. Using the equations represented by the lines in Figure 22, the pressure exponent g was found to be 0.5. The values of  $C_X$  at the different values of X were also determined. Figure 23 shows the variation of  $\log C_X$  with  $\log \frac{X - 0.40}{1 - X}$ ,  $X_0$  being equal to 0.40. From the Figure it can be seen that a straight line may be used to represent the data. Using the equation represented by this line, the following expression was obtained:

$$C_X = 6600 \left( \frac{X - 0.40}{1 - X} \right)^{1.21} \quad (38)$$

Substituting this expression for the integral in Equation (32),

$$L_c - L_0 = \frac{6600 G}{(1 - F_v) \bar{P}_c^{0.5}} \left( \frac{X - 0.40}{1 - X} \right)^{1.21} \quad (39)$$

Using Equation (39) and smoothed values of  $L_0$  from Figure 21, several values of X were computed for each bed depth. These values are compared with the experimental data in Figure 19. From the Figure it can be seen that Equation (39) gives a good approximation of the data. The differences between the calculated curves and the arithmetic-mean curves may be attributed to errors in the determination of the pressure exponent g.

The values of  $L_0$  used in these tests are somewhat greater at chamber pressures below 600 psia than are those predicted by Equation (27). The difference between the values is attributed to the fact that the atomization of hydrazine in these tests at the lower pressures was less than that which was used in the tests upon which Equation (27) is based.

In order to determine the values of all of the constants in Equation (32), extremely precise measurements of the variation of X with both  $\bar{P}_c$  and  $L_c$  would be required. For this reason and because of the scatter in the data, no attempt has been made to evaluate the individual values of d, e, a and  $\beta$ . For this purpose, laboratory studies would be required. In order to determine the values of  $E_a$  and  $\beta$  accurately, it would be



necessary to study the rate of dissociation of the ammonia over the H-7 catalyst at several different temperatures. In any event, Equation (39) should be sufficiently accurate for most engineering purposes.

b. Dissociation of ammonia over type H-A-3 catalyst. Bed depths of 1, 1 1/2, 2 1/2, 3 1/2, 4 1/2, 5 1/2, and 7 inches, using 1/8- by 1/8-inch cylinders of the H-A-3 catalyst were tested in the same manner as was described in Section VIII-B-2-a. In these tests, the ratio of  $G/\bar{P}_c$  was maintained constant at  $5.1 \times 10^{-5}$  in.<sup>2</sup>/sec  $\pm 3.6$  %. This low ratio of  $G/\bar{P}_c$  was used in order to limit the pressure drop across the bed. A minimum of four tests was made at each bed depth. In each test, a new charge of catalyst was used, and the chamber pressure was varied from about 150 to 750 psia in steps of 50 psi.

Representative data obtained in these tests are shown in Figure 24. The curves shown in the Figure were obtained by averaging the data, in the manner described in connection with the data obtained with the H-7 catalyst. Using smoothed data from these curves, plots of  $X$  vs  $L_c$  were prepared as shown in Figure 25. Only the curves at 200, 500, and 700 psia are shown; however, these curves are representative of all of the data. From the curves it can be seen that the influence on  $X$  of pressure is small relative to that of bed depth. For this reason and because of uncertainty in the true value of  $X_0$  using this catalyst, no attempt has been made to obtain a solution for Equation (32) as was done for the H-7 catalyst.<sup>a</sup> Instead, the data have been correlated in terms of residence time. For simplicity and because the ratio  $RT_c/M_g$  is virtually constant at all values of  $X$ , an effective residence time  $\theta_e$  has been defined as follows:

$$\theta_e = \frac{\bar{P}_c L_c (1 - F_V)}{G} \quad (40)$$

The variation of  $X$  with  $\theta_e$  for the H-A-3 catalyst is shown in Figure 26 for pressures of 200, 500, and 700 psia. The values of  $X$  used in the Figure are smoothed values obtained from the curves of  $X$  vs  $\bar{P}_c$ . The values of  $X$  obtained with the H-7 catalyst at a pressure of 500 psia are also shown in the Figure. It should be noted that the H-A-3 catalyst is much more active than the H-7 catalyst in the dissociation of ammonia.

The following equation should be used to determine the depth of the H-A-3 catalyst required to dissociate a given fraction of the ammonia:

$$L_c = \frac{\theta_e G}{\bar{P}_c (1 - F_V)} \quad (41)$$

The values of  $\theta_e$  in this equation should be taken from Figure 25. However, values of  $L_c$  less than those given by Equation (27) should never be used.

<sup>a</sup>A study of the data shown in Fig. 26 indicates that with the H-A-3 catalyst the pressure exponent 1-d+e in Eq. (32) is equal to that obtained with the H-7 catalyst; i.e., 1-d+e = 0.5.

## C. ESTIMATION OF PRESSURE DROP ACROSS CATALYST BEDS

## 1. Basic Factors

The flow of hydrazine-decomposition gases through a catalyst bed is accompanied by a loss in pressure. This loss in pressure must be limited for two reasons: (1) in order to minimize the injection pressure and therefore the weight of the feed system required for a given discharge pressure and (2) to prevent the development of forces sufficient to cause crushing of the catalyst particles, thereby producing an increased pressure loss and an unstable exhaust pressure.

The pressure losses associated with the passage of fluids through conduits of uniform cross-section are correlated by means of the dimensionless Fanning equation:

$$\Delta P = \frac{2fG^2L}{g_c D_c \rho} \quad (42)$$

The dimensionless friction factor  $f$  in Equation (42) is correlated as a function of the Reynolds number  $N_{Re}$ , which is defined as  $\frac{4r_h G}{\mu}$ . The hydraulic radius  $r_h$  is defined as the ratio of the wetted cross-sectional area of a conduit to its wetted perimeter; hence for a circular pipe  $N_{Re}$  becomes  $\frac{DG}{\mu}$ .

In order to utilize the Fanning equation for the correlation of pressure losses obtained in packed beds, it must be modified to include terms both for the free cross-sectional area which is available for flow and for the effective hydraulic radius of the path between the particles. The modifications of the Fanning equation which are necessary before satisfactory correlation can be achieved are largely dependent on the arrangement of the particles in the bed (Cf. Ref. 15). Because of the time required, hand-packed beds which conform to a particular geometric arrangement are not practical. As a result, beds are generally formed by pouring the particles into the chamber. If the particles are added to the chamber at such a rate that each comes to rest before another falls on top of it, minimum bridging occurs, and a high bulk density results. Beds formed in this manner are described as being in random dense arrangement. The opposite extreme, referred to as random loose arrangement, is obtained when all of the particles are simultaneously dumped into the chamber. In a random dense arrangement, the bulk density may be 25 % higher, and under the same conditions of flow the pressure loss may be nearly three times greater than pressure losses obtained with a loose arrangement (Cf. Ref. 15).

The over-all activity of a catalyst bed is influenced more by the weight of catalyst which is contained than by the total volume occupied. As a result, it is generally more desirable from the standpoint of efficient reactor design to utilize random dense arrangement of the catalyst particles. In this study (Cf. Section VII), an attempt was made to approximate the random dense arrangement.

The following dimensionless equation was proposed (Cf. Ref. 15) for the correlation of the pressure losses obtained in beds in random dense arrangement:

$$\Delta P = \frac{2f_d G^2 a_v L_c}{\rho_g F_v^{1.7}} \quad (43)$$

The dimensionless friction factor  $f_d$  was correlated by means of a modified Reynolds number  $N_{Red}$ , which is defined as  $\frac{G}{\mu a_v}$ . When  $f_d$  is plotted against  $N_{Red}$  on log-log paper, a smooth curve of gradually changing slope is obtained which may be approximated by two straight lines, as follows (Cf. Ref. 15):

$$f_d = 2.60/N_{Red}^{0.3}; \quad [10 < N_{Red} < 150] \quad (44)$$

$$f_d = 1.23/N_{Red}^{0.15}; \quad [150 < N_{Red} < 300] \quad (45)$$

The range of Reynolds numbers of practical interest in connection with the use of hydrazine as a monopropellant is greater than that covered by Equations (44) and (45). Therefore, it was necessary to determine the relationship between  $f_d$  and  $N_{Red}$  over the range  $300 < N_{Red} < 3000$ .

If the depth of catalyst bed in which hydrazine is present as a liquid is neglected, it can be assumed that the fluid flowing through the catalyst behaves as a perfect gas, and

$$\rho = \frac{\bar{P}_c M_g}{RT_c} \quad (46)$$

where  $\bar{P}_c$  is defined as the arithmetic-mean pressure in the bed.

Substituting from Equation (46) in Equation (43) and combining constants,

$$\Delta P_c = f_d K' \left( \frac{\bar{T}_c}{M_g} \right) \left( \frac{a_v}{F_v^{1.7}} \right) \frac{G^2 L_c}{\bar{P}_c} \quad (47)$$

The barred quantities in Equation (47) refer to average values in the bed. Over the range of values of  $X$  encountered in this study ( $0.25 < X < 0.75$ ), the maximum variation of  $T_c/M_g$  is less than 5%. For this reason, an average value of 165 corresponding to an  $X$  value of 0.50 may be used for pure hydrazine. Combining this value with  $K'$ ,

$$P_c = K'' f_d \left( \frac{a_v}{F_v^{1.7}} \right) \frac{G^2 L_c}{\bar{P}_c} \quad (48)$$

The viscosity of the gases produced by the adiabatic decomposition of pure hydrazine was calculated using the method outlined in Reference 15. The viscosity varied from 0.038 centipoise at a value of  $X$  of 0.25 to 0.029 centipoise at an  $X$  value of 0.75. In computing the values of  $N_{Red}$ , an average viscosity of 0.033 centipoise was used. With this value of  $\mu$ , using the dimensions shown in Table I,

$$N_{Red} = 5.41 \times 10^5 \frac{G}{a_v} \quad (49)$$

With  $f_d = K''' N_{Red}^f$ , substituting in Equation (48), and combining constants,

$$\Delta P_c = K \left( \frac{a_v^{1-f}}{F_v^{1.7}} \right) (G)^{2+f} \frac{L_c}{P_c} \quad (50)$$

## 2. Experimental Determination

The pressure drop across the catalyst bed was measured in each of the tests described in the preceding sections. Figures 27 and 28 show representative plots of  $\bar{P}_c \cdot \Delta P_c$  vs  $\dot{\omega}$ , for both the H-7 (1/4-in. spheres) and the H-A-3 (1/8- by 1/8-in. cylinders) catalysts.

With the exception of the data obtained with 1-inch depths of catalyst, all of the data could be represented by straight lines.<sup>a</sup> It was also found that the scatter of the experimental points around the mean curves increased as the bed depth was decreased. This increase in scatter with decreasing bed depth is similar to that observed in the measurement of  $X$  and has been attributed to the same causes, namely, random variations in the packing of the bed and in the performance of the injector. It is believed that the scatter caused by nonreproducible packing of the bed is small relative to that caused by variations in injector performance.

It has been pointed out in Section VIII-B-2 that under the conditions of these tests (constant tank pressure and constant  $G/\bar{P}_c$ ), the degree of atomization of the injected hydrazine decreased with decreasing flow rate. The decrease in the atomization of the hydrazine is believed to have caused an increase in the depth of penetration of the liquid into the bed as the flow rate was decreased. This penetration of the liquid into the bed decreased the length of the path through which the decomposition gases had to pass, thereby reducing the pressure drop across the bed. Since the performance of the injector was not reproducible from test to test, the mean wetted

<sup>a</sup>Because of the scatter in the data, it was necessary to use trial and error methods in obtaining mean curves which were representative of the data obtained with a particular bed depth and at the same time consistent with the data obtained at other bed depths. As a first approximation, straight lines which gave the best apparent fit for the data were drawn. From these lines, values of  $\bar{P}_c \Delta P_c$  at several values of  $\dot{\omega}$  were determined. Using these data, cross-plots of  $\bar{P}_c \Delta P_c$  vs  $L_c$  at constant  $\dot{\omega}$  were prepared. Straight lines which gave the best apparent fit for these data were then drawn, and the values of  $\bar{P}_c \Delta P_c$  at the different flow rates were determined for a particular bed depth. These data were then used to draw adjusted lines through the plots of  $\bar{P}_c \Delta P_c$  vs  $\dot{\omega}$ . This process was repeated several times until the best and most consistent fit of all the data was obtained. The lines shown in the Figures were obtained in this manner.

depth  $L_w$  also varied from test to test. In the longer beds, the percentage variation of the effective bed depth  $L_c - L_w$  through which the decomposition gases had to travel was quite small; hence the scatter in the data was also small. As  $L_c$  was decreased, the percentage variation of  $L_c - L_w$ , and consequently the scatter, increased.

Figures 29 and 30 show the variation of  $\bar{P}_c \Delta P_c$  with  $L_c$  at constant flow rates. From the Figures it can be seen that, when the lines through the data are extrapolated to zero  $\bar{P}_c \Delta P_c$  (i.e., to zero pressure drop), a positive intercept  $L'_w$  is obtained. The value of  $L'_w$  is indicative of the mean wetted depth. When  $\log L'_w$  was plotted against  $\omega^2$ , straight lines were obtained as shown in Figure 31. The equations for these lines are as follows:

$$L'_w = \frac{1.46}{10^{2.10} \omega^2} \quad \text{H-7 catalyst} \quad (51)$$

$$L'_w = \frac{1.57}{10^{5.70} \omega^2} \quad \text{H-A-3 catalyst} \quad (52)$$

Since for a particular injector,  $\omega^2$  is proportional to  $\Delta P_1$ , which governs the degree of atomization of the hydrazine and therefore the depth of penetration of liquid hydrazine into the bed, it appears that  $\Delta P_1$  should be substituted for  $\omega^2$  in Equations (51) and (52). In the tests made with the H-7 catalyst,  $\omega^2 = 20.0 \times 10^{-4} \Delta P_1$ . In the tests made with the H-A-3 catalyst,  $\omega^2 = 8.2 \times 10^{-4} \Delta P_1$ . Substitution of these values in Equations (51) and (52) yields the following expressions:

$$L'_w = \frac{1.46}{10^{0.0042 \Delta P_1}} \quad \text{H-7 catalyst} \quad (53)$$

$$L'_w = \frac{1.53}{10^{0.0047 \Delta P_1}} \quad \text{H-A-3 catalyst} \quad (54)$$

It is possible that the close agreement between these equations for the two catalysts is coincidental. However, because of the observed variation of  $X$  and  $\bar{P}_c \Delta P_c$  with pressure, flow rate, and bed depth, and because of the observed decrease with  $\Delta P_1$  of the degree of atomization provided by both sizes of injector, it appears reasonable that  $\Delta P_1$  rather than catalyst activity or particle size should be the prime variable which governs  $L'_w$ .

The influences of chamber diameter and type of injector on  $L'_w$  have not been determined. However, it is

likely that the constants in Equations (53) and (54), if not the form of the equations themselves, would be markedly influenced by both chamber diameter and injector spray pattern. Further study of the influence of these two variables on  $L_w^1$  is being considered.

In order to determine the values of  $K$  and  $f$  in Equation (50), the slopes of the curves in Figures 29 and 30, i.e.,  $P_c \Delta P_c / (L_c - L_w^1)$ , were plotted against  $\dot{\omega}$  on log-log paper as shown in Figure 32. From the Figure it can be seen that both sets of data are best represented by straight lines. The values of  $f$  and  $K$  obtained from these lines, together with the range of Reynolds numbers (Cf. Eq. 50) covered with the two catalysts are as follows:

$$\begin{matrix} f = -0.20 \\ K = 1260 \end{matrix} \left\{ \begin{matrix} 1.8 \times 10^{-4} < \frac{G}{a_v} < 12 \times 10^{-4} \\ 100 < N_{\text{Red}} < 650 \end{matrix} \right\} \text{ H-A-3 catalyst}$$

$$\begin{matrix} f = 0 \\ K = 3900 \end{matrix} \left\{ \begin{matrix} 6.8 \times 10^{-4} < \frac{G}{a_v} < 37 \times 10^{-4} \\ 370 < N_{\text{Red}} < 2000 \end{matrix} \right\} \text{ H-7 catalyst}$$

The different values of  $f$  and  $K$  obtained over the two ranges of Reynolds numbers indicate that  $\log f_d$  is not linear with  $\log N_{\text{Red}}$ . For this reason, the slope of the curves of  $\bar{P}_c \Delta P_c$  vs  $\dot{\omega}$  should have decreased slightly as  $\dot{\omega}$  was increased. This curvature in the data could not be detected because of the scatter. In any event, the error resulting from the use of straight lines to represent the data should not be large. It is likely that part of the inability to detect curvature in the plots of  $\bar{P}_c \Delta P_c$  vs  $\dot{\omega}$  resulted from the assumption of constant values of  $\mu$  and  $T_c/M_g$ . However, as was indicated in Section VIII-A-4 the variation in these two parameters over the range of  $X$  values encountered was quite small.

After substituting the values of  $f$  and  $K$  in Equation (50), the following generally applicable expressions are obtained:

$$\begin{aligned} 1.85 \times 10^{-4} < \left( \frac{G}{a_v} \right) < 11.10 \times 10^{-4} \\ 100 < N_{\text{Red}} < 600 \end{aligned} \quad \Delta P_c = 1260 \left( \frac{\frac{a_v}{F_v}^{1.2}}{F_v^{1.7}} \right) \frac{G^{1.8} L_c}{\bar{P}_c} \quad (55)$$

$$\begin{aligned} 11.10 \times 10^{-4} < \left( \frac{G}{a_v} \right) < 55.5 \times 10^{-4} \\ 600 < N_{\text{Red}} < 3000 \end{aligned} \quad \Delta P_c = 3900 \left( \frac{\frac{a_v}{F_v}}{F_v^{1.7}} \right) \frac{G^2 L_c}{\bar{P}_c} \quad (56)$$

No allowance for  $L_w$  has been made in Equations (55) and (56) because of uncertainty relative to the influence of chamber diameter and injector design on this parameter. However, if injector pressure drops of 100 psi or greater are used and if reasonably uniform cross-sectional distribution of the injected hydrazine is provided,  $L_w$  should be fairly small, and the errors resulting from its omission in Equations (55) and (56) should also be small. In any case, the omission of  $L_w$  in these equations should result in conservative values of  $\Delta P_c$ .

In order to prevent crushing of the catalyst particles, thereby producing excessive pressure losses and an unstable exhaust pressure, it is necessary to design reaction chambers in such a way that  $\Delta P_c$  does not exceed certain limits which are determined by the physical properties of the catalyst. Based on the experience gained in this study, it is recommended that reaction chambers be designed to limit  $\Delta P_c$  to the following maximum values:

$$\Delta P_c \text{ max} = 35 \text{ psi} \quad \text{H-7 catalyst}$$

$$\Delta P_c \text{ max} = 20 \text{ psi} \quad \text{H-A-3 catalyst}$$

When mixtures containing nitric acid and/or water are to be used, it is recommended that the values of  $\Delta P_c$  given by Equations (55) and (56) be multiplied by the ratio  $(T_c/M_g)_M/165$ , where  $(T_c/M_g)_M$  is the value of this ratio for the particular mixture at  $X = 0.50$  (Cf. Eq. 7).

#### D. EQUATIONS FOR PREDICTING THE PERFORMANCE OF MONOPROPELLANT-HYDRAZINE REACTION CHAMBERS

The purpose of this section is to summarize the relationships which are recommended for use in the design of monopropellant hydrazine reaction chambers.

##### 1. Conditions Required for the Attainment of Predicted Performance

In order to obtain reproducible performance which conforms with that predicted by the relationships presented in this report, it is necessary in the design and operation of monopropellant-hydrazine reaction chambers to observe the following criteria:

1. Catalyst beds should be formed in such a manner (Cf. Section VII-C-1-b) that random dense arrangement of the catalyst particles is obtained.
2. Hydrazine should be injected into the reaction chamber as a highly atomized stream which is uniformly distributed across the upstream surface of the catalyst bed; with solid cone injectors, an injector pressure drop of at least 100 psi should be used.
3. The injector pressure drop, injection pattern, and feed-system arrangement should be such that oscillations in chamber pressure do not exceed  $\pm 2\%$  of the chamber pressure (Cf. Section VI-C).
4. In the absence of hydrazine nitrate, the water concentration in the hydrazine feed should not exceed 5 wt %.

5. In mixtures of hydrazine nitrate and water with hydrazine, the ratio of the weight fraction of hydrazine nitrate to that of water should be at least 1.7.
6. Reaction chambers should be designed to give hydrazine mass-flow rates of at least  $0.020 \text{ lb/in.}^2 \text{ sec.}$  In those cases where mass-flow rates below  $0.020 \text{ lb/in.}^2 \text{ sec}$  must be used, a ceramic liner or other means of limiting heat losses should be incorporated in the reaction chamber.
7. Catalysts should be prepared in strict accordance with the directions given in Reference 12 and should be stored in sealed containers.
8. When a bipropellant ignition system is used, the ratio of the nitric acid flow rate to that of the hydrazine should not exceed 0.30, and the propellants should be uniformly mixed so that local high temperatures and damage to the catalyst are prevented.

In reaction chambers designed and operated in accordance with these criteria, it should be possible to obtain ammonia dissociation within 10% and pressure drops within 20% of the values predicted by the relationships presented in this report.

## 2. Equations for Type H-7 Catalyst

The minimum bed depth  $L_0$  of the H-7 catalyst required for the complete decomposition of hydrazine is given by the following equation:

$$L_0 = 1 + \frac{8 \times 10^4 G}{a_v \bar{P}_c} \quad (27)$$

With bed depths equal to those given by Equation (27), 40% of the ammonia should be dissociated, and optimum performance (Cf. Section III) of the monopropellant in rocket thrust chambers should be obtained.

The bed depth  $L_c$  required for the dissociation of a given fraction  $X$  of ammonia is given by the following expression, which is obtained by combining Equations (27) and (39):

$$L_c = 1 + \frac{8 \times 10^4 G}{a_v \bar{P}_c} + \frac{6600G}{(1 - F_v) \bar{P}_c^{1/2}} \left( \frac{X - 0.40}{1 - X} \right)^{1.21} \quad (57)$$

Equation (57) is applicable over the range  $0.40 \leq X \leq 0.55$ . For higher values of  $X$ , the H-A-3 catalyst should be used.

The values of  $G$  in Equations (27) and (57) must be limited in order to prevent the development of excessive pressure drop across the catalyst bed. When the H-7 catalyst is used, reaction chambers should be operated in such a manner as to give pressure drops of less than 35 psi. For design purposes, it is recommended that a pressure drop  $\Delta P_c$  of 25 psi be used in Equations (55) or (56) for estimating the maximum allowable hydrazine mass-flow rate  $G_{\max}$ . Using this value of  $\Delta P_c$ , Equations (55) and (56) may be written as follows:



$$G_{\max} = 0.114 \left( \frac{F_v^{1.7} P_c}{a_v^{1.2} L_c} \right)^{0.56} ; 1.85 \times 10^{-4} < \left( \frac{G}{a_v} \right) < 11.1 \times 10^{-4} \frac{\text{lb}}{\text{in. sec}} \quad (57)$$

$$G_{\max} = 0.08 \left( \frac{P_c F_v^{1.7}}{a_v L_c} \right)^{0.50} ; 11.1 \times 10^{-4} < \left( \frac{G}{a_v} \right) < 55.5 \times 10^{-4} \frac{\text{lb}}{\text{in. sec}} \quad (58)$$

Wherever possible, it is recommended that reaction chambers be designed to give hydrazine mass-flow rates equal to those obtained from Equations (57) and (58). In this manner, the influences of heat losses and channeling will be minimized.

### 3. Equations for Type H-A-3 Catalyst

Type H-A-3 catalyst should be used only in those applications in which it is necessary or desirable to dissociate 50 % or more of the ammonia. The minimum bed depth of this catalyst should be computed from the following equation:

$$L_0 = 1 + \frac{8 \times 10^4 G}{a_v P_c} \quad (27)$$

The bed depth  $L_c$  of the H-A-3 catalyst required to dissociate a fraction  $X$  of the ammonia should be computed from the following equation, where  $\theta_e$  is the effective residence time shown in Figure 26:

$$L_c = \frac{\theta_e G}{P_c (1 - F_v)} \quad (41)$$

When the H-A-3 catalyst is used, reaction chambers should be so operated that the pressure drop across the catalyst bed is less than 20 psi. For design purposes, a pressure drop of 15 psi should be used in Equations (55) and (56) for estimating  $G_{\max}$ . With this value of  $\Delta P_c$ , Equations (55) and (56) may be written as follows:

$$G_{\max} = 0.11 \left( \frac{F_v^{1.7} P_c}{a_v^{1.2} L_c} \right)^{0.556} ; 1.85 \times 10^{-4} < \left( \frac{G}{a_v} \right) < 11.1 \times 10^{-4} \frac{\text{lb}}{\text{in. sec}} \quad (59)$$

$$G_{\max} = 0.062 \left( \frac{F_v^{1.7} P_c}{a_v L_c} \right)^{0.50} ; 11.1 \times 10^{-4} < \left( \frac{G}{a_v} \right) < 55.5 \times 10^{-4} \frac{\text{lb}}{\text{in. sec}} \quad (60)$$

It is recommended that reaction chambers be designed to give hydrazine flow rates equal to those indicated by Equations (59) and (60).

#### E. INFLUENCE OF ADDITIVES ON THE PERFORMANCE OF MONOPROPELLANT HYDRAZINE

A systematic investigation of additives and impurities in hydrazine has not been made. However, certain observations have been made which are summarized in the following paragraphs.

##### 1. Water

The addition of up to 5 wt % water to hydrazine did not appear to have an appreciable influence on the performance obtained in a particular reaction chamber. When this concentration of water was exceeded, however, the amount of catalyst required for the complete decomposition of hydrazine was increased (Cf. Ref. 12), and the amount of ammonia which could be dissociated with a given residence time over a particular catalyst was decreased. This effect of higher concentrations of water has been attributed to the lowering of the temperatures in the catalyst bed, thereby reducing the rates of reaction and increasing the residence time required to accomplish the decomposition of a given amount of hydrazine or ammonia. The presence of water may also be related to adsorption phenomena in which water preferentially occupies the active centers of the catalyst surface, thereby reducing the effective surface available for the desired reactions.

##### 2. Aniline

At the present time, the concentration of commercial hydrazine involves an azeotropic distillation which utilizes aniline as the entraining agent. As a result, commercial hydrazine contains some (up to 3 wt %) aniline. For this reason, tests were made to determine the influence of aniline on the performance of hydrazine-monopropellant reaction chambers. Concentrations up to 10 wt % were tested. No detectable influence on the stability or smoothness of the operation of the reaction chambers could be detected, and deposition of carbon or other solid materials in the catalyst bed or heat exchanger was not observed. No measurements were made of the influence of aniline concentration on the minimum residence time required for the complete decomposition of hydrazine or the dissociation of a given fraction of ammonia. However, since the presence of aniline should reduce the temperatures at all points in the catalyst bed, some decrease in the rates of hydrazine and ammonia decomposition should result. The influence of a given weight fraction of aniline should not be greater than that of an equal weight of water. For this reason, no difficulties should be encountered in the operation of reaction chambers which contain as much as 5 wt % aniline.

##### 3. Hydrazine Nitrate

The addition of hydrazine nitrate to hydrazine raises the temperature at all points in the bed, and for this reason the rate of decomposition of hydrazine is increased. In an earlier study (Cf. Ref. 12), it was found that when hydrazine containing 20 wt % nitric acid was decomposed over 3/16- by 3/16-inch cylinders of the H-7 catalyst, the minimum residence time required for the complete decomposition of hydrazine was approximately one-half that required with pure hydrazine. In gas-analysis studies made with hydrazine which contained 5, 10, 15, and 20 wt % nitric acid, it was found that the value of X in Equation (7) was only slightly greater than that which was

obtained (Cf. Eq. 3) with concentrated hydrazine. From these observations, it has been concluded that the increase in temperature caused by the addition of nitric acid has only a small influence on the rate of dissociation of ammonia. For this reason, it is recommended that the values of X given by Equations (41) or (57) for concentrated hydrazine be used in Equation (7) for estimating the performance of hydrazine--hydrazine nitrate mixtures.

When mixtures of hydrazine, hydrazine nitrate and water were used, it was found that effects equivalent to those observed with water concentrations of more than 5 wt % in pure hydrazine were obtained when the weight fraction of hydrazine nitrate to that of the water was less than 1.7. From this observation and because of the fact that the increased temperatures obtained with the mixtures did not appreciably increase the amount of ammonia dissociation which could be achieved with a given residence time, it has been concluded that the presence of water tends to inhibit the activity of the catalyst in the dissociation of ammonia. The effect of this reduction of catalyst activity is apparently offset by the higher temperatures obtained when the ratio of the hydrazine nitrate concentration to that of the water is above 1.7. This inhibition of catalyst activity by water has been observed with ammonia synthesis catalysts (Cf. Ref. 13), where it was found that water acted as a poison which when present in sufficient amounts materially reduced the activity of the catalysts.

#### F. INFLUENCE OF OPERATING TIME AND REPEATED USE ON CATALYST PERFORMANCE

In order to obtain an indication of the operational reliability of the H-7 and H-A-3 catalysts, a series of tests was made using reaction chambers similar to those shown in Figures 4, 5, and 9. A single charge of catalyst was used to make ten tests, each test lasting for a minimum of 10 minutes. From these tests it was found that the pressure drop across the catalyst bed and the smoothness of operation were virtually uninfluenced by operating time or the number of ignition periods to which the catalyst was subjected. It was also found that the fraction of ammonia which was dissociated in a particular test was independent of the operating time. However, it was found that, when bipropellant ignition was used, the amount of ammonia which could be dissociated by a given charge of catalyst tended to decrease from test to test. The total decrease in the amount of ammonia which could be dissociated after ten tests with the same charge of catalyst was approximately 10 %. This decrease in catalyst activity has been attributed to damage to the catalyst surface caused by the bipropellant starting technique. However, the effect of repeated ignition does not appear sufficiently serious to cause any difficulty in systems where a single charge of catalyst must be used several times. No appreciable decrease in catalyst activity with repeated ignition was observed when an electrical ignition system was used. From the results of these tests, it has been concluded that with proper ignition and suitable operating conditions (good injection, reasonable pressure drop, and proper feed-system arrangement) a single charge of either H-7 or H-A-3 catalyst can be used in a single firing for an indefinite period of time without significant deterioration in the properties of the catalyst. It has also been concluded that a single charge of either catalyst may be used in a large number of separate firings without marked decrease in activity.

IX. EXPLOSION HAZARD INVOLVED IN THE USE OF HYDRAZINE DECOMPOSITION GASES TO PRESSURIZE THE OXIDIZER (RFNA) STORAGE TANK OF THE CORPORAL FLIGHT VEHICLE

The propulsion system of the Corporal flight vehicle consists of the following principal parts: (1) a tank for the storage of the fuel ( a mixture of aniline, furfuryl alcohol, and hydrazine), (2) a tank for the storage of the oxidizer (RFNA containing 12 wt %  $\text{NO}_2$ ), (3) a 20,000-pound thrust combustion chamber, and (4) a high-pressure multicell storage tank which is used to supply compressed air for the pressurization of the propellant tanks. In order to displace the propellants at the desired rate, it is necessary to pressurize the propellant tanks to about 450 psia. For this purpose, nearly 26 cu ft (325 lb) of air must be charged into the multicell storage tank at a pressure of about 2500 psi. The weight of the air-storage tank when fully pressurized is approximately 950 pounds.

Because of the large size and weight of the compressed-air pressurization system and because of the large amount of ground-handling equipment (compressors, dryers, storage cylinders, etc.) required to service the system in the field, this Laboratory proposed (Cf. Ref. 18) the use of a hydrazine mono-propellant gas-generation system. In a preliminary design study, it was estimated that the total weight of a hydrazine-monopropellant gas-generation system suitable for use in the Corporal flight vehicle would weigh less than 250 pounds and would permit a weight saving of approximately 700 pounds. This weight saving was reflected in greater range and/or payload capacity of the vehicle. Because of the possibility of using a prepackaged system, it was also anticipated that the use of the gas-generation system would materially simplify the servicing of the vehicle in the field. The full details of the development of gas-generation systems for use in the Corporal vehicle will be discussed in a separate report.

In the course of the development of the hydrazine-monopropellant gas-generation system for use in the Corporal missile, it was found that reliable-mechanical seals between the pressurizing gases, and the propellants could not be developed for practical use. For this reason, it was necessary to bring the pressurizing gases into direct contact with the propellants. Because of the presence of large amounts of ammonia and hydrogen in the hydrazine decomposition gases, an explosion hazard was involved when these gases were used to pressurize tanks containing RFNA.

In order to evaluate the probability of explosion when hydrazine decomposition gases were brought into contact with RFNA, a large number of laboratory-scale tests were made in which mixtures of ammonia and hydrogen at various temperatures were used to pressurize rapidly small heated vessels (up to 165°F) which contained RFNA (Cf. Refs. 19, 20, and 21). The effects of gas temperature, ammonia concentration, and pressurization rates were studied. From these tests it was found that the principal factors which caused explosions were ammonia concentration and the presence of small amounts of organic substances, such as transmitting oil in gages, etc. In the absence of organic materials and with ammonia concentrations of less than 5 mol %, no explosions were encountered in over twenty tests in which RFNA (containing 12 wt %  $\text{NO}_2$ ) at 120°F was rapidly pressurized (about 150 psi/sec) with hydrogen at a temperature of from 600 to 800°F. When the concentration of ammonia in the gases was increased above 5 %, the frequency of explosive reaction increased until, with about 20 mol % ammonia present in the hydrogen, explosions

were obtained in all of the tests made.

As originally developed, the hydrazine-monopropellant gas-generation system used the H-7 catalyst. With this catalyst (Cf. Section VIII-B-2-a), it was not found practicable to dissociate more than about 55 % of the ammonia. As a result, the decomposition gases produced with this catalyst contained about 25 mol % ammonia and could not be used for the pressurization of tanks which contained RFNA.

In an effort to decrease the concentration of ammonia in the hydrazine decomposition gases, a number of different catalysts were prepared and tested (Cf. Section IV). In the course of this investigation, the FM-type catalyst was discovered (Cf. Ref. 13). With this catalyst, using concentrated hydrazine, it was found possible to dissociate up to 75 % of the ammonia. However, since the decomposition gases produced with this catalyst contained over 12 mol % ammonia, it was necessary before pressurization of RFNA tanks could be attempted to reduce the ammonia concentration to about 5 mol % through the addition of hydrazine nitrate to the hydrazine. For this purpose, a mixture consisting of 20 wt %  $\text{HNO}_3$  and 6 wt % water in hydrazine was developed. With this mixture, it was found possible, using the FM catalyst, to produce gases which contained approximately 5 mol % ammonia. The reaction chamber and arrangement of catalyst used to obtain this concentration of ammonia are shown in Figure 8. A residence time of about 10 milliseconds (Cf. Eq. 8) was used to insure complete decomposition of the hydrazine. The residence time in the FM catalyst was about 20 milliseconds. In over fifty tests made with this arrangement of catalysts, gas analyses (Cf. Section VII-B-2) showed that the maximum concentration of ammonia in the decomposition gases was 7 mol %, whereas the average concentration in all of the tests was less than 5.5 mol %.

In order to determine the probability of explosion involved in the pressurization of tanks containing RFNA, a series of tests was made in which a number of small aluminum tanks containing RFNA at 165°F were rapidly pressurized (150 psi/sec) with hydrazine decomposition gases at a temperature of about 800°F. (The decomposition gases from the reaction chamber were cooled in a heat exchanger as shown in Fig. 15). Thirty tests of this type were made without the occurrence of an explosion or the indication of any chemical reaction in the tanks.

Since the ullage and cross-sectional area of the tanks used in these tests was considerably smaller than those which would be encountered in the oxidizer tank of the Corporal vehicle, additional tests were made using 30-inch-diameter spheres which were filled in such a manner that the ullage and the area of the acid surface in contact with the gases were equal to those in the tanks of the flight vehicle. In these tests, the tanks were rapidly pressurized with hydrazine decomposition gases. In the course of these tests, several explosions occurred which were subsequently attributed to the presence of aniline, from the manufacturing process, in the hydrazine. No aniline was present when the small-scale pressurizing tests were made.

Because of the hazards involved in the pressurization of the oxidizer tank of the Corporal vehicle with hydrazine decomposition gases, the use of the monopropellant for this purpose was abandoned. At the

present time, the hydrazine-monopropellant gas-generation system is being considered for possible use in the pressurization of the fuel tank of the Corporal flight vehicle. A second gas-generation system, using an oxidizer-rich RFNA-hydrazine gas generator, is being studied for possible use in the pressurization of the oxidizer tank of the flight vehicle.

#### X. CONCLUSIONS

In the course of this investigation, over 2,000 successful tests of monopropellant-hydrazine reaction chambers have been made. These tests were carried out using hydrazine or mixtures of hydrazine, hydrazine nitrate, and water in reaction chambers having diameters of 1, 2, 3 1/2, 4 7/8, and 6 inches. Chamber pressures from 100 to 800 psia and hydrazine feed rates from 0.004 to 0.11 lb/in.<sup>2</sup> sec were used. Based on these tests, it has been concluded that, using the operating procedures and design relationships outlined in this report, hydrazine may be made to perform reliably and efficiently over a very wide range of conditions. Further, with the two catalysts developed in this and an earlier study (Cf. Ref. 12), it should be possible to achieve optimum or near-optimum performance of the monopropellant in all applications for which it is thermochemically suited.

The primary limitation to the general use of concentrated hydrazine is its high freezing point (34°F). For most applications, this limitation may be circumvented by mechanical means (heated or insulated tanks in small units) or through the use of additives such as hydrazine nitrate and/or water which lower the freezing point. With presently developed catalysts, the fractional dissociation of ammonia obtained with these mixtures is equivalent to that obtained with concentrated hydrazine, provided the ratio of the weight fraction of hydrazine nitrate to that of the water is greater than about 1.7. The use of mixtures in which this ratio is less than 1.7 is not recommended because of the unstable operation which has been obtained with such mixtures. Since there is a limit to the amount of water which can be added to mixtures of hydrazine and hydrazine nitrate, there is also a lower limit to the temperature of the decomposition gases which can be produced by mixtures that freeze at or below a specified point. However, it is possible with presently developed catalysts to use mixtures which freeze at -40°F or below and still obtain exhaust temperatures of about 1700°F; e.g., a mixture consisting of 74 wt % N<sub>2</sub>H<sub>4</sub>, 16 wt % HNO<sub>3</sub>, and 10 wt % water (Cf. Table IV), which freezes at about -40°F, may be decomposed over the H-A-3 catalyst to give gases at about 1700°F. Therefore, it is possible from the standpoint of performance to use low-freezing mixtures of hydrazine, hydrazine nitrate, and water in nearly all of the applications for which concentrated hydrazine is suited. The chief disadvantages of the mixtures relative to concentrated hydrazine are their greater thermal sensitivity and the greater care which must be exercised in their storage and handling. However, with suitable operating procedures and reasonable safety precautions, no major difficulties should be encountered in the use of these mixtures.

Based on the observed extent of the ammonia dissociation obtained when hydrazine was decomposed without the use of a catalyst, it has been concluded that the initial decomposition of hydrazine in adiabatic flow

systems is best represented by the following equation:



At the present time it is not possible to establish definitely the rate-controlling mechanisms involved in the primary decomposition of hydrazine. However, because of the influence of the degree of atomization of hydrazine on the depth of penetration of liquid hydrazine into the bed, it would appear that the rates of evaporation and heat transfer are extremely important in controlling the over-all rate of the decomposition reaction. The fact that water when present in excess of 5 wt % materially increases the depth of bed required to decompose the hydrazine completely may also be related to evaporation and heat-transfer phenomena. The presence of water in the hydrazine has two effects: (1) It decreases the reaction temperature; hence the temperature at the surface of the catalyst particles is lowered, thereby reducing the amount of heat which can be transferred to the liquid stream in a given volume of catalyst. (2) It increases the heat required to evaporate the feed. These two effects might easily explain the adverse influence of water on the operation of hydrazine-monopropellant reaction chambers. The influence of nitric acid in the hydrazine may likewise be explained in terms of heat-transfer and evaporation rates. The presence of nitric acid raises the temperature of the catalyst surface, thereby increasing the rates of heat transfer. As a result the depth of bed required for decomposition of the hydrazine is reduced.

TABLE I  
NOMENCLATURE

- A = Feed-composition factor, defined by Eq. (17).
- a = Moles of hydrazine in mixture with b moles of  $\text{HNO}_3$  and c moles of water.
- $a_v$  = Geometric surface area of catalyst particles in a unit volume of catalyst bed ( $\text{in.}^2/\text{in.}^3$ ).
- B = Feed-composition factor, defined by Eq. (18).
- b = Moles of nitric acid in mixture with a moles of hydrazine and c moles of water.
- $C^*$  = Characteristic velocity (ft/sec).
- $C_x$  = Value of integral in Eq. (32) for the interval 0.40 to X.
- c = Moles of water in mixture with a moles of hydrazine and b moles of water.
- D = Diameter (in.).
- $D_c$  = Diameter of reaction chamber (in.).
- $D_m$  = Throat diameter of main discharge nozzle b in Fig. 16 (in.).
- $D_p$  = Nominal particle diameter (spheres or cylinders) (in.).
- $D_s$  = Throat diameter of sample nozzle a in Fig. 16 (in.).
- d = Exponent in Eq. (28), constant for a particular catalyst.
- $E_a$  = Apparent energy of activation involved in the catalytic dissociation of ammonia (kcal/mol).
- e = Exponent in Eq. (28), constant for a particular catalyst.
- $e_N$  = Base of natural logarithms.
- $F_v$  = Porosity of catalyst beds.
- f = Exponent or friction factor.
- $f_d$  = Modified friction factor defined by Eq. (43).
- G = Mass-flow rate of hydrazine per unit area of cross-sectional area of reaction chamber ( $\text{lb}/\text{in.}^2 \text{ sec}$ ).
- g = Pressure exponent = d - e = constant for a particular catalyst.
- $g_c$  = Gravitational constant = 32.2 ft/sec.
- $H_p$  = Enthalpy of products of the reaction represented by Eq. (9) at  $T_B$  (Btu/mol).
- $H_v$  = Enthalpy of hydrazine vapor at  $T_B$  (Btu/lb mol).
- $I_{sp}$  = Specific impulse,  $P_c/P_e = 20.4$  (sec).
- K = Experimentally determined constant in Eq. (50).
- $K_o$  = Discharge coefficient of gas-metering orifice in gas-analysis system (g in Fig. 16).
- $K_T$  = Proportionality constant in Eq. (28).
- L = Depth of catalyst (in.).
- $L_A$  = Depth of zone A (in.).
- $L_B$  = Depth of zone B (in.).
- $L_c$  = Total depth of catalyst (in.).



TABLE I (Cont'd)

- $L_0$  = Depth of catalyst required for complete decomposition of hydrazine (in.).  
 $L_w$  = Depth of penetration of liquid hydrazine into the catalyst bed (in.).  
 $L'_w$  = Apparent depth of penetration of liquid hydrazine into the bed (in.).  
 $L_X$  = Depth of catalyst required to dissociate a fraction X of the ammonia (in.).  
 $M_g$  = Average molecular weight of decomposition gases (lb/mol).  
 $M_o$  = Average molecular weight of gases leaving gas-analysis system (lb/mol).  
 $N_{Re}$  = Reynolds number =  $\frac{DG}{\mu}$   
 $N_{Red}$  = Modified Reynolds number =  $\frac{G}{\mu_{av}}$   
 $N = n_a/(1 - n_a)$ .  
 $n_a$  = Mol fraction of ammonia in decomposition gases.  
 $n_H$  = Mol fraction of hydrogen in decomposition gases.  
 $n_N$  = Mol fraction of nitrogen in decomposition gases.  
 $n_w$  = Mol fraction of water in decomposition gases.  
 $P_c$  = Chamber pressure at exit of catalyst bed (psia).  
 $\bar{P}_c$  = Average pressure in catalyst bed =  $P_c + 1/2 \Delta P_c$  (psia).  
 $P_e$  = Exhaust pressure (psia).  
 $P_o$  = Pressure upstream from gas-metering orifice in gas-analysis system (psia).  
 $P_{H_2}$  = Partial pressure of hydrogen (psia).  
 $P_{NH_3}$  = Partial pressure of ammonia (psia)  
 $R$  = Perfect gas constant =  $10.73 \frac{\text{psi cu ft}}{\text{mol } ^\circ R} = 2.025 \times 10^4 \frac{\text{psi cu in.}}{\text{mol } ^\circ R}$   
 $r_A$  = Rate of decomposition of hydrazine in zone A (mol/lb sec).  
 $r_B$  = Rate of decomposition of hydrazine in zone B (mol/lb sec).  
 $r_C$  = Rate of dissociation of ammonia (mol/lb sec).  
 $r_h$  = Hydraulic radius (in.).  
 $S$  = Gas-analysis system factor, defined by Eq. (19).  
 $T$  = Temperature ( $^\circ K$ ).  
 $T_B$  = Boiling point of hydrazine at  $\bar{P}_c$  ( $^\circ R$ ).  
 $T_C$  = Adiabatic reaction temperature ( $^\circ R$  or  $^\circ F$ , as indicated).  
 $T_e$  = Exhaust temperature ( $^\circ R$  or  $^\circ F$ , as indicated).  
 $V_c$  = Volume of catalyst bed in reaction chamber (cu in.).  
 $X$  = Fraction of ammonia dissociated.  
 $X_o$  = Fraction of ammonia dissociated at  $L_o$ .  
 $Y$  = Weight fraction of hydrazine in feed to reaction chamber.

TABLE I (Cont'd)

$Y_A$  = Fraction of hydrazine which must be decomposed in order to release heat required to evaporate  $1 - Y_A$  moles of hydrazine at  $T_B$ .

$Y_B$  = Equilibrium fraction of hydrazine decomposed under adiabatic conditions.

$y$  = Fraction of hydrazine decomposed.

$Z$  = Weight fraction of nitric acid in feed to reaction chamber.

$\alpha$  = Constant.

$\beta$  = Constant.

$\Delta H_{T_e}^{T_c}$  = Change in enthalpy involved in cooling decomposition gases from  $T_c$  to  $T_e$  (Btu lb).

$\Delta L_X = L_X - L_0$  (in.).

$\Delta P_c$  = Pressure drop across catalyst bed (psi).

$\Delta P_o$  = Pressure drop across gas-metering orifice in gas-analysis system (psi).

$\Delta P_i$  = Pressure drop across injector (psi).

$\theta_c$  = Residence time, defined by Eq. (8)(sec).

$\theta_e$  = Effective residence time, defined by Eq. (40).

$\rho$  = Density of decomposition gases (lb/cu ft).

$\rho_c$  = Density of catalyst particles (lb/cu in.).

$\dot{w}$  = Hydrazine feed rate (lb/sec).

$\dot{w}_o$  = Flow rate of gases leaving gas-analysis system (lb/sec).

$\dot{w}_g$  = Flow rate of decomposition gases entering gas-analysis system (lb/sec).

TABLE II  
CALCULATED PERFORMANCE AS A MONOPROPELLANT OF CONCENTRATED HYDRAZINE

LOX (% NH <sub>3</sub> dissoc- iated)	H <sub>2</sub> O (wt %)	Gas Composition (mol %)				M <sub>g</sub> (lb/mol)	ΔH <sub>R</sub> (Btu/lb)	T <sub>c</sub> (°K)	C* (ft/sec)	I <sub>sp</sub> (sec)	Change in Enthalpy Between T <sub>c</sub> and T <sub>g</sub> ΔH <sub>T,c</sub> (Btu/lb)													
		NH <sub>3</sub>	H <sub>2</sub>	H <sub>2</sub> O	H <sub>2</sub> O						1600°K 1500°K	2240°K 1500°K	2060°K 1400°K	1880°K 1300°K	1200°K 1100°K	1240°K 1000°K	1160°K 900°K	900°K 700°K	800°K 600°K	620°K 400°K	260°K 80°K			
0.0	0.0	80.00	20.00	0.00	0.00	19.23	1500	1645	4300	191.0	67	202	335	464	599	711	828	940	1047	1149	1246	1336	1421	1500
	5.0	75.74	18.94	0.00	5.32	19.17	1410	1559	4200	184.8														
	10.0	71.52	17.87	0.00	10.61	19.11	1320	1468	4100	178.5														
20.0	0.0	55.20	24.10	20.70	0.00	16.58	1335	1500	4375	191.5	-	0	132	262	388	510	629	744	854	960	1061	1145	1249	1335
	5.0	52.64	22.99	19.75	4.62	16.65	1254	1412	4238	185.3														
	10.0	50.09	21.86	18.77	9.28	16.71	1172	1322	4092	178.9														
40.0	0.0	36.36	27.28	36.36	0.00	14.59	1171	1348	4366	189.5	-	-	-	59	186	310	431	548	661	771	877	979	1077	1171
	5.0	34.83	26.14	34.83	4.20	14.73	1097	1272	4190	182.3														
	10.0	33.35	25.05	33.35	8.25	14.87	1024	1196	4026	175.2														
60.0	0.0	21.62	29.72	48.66	0.00	13.00	1006	1127	4292	185.2	-	-	-	-	-	110	232	352	468	582	692	800	904	1006
	5.0	20.82	28.63	46.89	3.66	13.18	942	1110	4111	177.1														
	10.0	20.01	27.52	45.85	7.42	13.37	876	1030	3921	169.0														
80.0	0.0	9.75	31.70	58.55	0.00	11.71	841	1026	4180	177.5	-	-	-	-	-	-	34	156	275	392	508	621	732	841
	5.0	9.43	30.65	56.61	3.31	11.92	785	948	3980	170.4														
	10.0	9.09	29.56	54.60	6.75	12.14	724	884	3765	162.7														
100.0	0.0	0.00	33.33	66.67	0.00	10.69	677	867	3950	169.0	-	-	-	-	-	-	-	-	82	203	323	442	560	677
	5.0	0.00	32.31	64.67	3.02	10.91	629	804	3768	163.0														
	10.0	0.00	31.28	62.54	6.18	11.14	579	738	3570	156.5														

TABLE III  
CALCULATED PERFORMANCE AS A MICROPELLANT OF A MIXTURE CONSISTING OF 74 WT %  $H_2$ , 20 WT %  $HNO_3$ , AND 6 WT %  $H_2O$ <sup>a</sup>

LOX (% $H_2$ dissolved)	Gas Composition (mol %)				$H_2$ (lb/mol)	$\Delta H_R$ (Btu/lb)	$T_c$ (°K)	$C^*$ (ft/sec)	$I_{sp}$ (sec)	Change in Enthalpy Between $T_c$ and $T_0$ $\Delta H_{T_c}^0$ (Btu/lb)														
	$H_2$	$H_2$	$H_2O$	$H_2O$						2600°K	2400°K	2200°K	2000°K	1800°K	1600°K	1400°K	1200°K	1000°K	800°K	600°K	400°K	260°K	80°K	
0	50.72	23.72	0	25.56	19.89	1503	1790°K	4400	193.5	112.1	231.6	349.7	464.9	577.6	687.0	793.2	896.2	995.4	1090.8	1181.6	1268.4	1350.9	1429.2	1503.3
20	36.84	26.14	13.81	23.21	18.06	1402	1691	4450	195.0	-	107.6	225.3	340.7	453.6	563.5	670.5	774.5	875.3	972.3	1065.6	1155.2	1241.4	1323.7	1402.3
40	25.30	28.15	25.30	21.25	16.54	1302	1585	4474	194.4	-	-	101.1	216.6	329.7	440.1	548.9	653.0	755.1	854.1	949.5	1042.2	1131.6	1217.8	1301.4
60	15.55	29.85	35.00	19.60	15.25	1201	1480	4435	192.6	-	-	-	92.3	205.7	316.6	425.3	531.1	634.6	735.6	833.5	929.1	1021.6	1112.4	1200.4
80	7.22	31.31	43.29	18.18	14.15	1099	1367	4408	190.0	-	-	-	81.7	193.8	302.4	409.6	514.9	617.4	717.8	816.1	911.0	1006.5	1099.4	-
100	0.0	32.56	50.48	16.96	13.20	998.3	1262	4344	186.6	-	-	-	-	-	79.6	179.6	288.3	394.7	499.4	601.7	702.9	802.4	900.9	998.4

<sup>a</sup>Freezing point of the mixture was -38°K.

TABLE IV  
CALCULATED PERFORMANCE AS A MONOPROPELLANT OF A MIXTURE CONSISTING OF 70 WT %  $H_2H_4$ , 20 WT %  $HNO_3$ , AND 10 WT %  $H_2O^a$

100X (% $H_2$ , dissociated)	Gas Composition (mol %)				$M_g$ (lb/mol)	$\Delta H_g$ (Btu/lb)	$T_c$ (°K)	$C^*$ (ft/sec)	$I_{sp}$ (sec)	Change in Enthalpy Between $T_c$ and $T_e$ $\Delta H_{T_c}^{T_e}$ (Btu/lb)																	
	$NH_3$	$H_2$	$H_2$	$H_2O$						2600°F	2420°F	2240°F	2000°F	1880°F	1700°F	1520°F	1340°F	1160°F	980°F	800°F	600°F	440°F	260°F				
										1700°K	1600°K	1500°K	1400°K	1300°K	1200°K	1100°K	1000°K	900°K	800°K	700°K	600°K	500°K	400°K	300°K			
0	47.28	22.83	0	29.89	19.84	1398	1712°K	4300	189.5	13.7	132.1	249.4	363.9	475.5	584.3	690.0	792.2	891.7	985.4	1075.9	1162.4	1244.7	1322.8	1398			
20	34.55	25.18	12.96	27.31	18.12	1302	1616	4336	189.3	-	16.3	133.2	247.8	359.7	468.9	575.3	678.4	778.4	874.8	967.5	1056.8	1142.2	1224.1	1302			
40	23.86	27.15	23.85	25.14	16.68	1208	1515	4340	188.2	-	-	17.0	131.7	243.8	353.4	460.6	564.8	666.1	764.0	859.1	951.0	1039.7	1125.3	1208			
60	14.73	28.84	33.15	23.23	15.45	1114	1414	4320	186.9	-	-	-	15.6	127.9	238.1	347.9	451.1	553.8	653.6	750.7	845.3	937.2	1026.6	1114			
80	6.86	30.29	41.16	21.69	14.39	1020	1311	4272	184.2	-	-	-	-	12.1	122.7	231.2	337.4	441.4	543.0	642.3	739.5	834.6	927.9	1020			
100	0	31.54	48.16	20.30	13.47	926	1208	4205	180.5	-	-	-	-	-	-	7.3	116.5	223.7	329.1	432.4	533.9	633.8	732.1	829.1	926		

<sup>a</sup> Freezing point of the mixture was -60°F.

TABLE V  
CALCULATED PERFORMANCE AS A MONOPROPELLANT OF A MIXTURE CONSISTING OF 74 WT %  $H_2$ , 16 WT %  $NO_2$ , AND 10 WT %  $H_2O^a$

100X (% $H_2$ dissoc- iated)	Gas Composition (mol %)				$\bar{M}_g$ (lb/mol)	$\Delta H_g$ (Btu/lb)	$T_c$ (°K)	$C^*$ (ft/sec)	$I_{sp}$ (sec)	Change in Enthalpy Between $T_c$ and $T_e \Delta H_{T_c}^{T_e}$ (Btu/lb)																	
	$H_2$	$H_2O$	$H_2$	$H_2O$						2420° K	2240° K	1600° K	1500° K	1400° K	1300° K	1200° K	1100° K	1000° K	900° K	800° K	700° K	600° K	500° K	400° K	300° K		
0	52.27	21.82	0	25.91	19.69	1360	1653	4150	186.1	64.5	135.0	302.7	417.4	529.1	637.5	742.4	843.5	940.4	1033.0	1121.4	1205.2	1284.6	1359.9				
20	37.86	24.49	14.19	23.46	17.82	1255	1546	4265	186.6	-	55.6	173.3	288.3	400.5	509.8	615.8	718.3	817.2	912.2	1003.6	1091.0	1174.6	1254.8				
40	25.94	26.70	25.93	21.43	16.28	1150	1437	4270	186.8	-	-	43.9	159.1	271.9	382.0	489.1	593.1	693.9	791.4	885.7	976.7	1064.5	1149.6				
60	15.92	28.55	35.81	19.72	14.99	1045	1326	4240	184.2	-	-	-	30.1	143.3	254.2	362.4	468.0	570.7	670.6	767.9	862.5	954.5	1044.5				
80	7.37	30.13	44.23	18.27	13.88	939	1213	4178	180.0	-	-	-	-	14.8	126.5	235.8	342.9	447.5	549.9	650.2	748.3	844.5	939.3				
100	0	31.50	51.40	17.01	12.93	834	1098	4095	175.5	-	-	-	-	-	-	109.1	217.7	324.3	429.0	532.3	634.0	734.5	834.1				

<sup>a</sup>Freezing point of the mixture was -38°F.

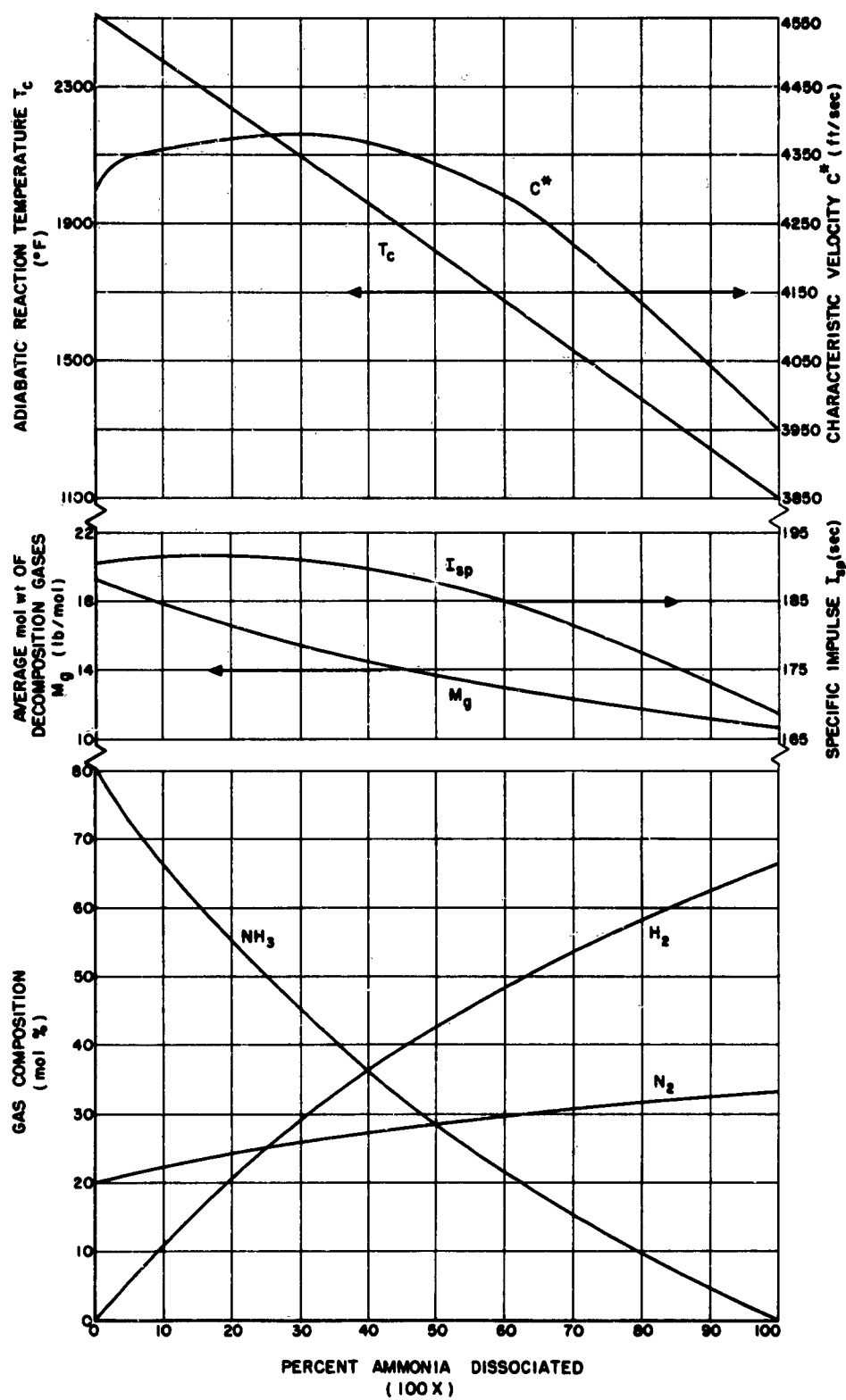


Figure 1. Calculated Performance of Hydrazine

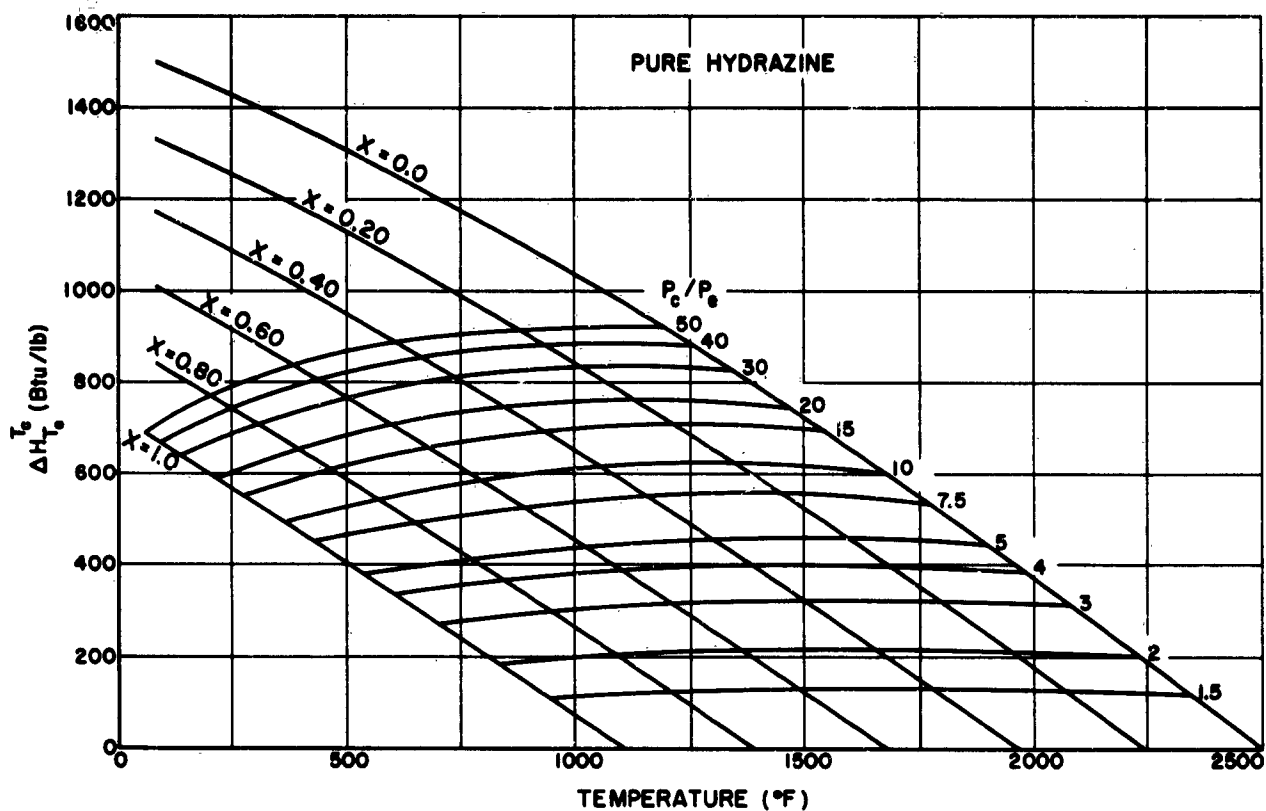


Figure 2. Change in Enthalpy Associated with Cooling of Hydrazine Decomposition Gases

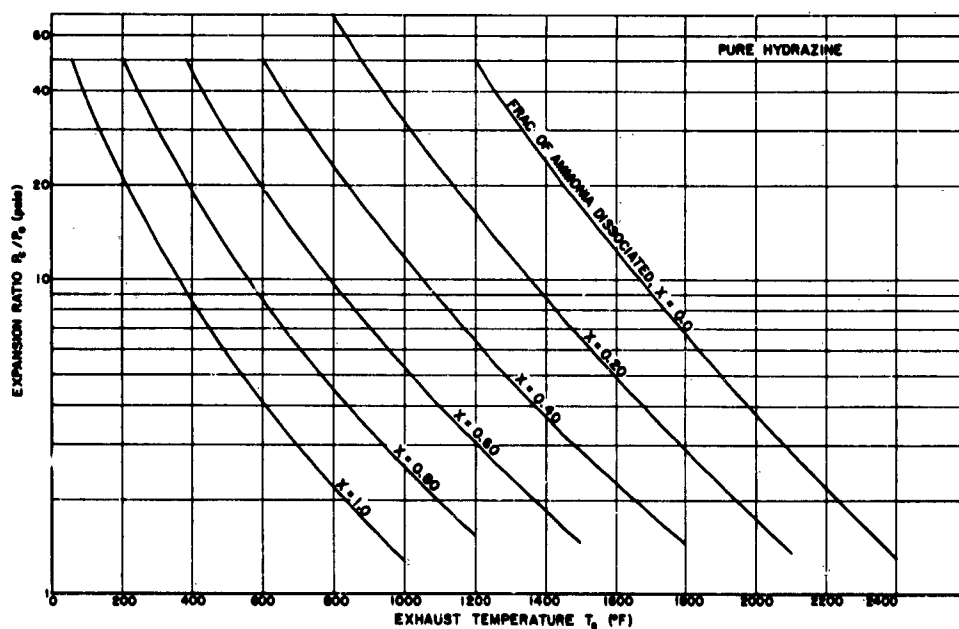


Figure 3. Variation of Exhaust Temperature with Pressure Ratio (Concentrated Hydrazine)



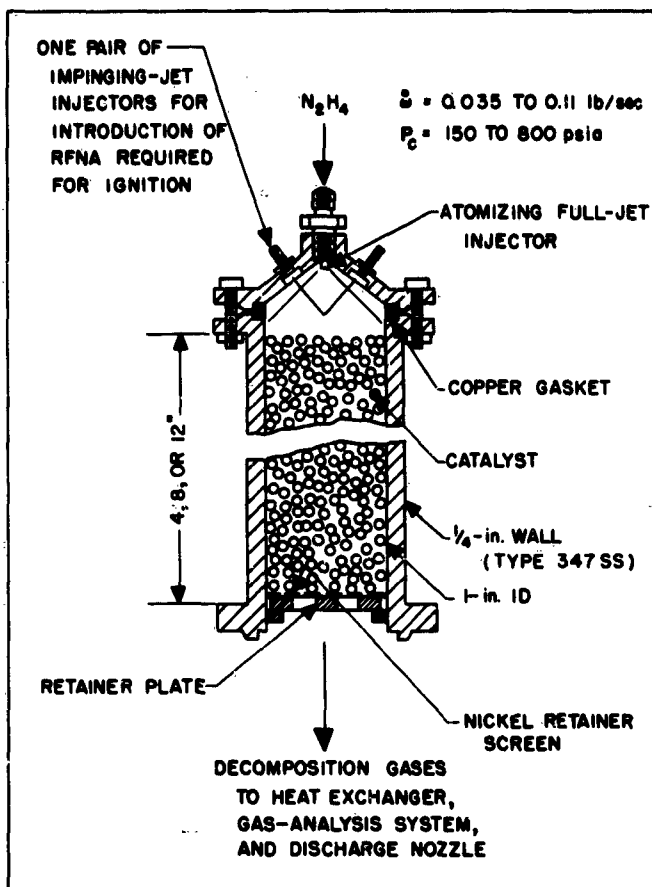


Figure 4. Reaction Chamber of 1-Inch Diameter.

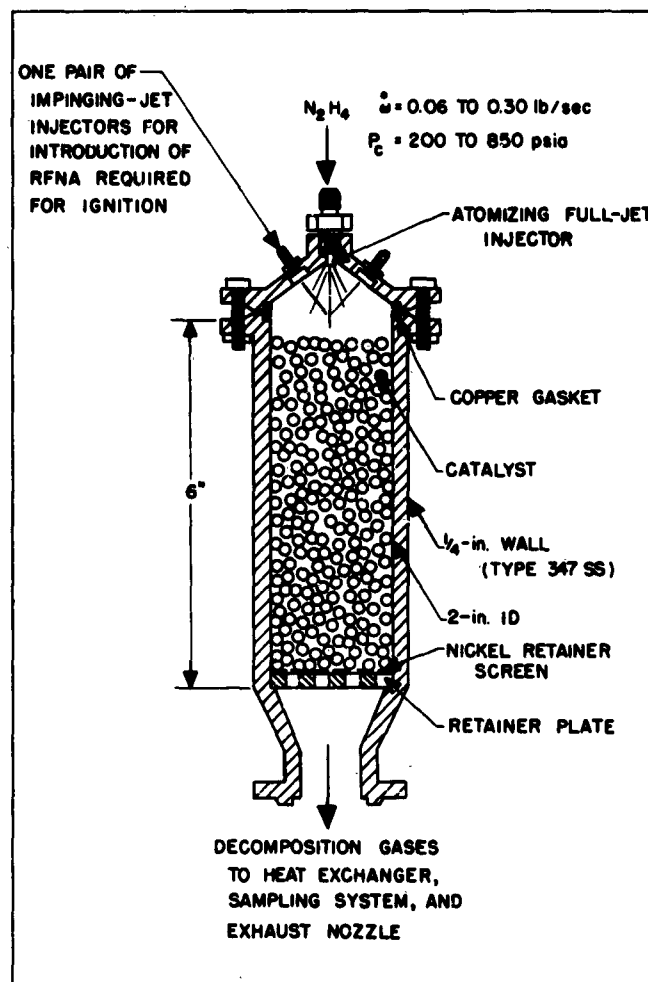


Figure 5. Reaction Chamber of 2-Inch Diameter

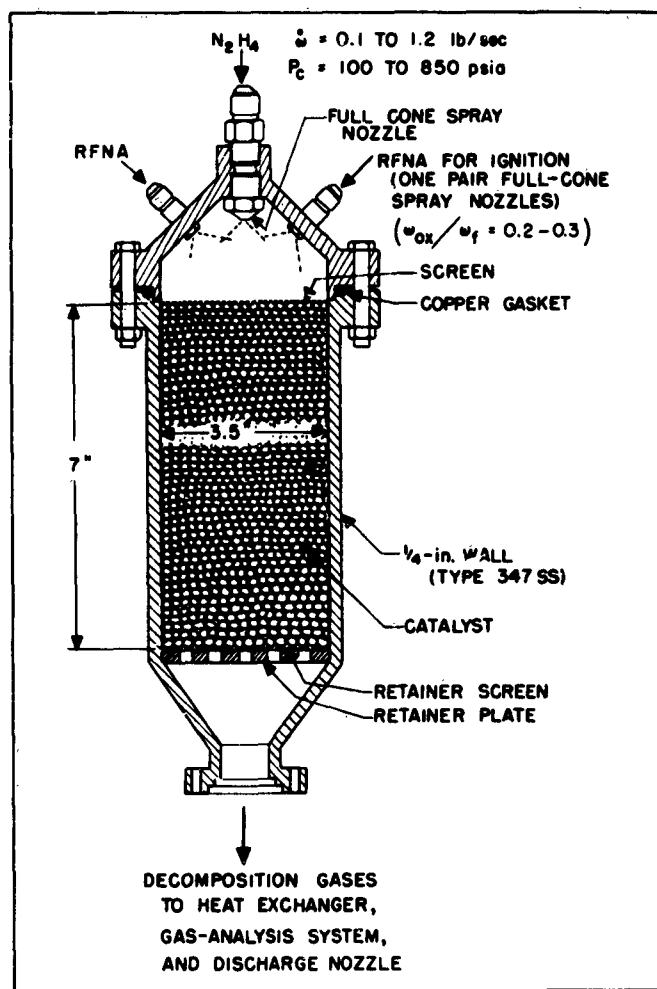


Figure 6. Reaction Chamber of 3 1/2-Inch Diameter

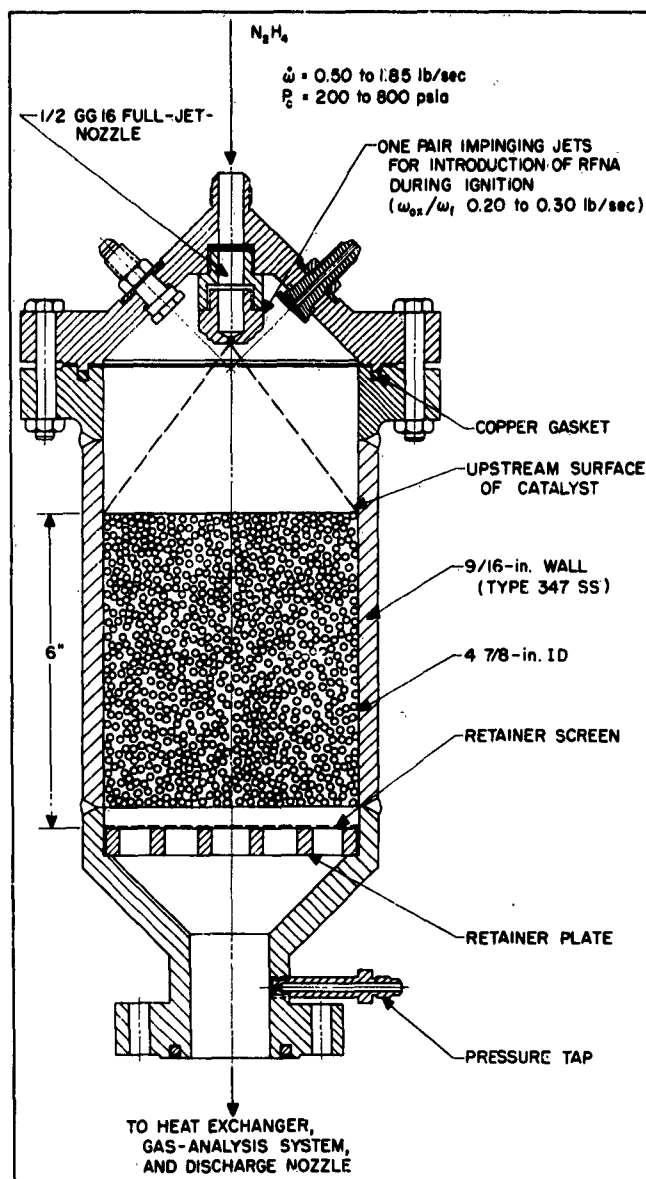


Figure 7. Reaction Chamber of 4 7/8-Inch Diameter

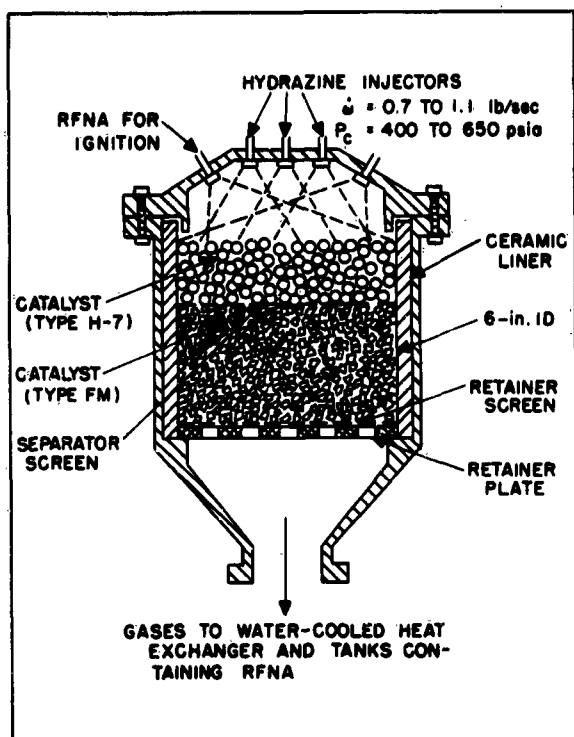


Figure 8. Reaction Chamber of 6-Inch Diameter, Showing Catalyst-Bed Arrangement Used to Generate Gases for Pressurization of Tanks Containing RFNA

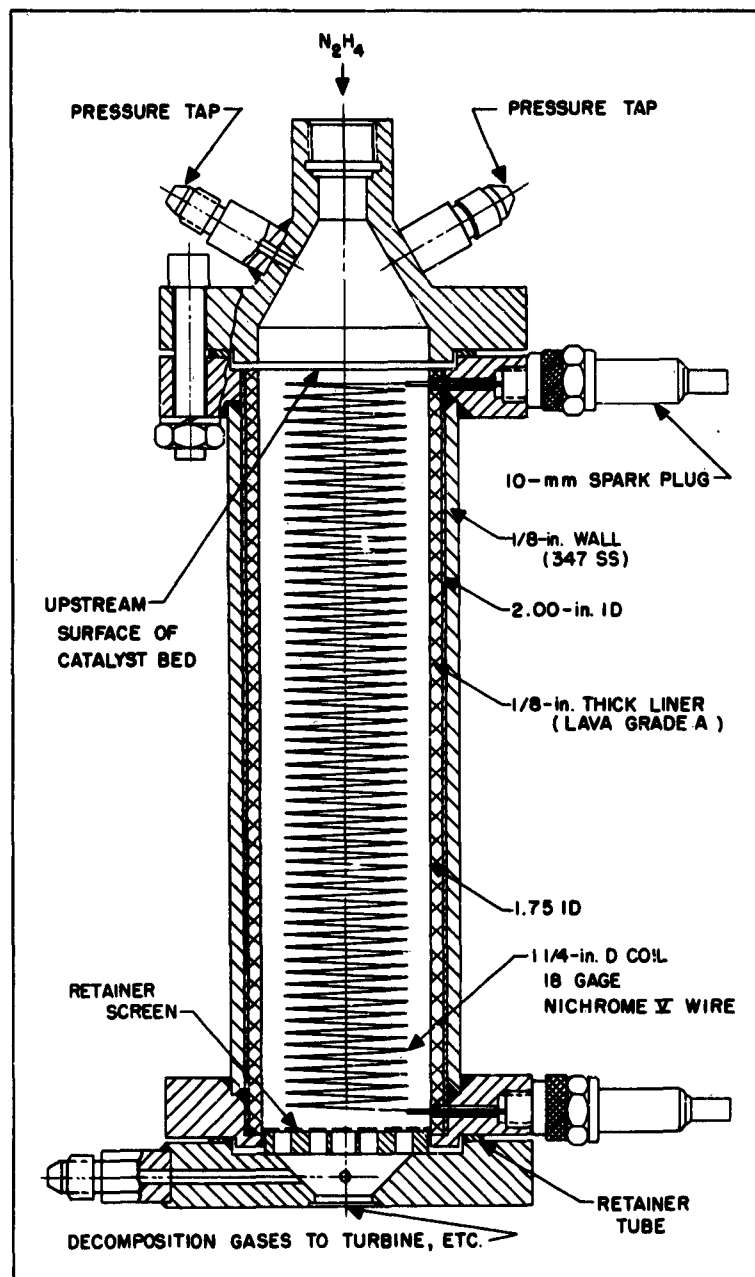


Figure 9. Reaction Chamber with Electrical Ignition System

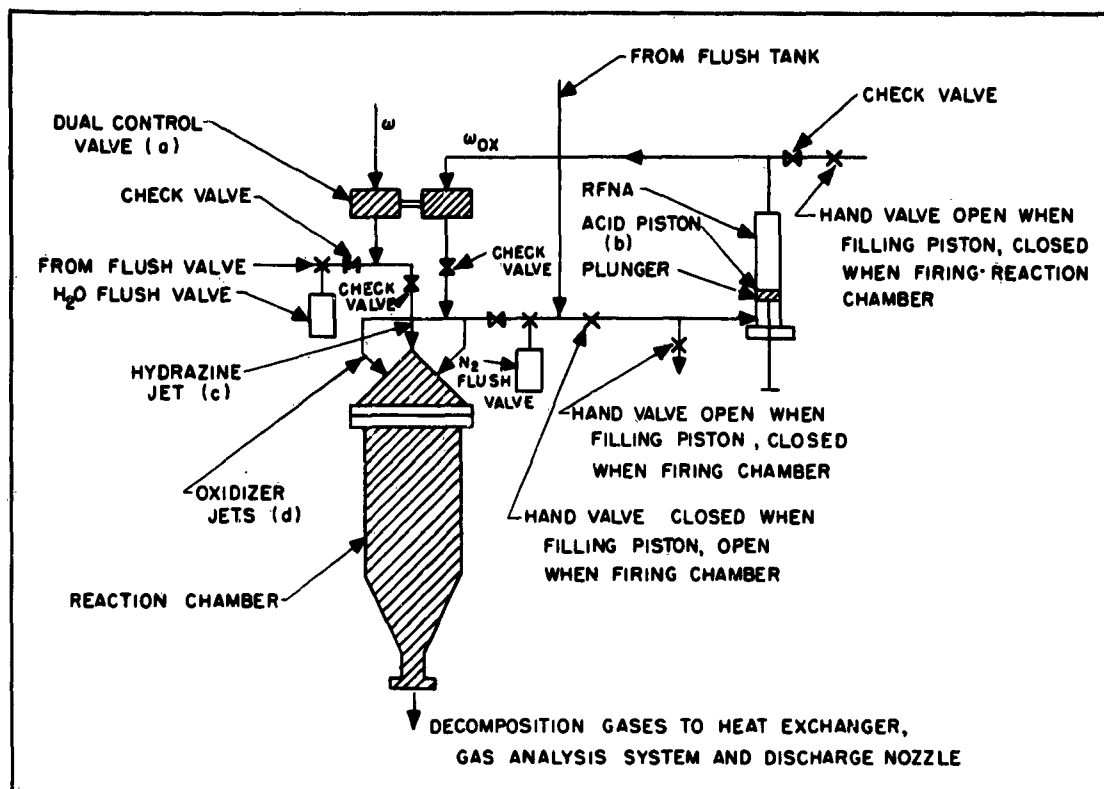


Figure 10. Bipropellant Ignition System

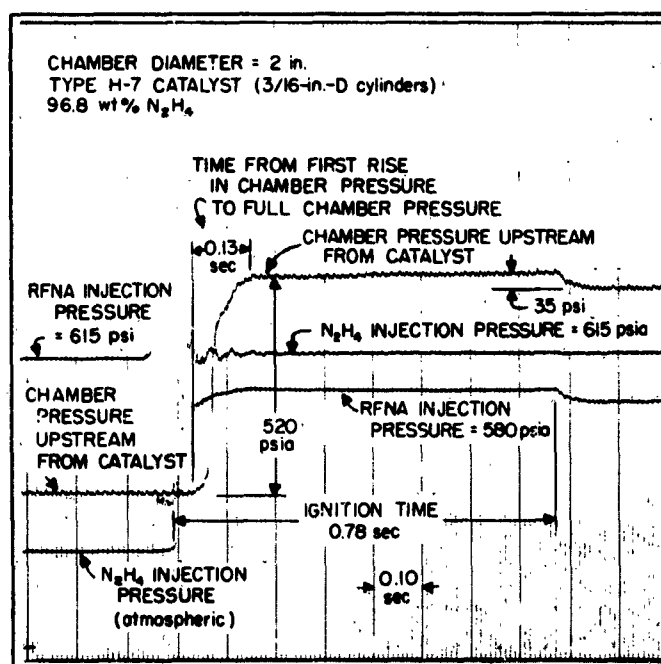


Figure 11. Typical Pressure Record Obtained During Ignition Period Using Bipropellant Starting Technique

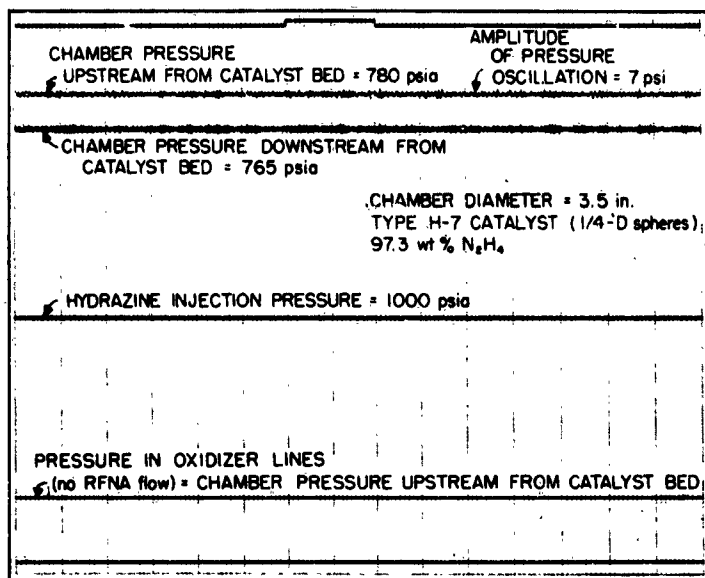


Figure 12. Typical Pressure Record Obtained with Proper Injection and Feed-System Arrangement

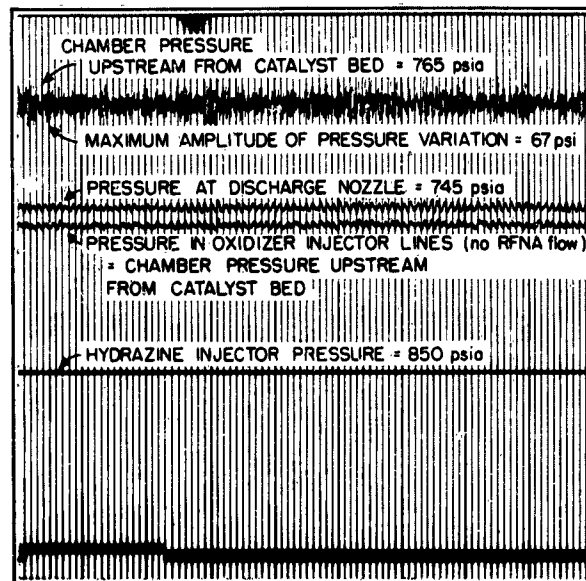


Figure 13. Pressure Instability Caused by Improper Atomization and/or Nonuniform Cross-Sectional Distribution of Injected Hydrazine

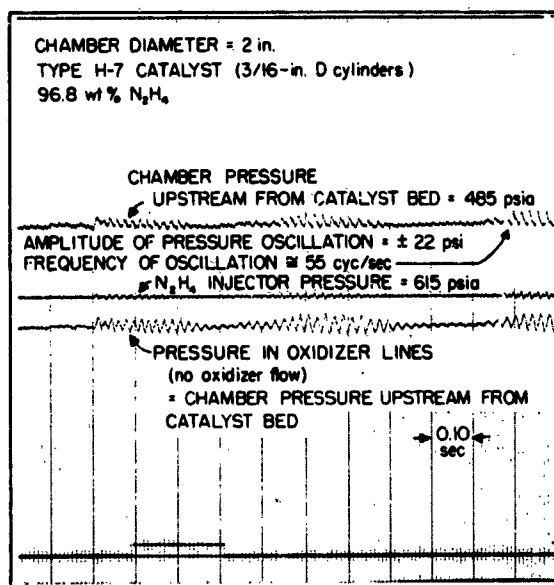


Figure 14. Pressure Instability Caused by Harmonic Coupling Between Reaction Chamber and Hydrazine Feed System

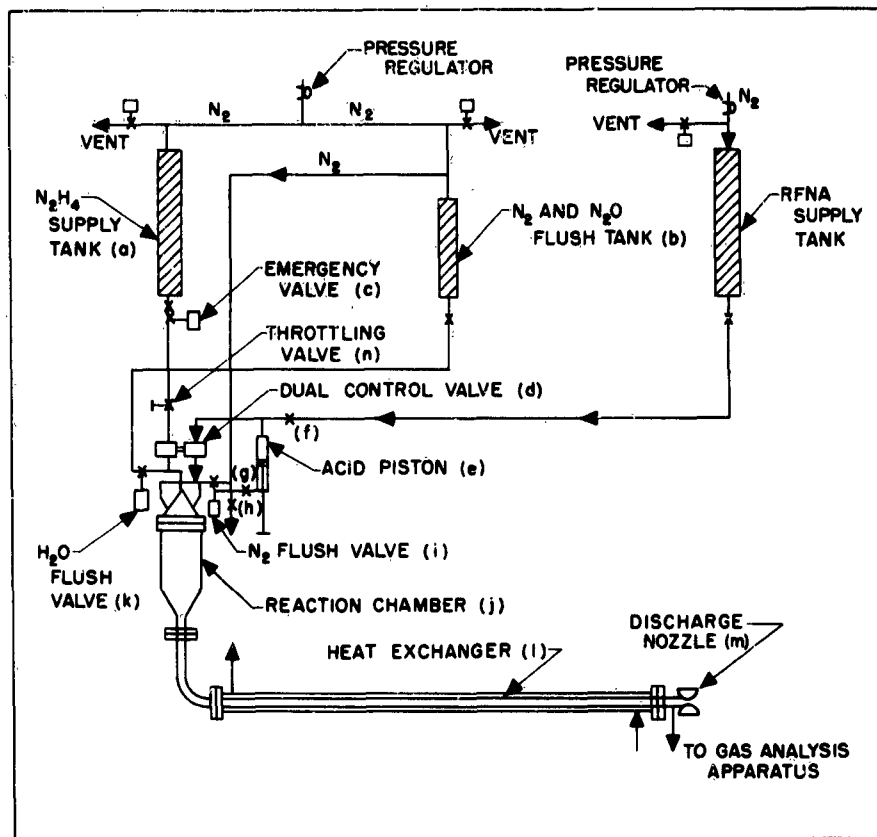


Figure 15. Arrangement of Apparatus Used in Testing of Hydrazine-Monopropellant Reaction Chambers

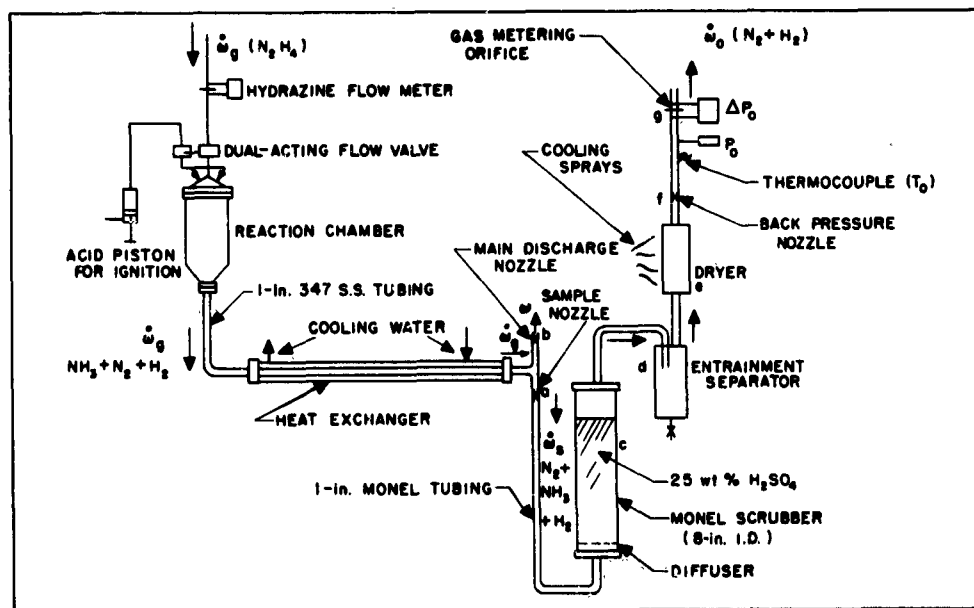


Figure 16. Apparatus Used for Continuous Analysis of Hydrazine Decomposition Gases

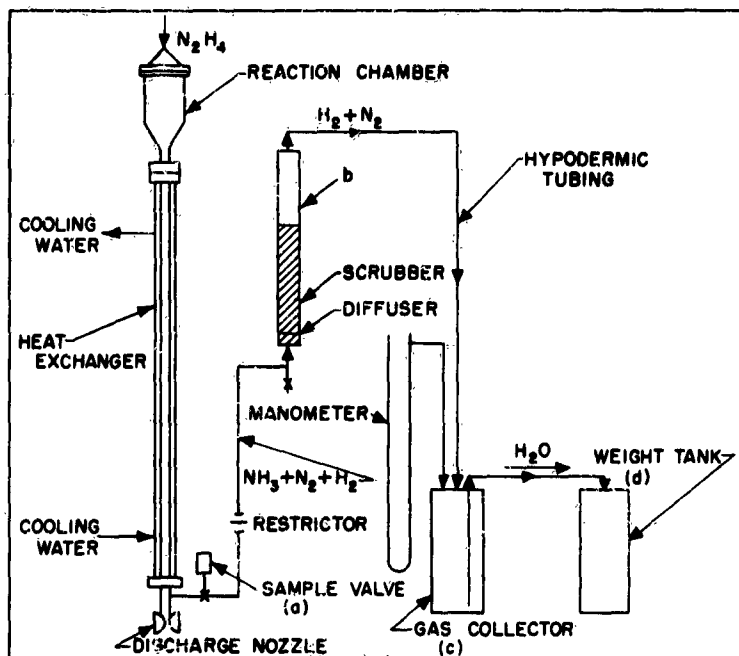
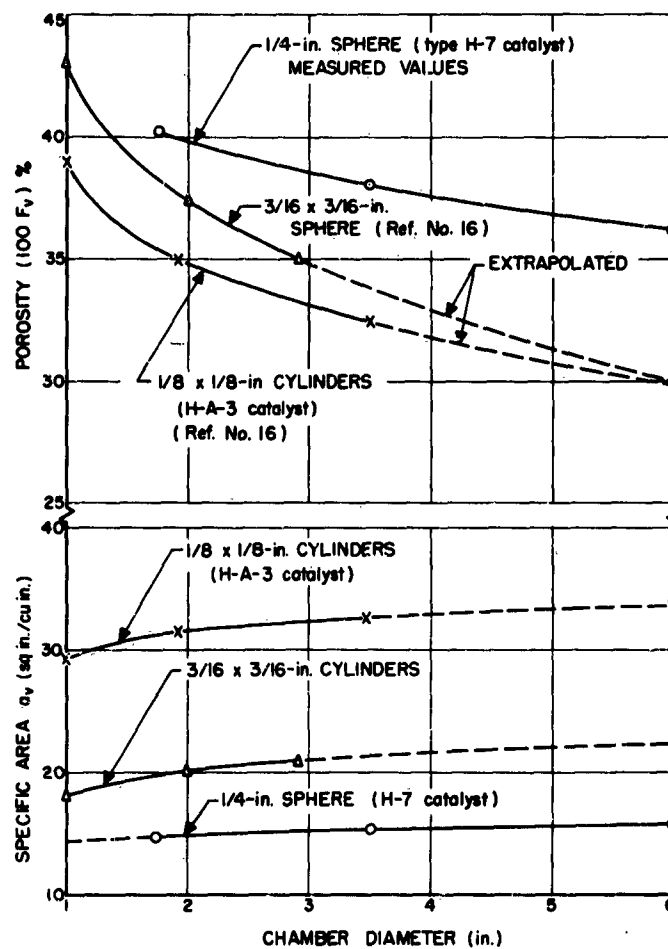


Figure 17  
Apparatus Used for Intermittent Analysis of  
Hydrazine Decomposition Gases

Figure 18  
Variation of Porosity  $F_v$  and Specific Area  $a_v$   
( $\text{in.}^2/\text{in.}^3$ ) with Chamber Diameter



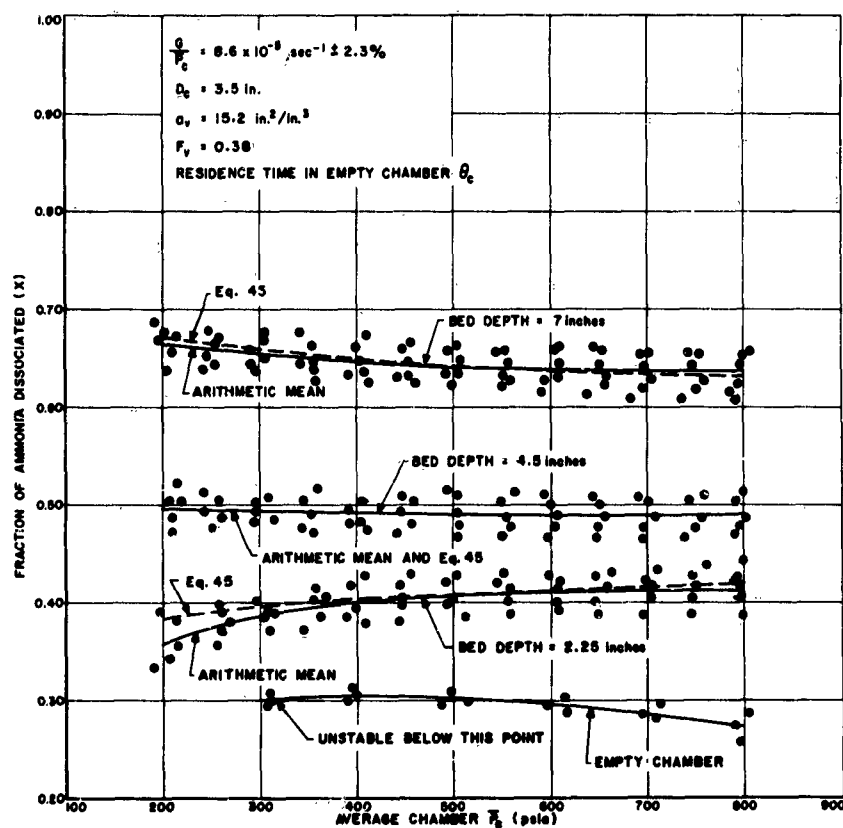


Figure 19. Influence of Chamber Pressure on Dissociation of Ammonia over Type H-7 Catalyst (1/4-In. Spheres)



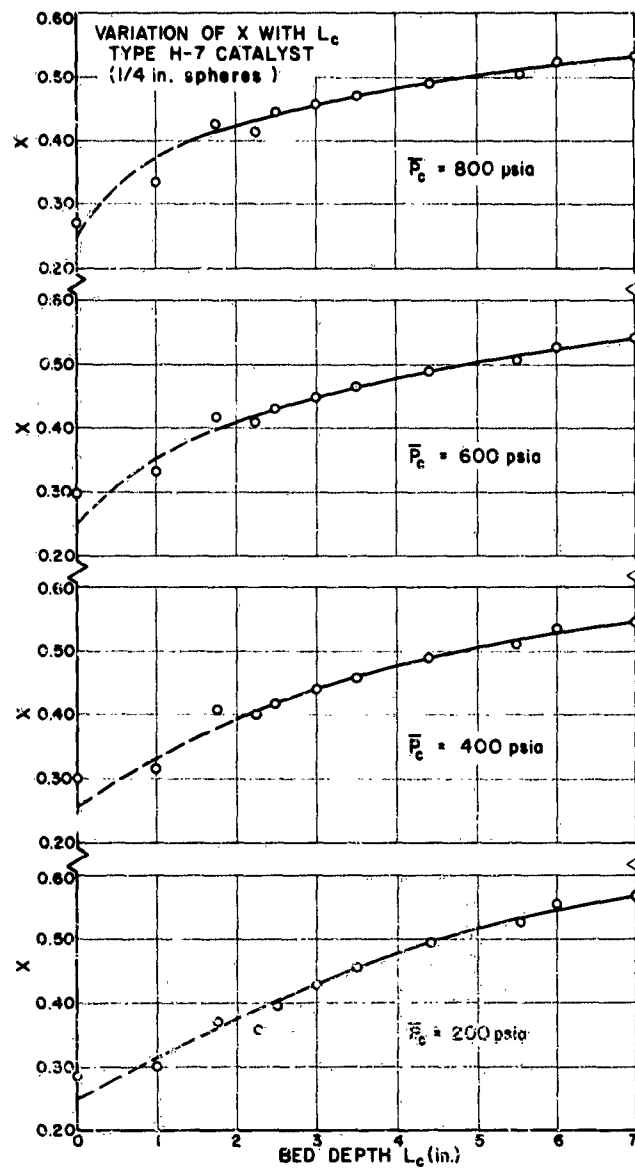


Figure 20. Influence of Bed Depth on the Dissociation of Ammonia over Type H-7 Catalyst

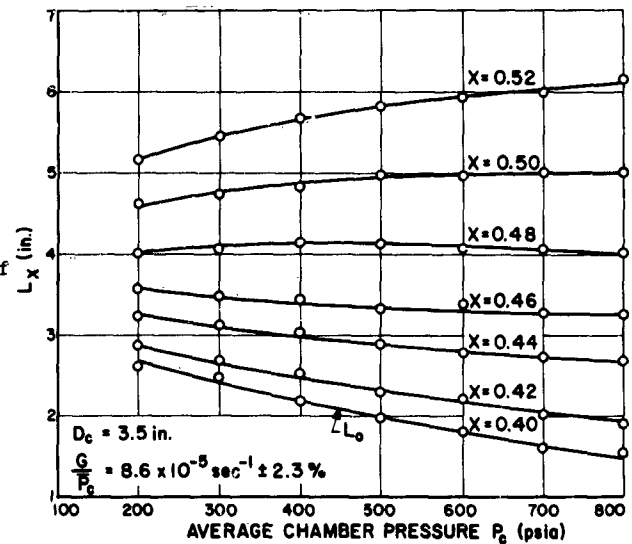


Figure 21. Influence of Chamber Pressure on Depth of Type H-7 Catalyst Required to Dissociate Various Fractions of Ammonia

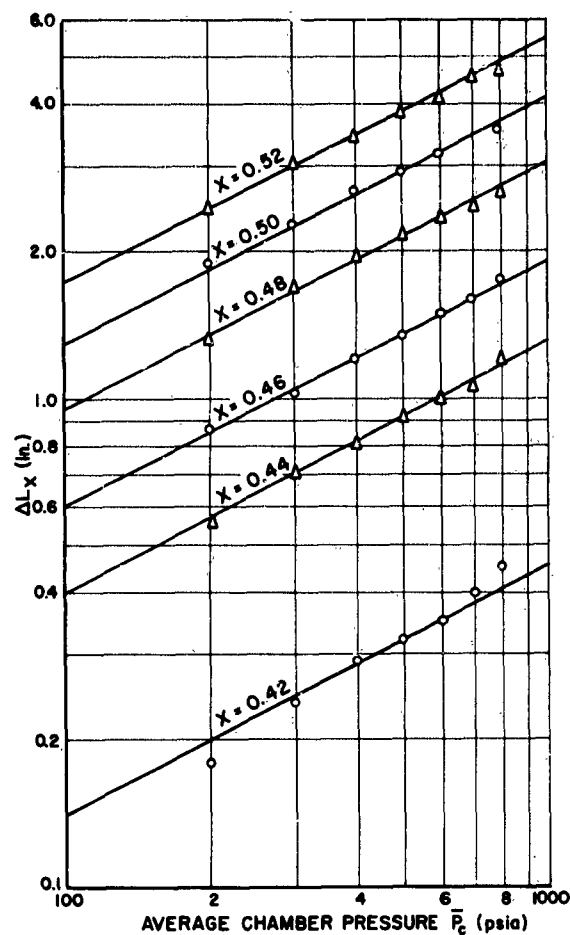


Figure 22. Influence of Chamber Pressure on Incremental Bed Depth  $\Delta L_x$  Required with Type H-7 Catalyst to Dissociate Various Fractions of the Ammonia

$$C_X = \int_{0.40}^X \frac{\beta (5+4)^{d-e} X^e e_n \frac{2.11-X}{(1-X)^d} dX}{(1-X)^d}$$

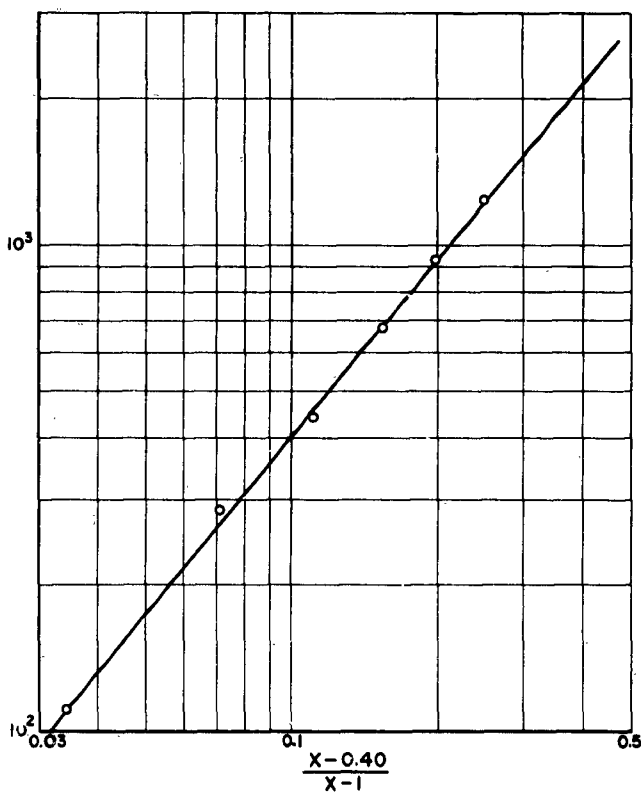


Figure 23. Curves Used in the Determination of Equation (38)

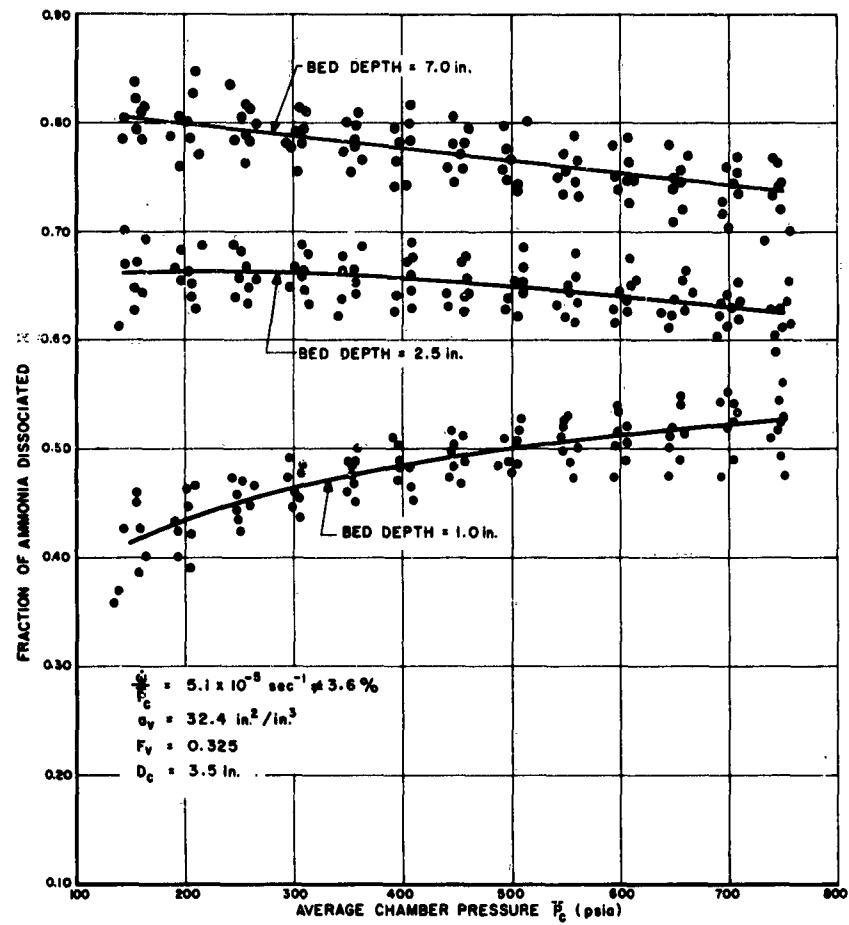


Figure 24. Influence of Chamber Pressure on Dissociation of Ammonia over Type H-A-3 Catalyst (1/8- by 1/8-In. Cylinders)

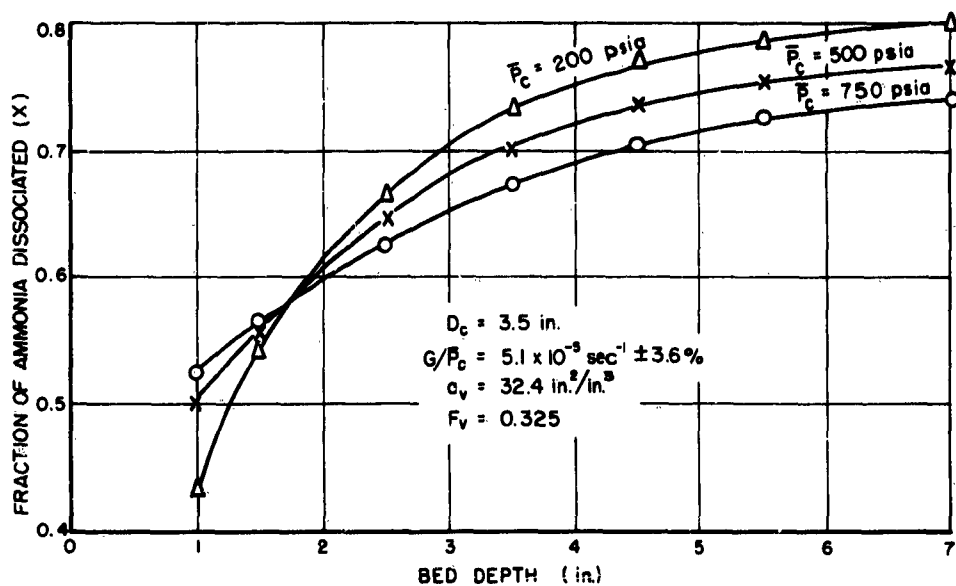
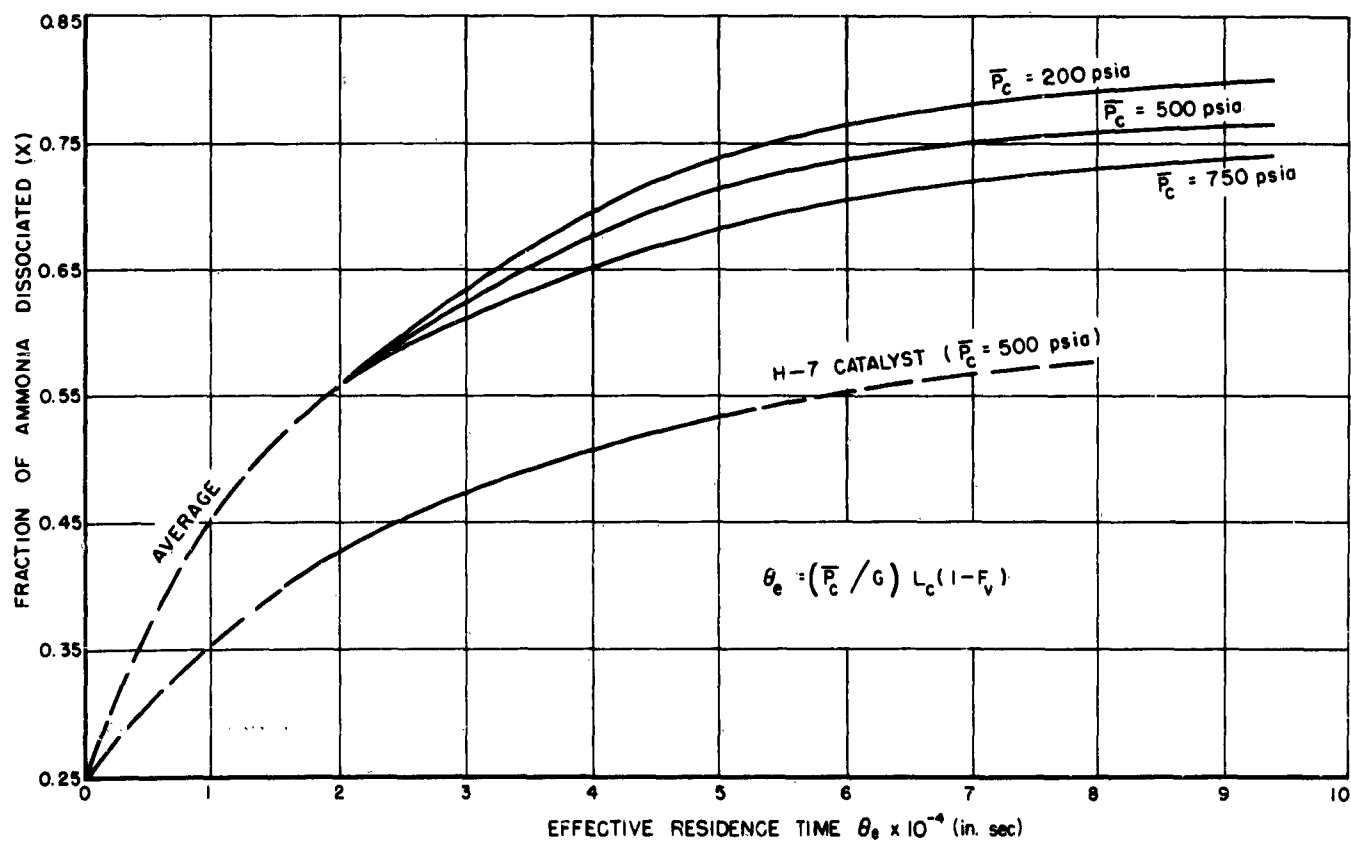


Figure 25. Influence of Bed Depth on Dissociation of Ammonia over Type H-A-3 Catalyst

Figure 26. Influence of Residence Time  $\theta_e$  on the Extent of Ammonia Dissociation over Type H-A-3 Catalyst

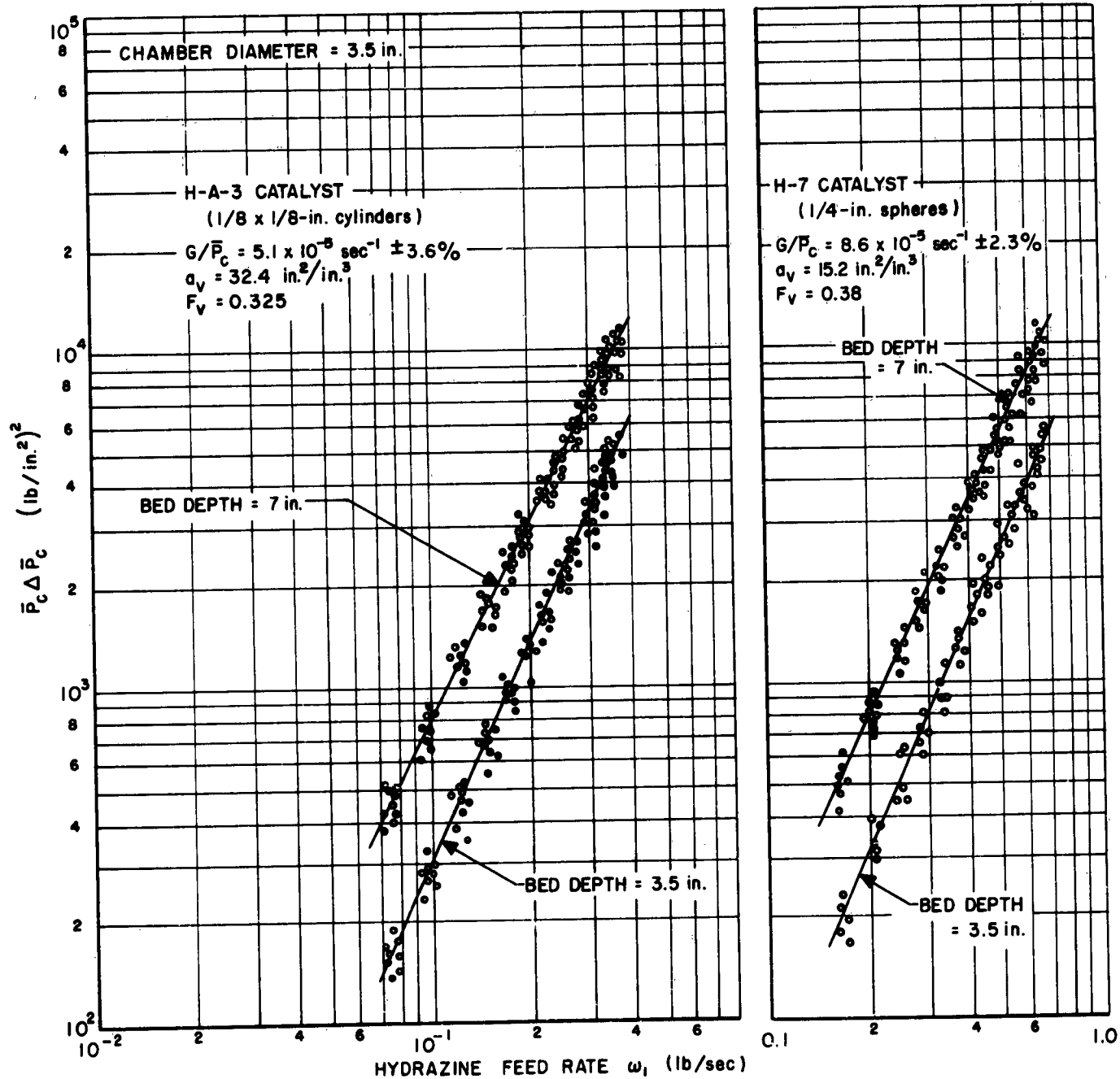


Figure 27. Variation of Pressure Drop with Hydrazine Feed Rate

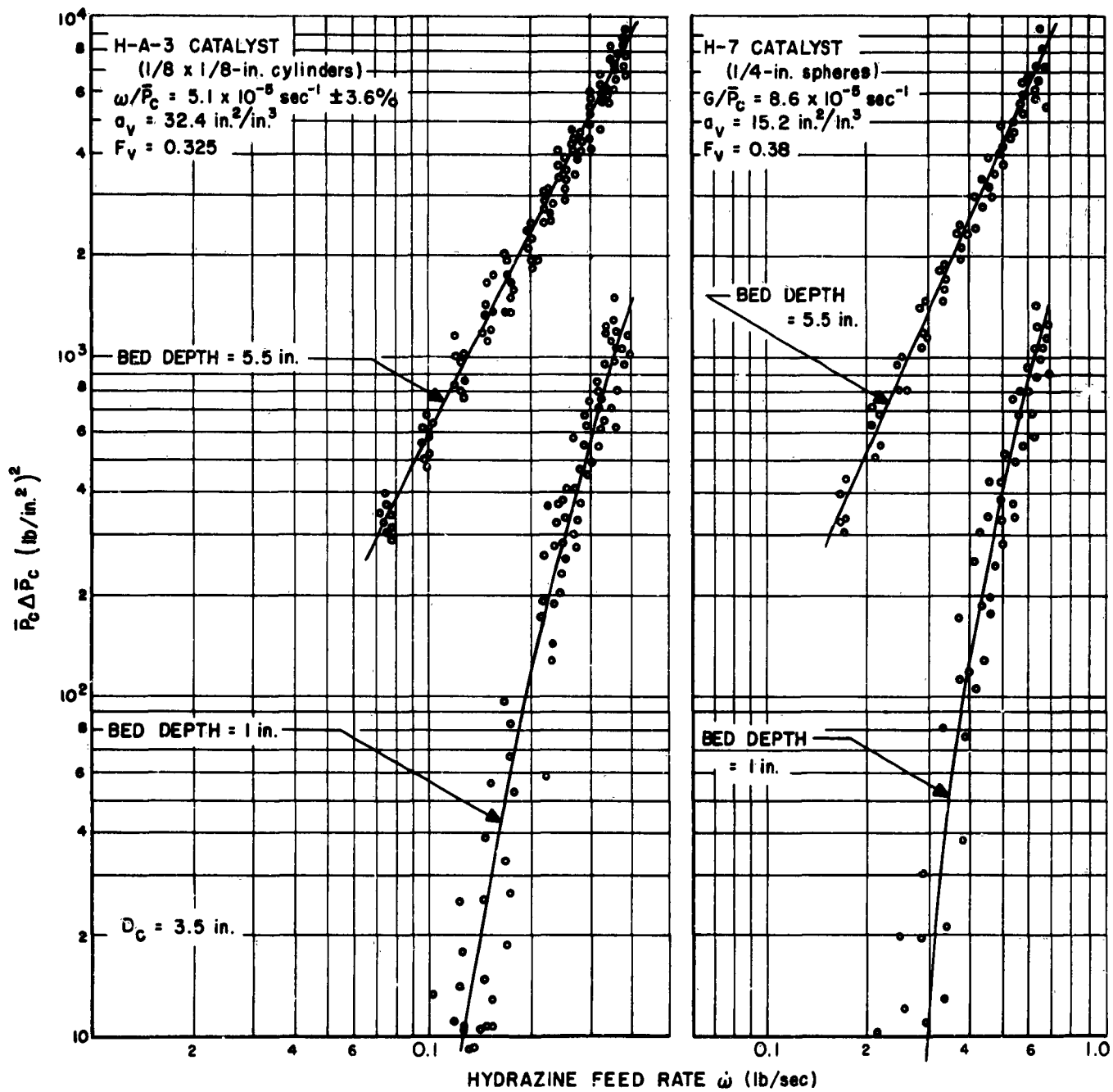


Figure 28. Variation of Pressure Drop with Hydrazine Feed Rate

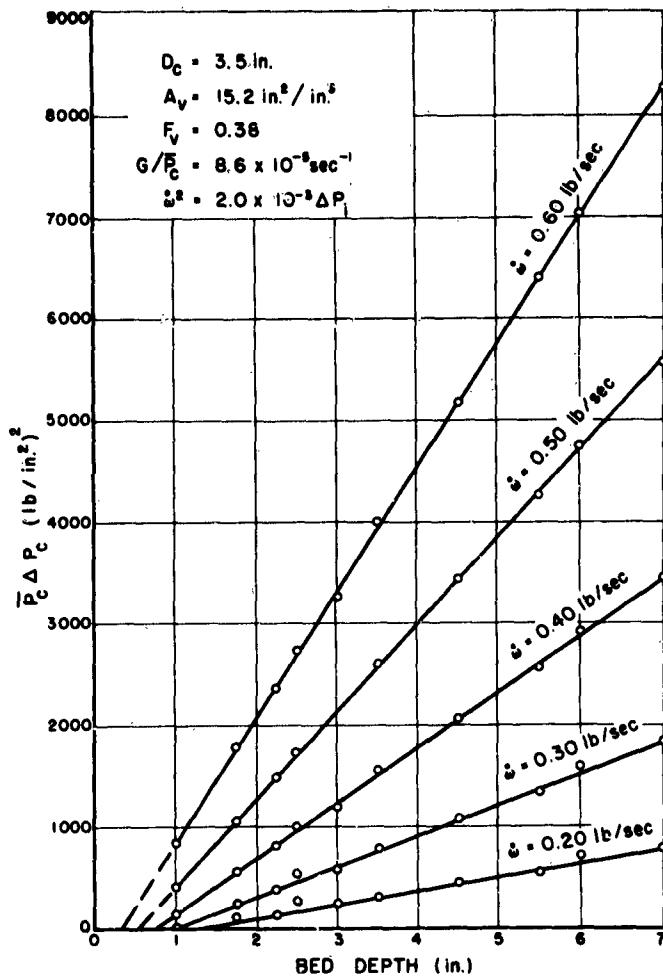


Figure 29. Variation of Pressure Drop with Bed Depth in Type H-7 Catalyst (1/4-In. Spheres)

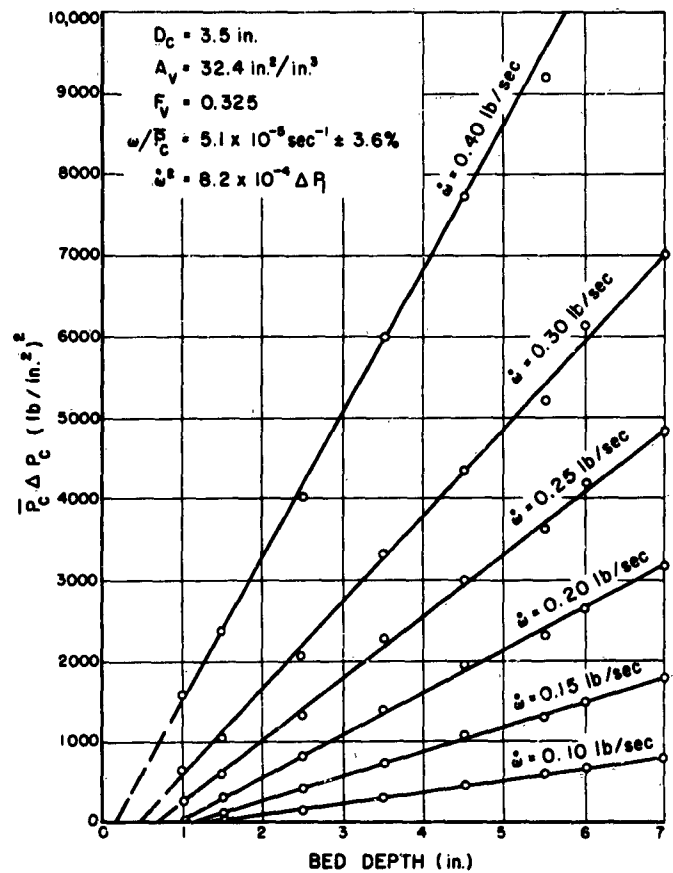
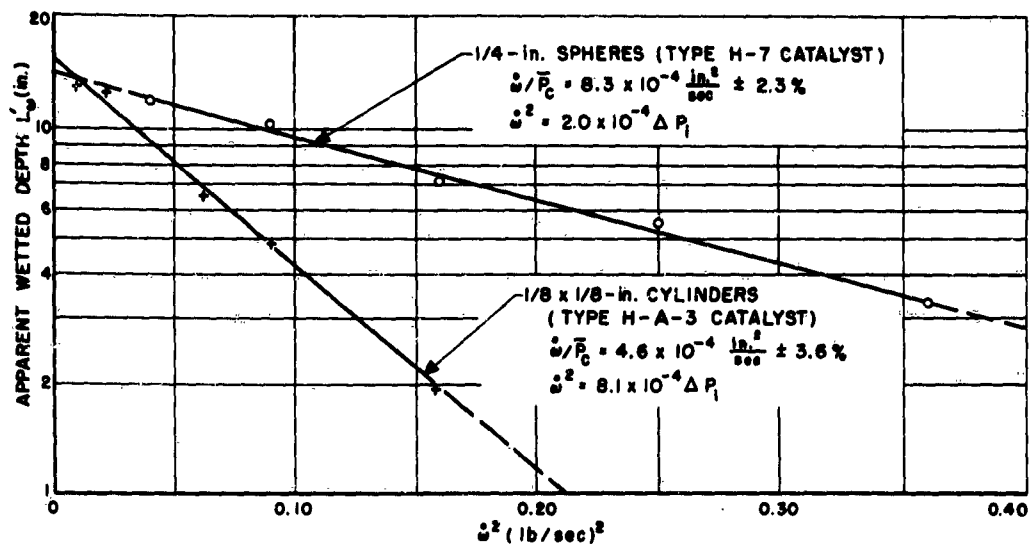
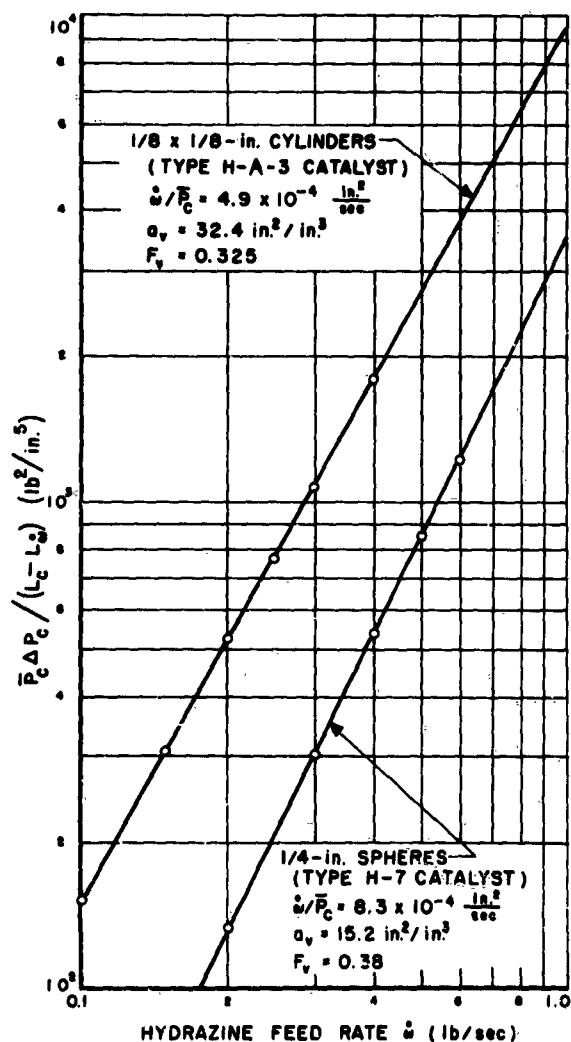


Figure 30. Variation of Pressure Drop with Bed Depth in Type H-A-3 Catalyst (1/8- by 1/8-In. Cylinders)

Figure 31. Variation of Apparent Wetted Depth  $L'$  With Flow RateFigure 32  
Curves Used in Evaluation of  
Constants in Equation (50)



## REFERENCES

1. Thomas, D. D., The Thermal Decomposition of Hydrazine, Progress Report No. 9-14. Pasadena: Jet Propulsion Laboratory, August 6, 1947.
2. Yost, M., Systematic Inorganic Chemistry. New York: Prentice-Hall Publishing Company, 1944.
3. Bichowsky, F. R., and Rossini, F. R., The Thermochemistry of the Chemical Substances. New York: Reinhold Publishing Company, 1936.
4. Hirschfelder, J. O., McClure, F. T., Curtiss, C. F. and Osborne, D. W., Thermodynamic Properties of Propellant Gases, OSRD Report No. 1087, Wash.: Library of Congress, November, 1942.
5. Murray, R. C. and Hall, A. R., "Flame Speeds in Hydrazine Vapour and in Mixtures of Hydrazine and Ammonia with Oxygen," Transactions Faraday Society, 47:743-751, 1951.
6. Hirschfelder, J. O., Curtiss, C. F. and Campbell, D. E., "The Theory of Flame Propagation - IV," Journal of Physical Chemistry, 57:403-417, 1953.
7. Adams, G. K., and Stocks, G. W., "The Combustion of Hydrazine," Article in Fourth Symposium (International) on Combustion. Baltimore: Williams and Wilkins Company, 1953, pp. 239-248.
8. Audrieth, L. R. and Ogg, B. A., The Chemistry of Hydrazine. New York: John Wiley and Sons, Inc., 1951.
9. Altman, D., and Thomas, D. D., Evaluation of Hydrazine as a Monopropellant and a Gas Generant, Progress Report No. 9-36. Pasadena: Jet Propulsion Laboratory, April 17, 1949.
10. Combined Bimonthly Summary No. 2 (August 20, 1947, to October 20, 1947). Pasadena: Jet Propulsion Laboratory, November 20, 1947 (Confidential).
11. Elverum, G. W., Jr., and Cole, L. G., Some Physical Chemical Studies of System Hydrazine - Hydrazine Nitrate - Water, Memorandum No. 20-79. Pasadena: Jet Propulsion Laboratory, December 30, 1952 (Confidential).
12. Grant, Arthur F., Jr., Development of Hydrazine as a Monopropellant and Gas Generant, Report No. 9-1. Pasadena: Jet Propulsion Laboratory March 1, 1950 (Confidential).
13. Grant, Arthur F., Jr., Catalysts for the Thermal Decomposition of Hydrazine When Used as a Monopropellant or as a Gas Generant, Publication No. 15. Pasadena: Jet Propulsion Laboratory, February 2, 1953 (Confidential).
14. Storch, H. H., Columbic, N., Anderson, R. B., The Fischer-Tropsch and Related Syntheses. New York: John Wiley and Sons, Inc., 1951.
15. Hougen, O. A., and Watson, K. M., Chemical Process Principles, Volume III - Kinetics and Catalysis. New York: John Wiley and Sons, Inc., 1947.
16. Brown, G. G., et al, Unit Operations. New York: John Wiley and Sons, Inc., 1950.
17. Egloff, G., Catalysis. New York: Reinhold Publishing Company, 1940.
18. Dunn, L. G., Meeks, Paul J., Denison, Frank G., Jr., Present Status of the Corporal E Development, Memorandum No. 4-59. Pasadena: Jet Propulsion Laboratory, March 17, 1950 (Secret).

## REFERENCES (Cont'd)

19. Combined Bimonthly Summary No. 27 (October 20, 1951, to December 20, 1951). Pasadena: Jet Propulsion Laboratory, January 20, 1952 (Confidential).
20. Combined Bimonthly Summary No. 28 (December 20, 1951, to February 20, 1952). Pasadena: Jet Propulsion Laboratory, March 20, 1952 (Confidential).
21. Combined Bimonthly Summary No. 30 (April 20, 1952, to June 20, 1952). Pasadena: Jet Propulsion Laboratory, July 20, 1952 (Confidential).

## APPENDIX

## Sample Calculations

The purpose of these calculations is to illustrate the use of the equations and Figures presented in this report.

## EXAMPLE I.

It is desired to design a monopropellant gas generator which is to be used to drive a turbine-pump combination in the propellant transfer system of a rocket vehicle. The characteristics and operating requirements of the turbine are as follows:

brake horsepower	= 350
efficiency	= 35 %
inlet pressure to turbine nozzles $P_c$	= 300 psia
exhaust pressure $P_e$	= 15 psia
maximum inlet-gas temperature, $T_c$	= 1900°F

The gas generator is to utilize either of the following:

1. Concentrated hydrazine containing not more than 5 wt % impurities.
2. A mixture of 74 wt %  $N_2H_4$ , 16 wt %  $HNO_3$ , and 10 wt %  $H_2O$  (Cf. Table V).

## A. Concentrated Hydrazine

In designing the reaction chamber, it is necessary to determine the chamber diameter  $D_c$ , bed depth  $L_c$ , type of catalyst (H-A-3 or H-7), and the maximum and minimum hydrazine-injection pressures.

The lower limit of ammonia dissociation permissible with pure hydrazine in this application is that which will give a temperature  $T_c$  of 1900°F. Accordingly (Cf. Fig. 1), it will be necessary to dissociate at least 45 % of the ammonia. Since a deviation of  $\pm 10$  % from the values of  $X$  predicted by the equations presented in this report must be anticipated, it is necessary to design the reaction chamber in such a manner as to dissociate 50 % of the ammonia. In such a reaction chamber, the values of  $X$  obtained should be between 0.45 and 0.55, and the temperature of the gases entering the nozzles of the turbine should therefore be between 1750 and 1900°F.

In designing the reaction chamber, it must be anticipated that the purity of the hydrazine will vary between 95 and 100 wt %. Consequently, two extremes of performance of the monopropellant must be expected: maximum performance (minimum flow rate of  $N_2H_4$  required to develop 350 brake hp) obtained with pure hydrazine at  $X = 0.45$ , and minimum performance (maximum flow rate of  $N_2H_4$  required to develop 350 brake hp) obtained with hydrazine containing 5 wt % impurities at  $X = 0.55$ . The reaction chamber must be designed to accommodate the maximum hydrazine flow rate, whereas the hydrazine feed system must be designed to accommodate both the maximum and minimum flow rates of hydrazine.

In computing the flow rates of hydrazine required to develop 350 brake hp, it is assumed that the

efficiency of the turbine is constant and unaffected by variations in X or in hydrazine purity.

1. Maximum performance (pure  $N_2H_4$ ,  $X = 0.45$ ). With pure  $N_2H_4$  at  $X = 0.45$ ,  $T_c = 1900^\circ F$ , and  $P_c/P_e = 20.0$ , the isentropic exhaust temperature (Cf. Fig. 3) is  $785^\circ F$ . From Figure 2 at  $X = 0.45$  and  $T_e = 785^\circ F$ , the isentropic conversion of enthalpy to kinetic energy,  $\Delta h_{785}^{1900}$  is 740 Btu/lb. The minimum flow rate of hydrazine required to develop 350 brake hp will be as follows:

$$\dot{w} \left( \frac{lb}{sec} \right) = \frac{350}{0.35} (hp) \left( \frac{1}{740} \right) \left( \frac{lb}{Btu} \right) (0.707) \left( \frac{Btu}{hp/sec} \right) = 0.955 lb/sec$$

2. Minimum performance (95 wt %  $N_2H_4$ ,  $X = 0.55$ ). It is assumed that a maximum of 5 wt % impurities in the hydrazine will reduce  $T_c$  to the same extent as 5 wt % water, but that these impurities will not change the value of  $\bar{C}_p$ , the average isobaric specific heat of the decomposition gases. As a result, since  $T_e = T_c \left( \frac{P_c}{P_e} \right)^{\frac{\gamma}{\gamma-1}}$ , the exhaust temperature  $T_e$  obtained with hydrazine containing 5 wt % water is given by the following expression, where the primed values refer to pure  $N_2H_4$  at  $X = 0.55$  and where  $T_c = 1610^\circ F$  is the adiabatic reaction temperature obtained (Cf. Table II) at  $X = 0.55$  with hydrazine containing 5 wt % water:

$$T_e = \frac{T_c' T_e'}{T_c'} = \frac{(655 + 460) (1610 + 460)}{(1750 + 460)} = 585^\circ F$$

Since  $\bar{C}_p$  is assumed to be unaffected by the presence of water, the value of  $\Delta h_{585}^{1610}$  for hydrazine containing 5 wt % water will be as follows:

$$\Delta h_{585}^{1610} = 720 \frac{1610 - 585}{1750 - 655} = 674 Btu/lb$$

The maximum flow rate of hydrazine required to develop 350 brake hp will be  $350 \times 0.707 / 0.35 \times 674$ , or 1.05 lb/sec.

The hydrazine flow rate required to develop 350 brake hp with all normal variations in generator performance ( $0.45 < X < 0.55$ ) and hydrazine purity (95 to 100 wt %) will be in the range 0.955 to 1.05 lb/sec.

Since the reaction chamber is to be designed to dissociate only 50 % of the ammonia, the H-7 catalyst should be used. This catalyst will be used in the form of 1/4-inch-diameter spheres.

It is assumed that  $G/a_v$  will be greater than  $11.1 \times 10^{-4}$  lb/in. sec. Consequently, Equation (58) may be used in estimating  $G_{max}$ , which will also be used as the designed mass-flow rate of hydrazine in the reaction chamber. From Equation (58),

$$G_{max} = \frac{4 \dot{w}_{max}}{\pi D_c^2} = \frac{4 \times 1.05}{\pi D_c^2} = \frac{1.336}{D_c^2} = 0.08 \left( \frac{\bar{P}_c \bar{P}_e^{1.7}}{a_v L_c} \right)^{1/2} \quad (61)$$

Equation (58) is based on a pressure drop through the catalyst bed  $\Delta P_c$  of 25 psi. Using this value of  $\Delta P_c$  and assuming a pressure drop of 5 psi between the catalyst bed and the entrance to the nozzles of the turbine,  $\bar{P}_c = 300 + 5 + \frac{25}{2} = 317.5$  psia. Substituting this value of  $\bar{P}_c$  in Equation (61) and solving for  $L_c$ ,

$$L_c = 1.137 \frac{D_c^{1.7} \bar{P}_c^{1.7}}{a_v} \quad (62)$$

From Equation (57), the depth  $L_c$  of the H-7 catalyst required to dissociate 50 % of the ammonia is as follows:

$$L_c = 1 + \frac{8 \times 10^4 \times 1.336}{317.5 D_c^2 a_v} + \frac{6600 \times 1.336}{17.85 (1-F_v) D_c^2} \left( \frac{0.5 - 0.4}{1.0 - 0.5} \right)^{1.21} =$$

$$1 + \frac{336.7}{a_v D_c^2} + \frac{70.6}{(1-F_v) D_c^2} \quad (63)$$

Combining Equations (62) and (63) and eliminating  $L_c$ ,

$$1.137 D_c^2 (D_c^2 F_v^{1.7} - a_v) = 336.7 + \frac{70.6 a_v}{(1-F_v)} \quad (64)$$

A trial-and-error solution of Equation (64), using the values of  $a_v$  and  $F_v$  given in Figure 18, gave a value of  $D_c$  of 4.75 inches. Using this value of  $D_c$  in Equation (62),  $L_c$  was found to be 7.0 inches. The values of  $a_v$  and  $F_v$  from Figure 18 at  $D_c = 4.75$  inches were  $15.6 \text{ in.}^2/\text{in.}$  and 0.370, respectively. The value of  $G/a_v$  is  $38 \times 10^{-4} \text{ lb/in. sec}$  and the use of Equation (58) for the estimation of  $G_{\max}$  was justified.

In order to insure proper atomization of the injected hydrazine (a solid-cone injector is assumed) and minimize oscillations in the chamber pressure, the injector pressure drop  $\Delta P_i$  must be 100 psi or  $0.30 P_{c \max}$ , whichever is the greater. If the nozzles of the turbine are designed to give a back pressure of 300 psia with a maximum flow rate of hydrazine (1.05 lb/sec), the total throat area  $A_N$  of the nozzles will be as follows, where 4130 ft/sec (Cf. Table II) is the characteristic velocity  $C^*$  obtained at  $X = 0.55$  with hydrazine containing 5 wt % water:

$$A_N = \frac{C^* \dot{w}}{P_{cgc}} = \frac{4130 \times 1.05}{300 \times 32.2} = 0.449 \text{ in.}^2$$

With pure  $N_2H_4$  at  $X = 0.55$ ,  $C^*$  (Cf. Fig. 1) is 4350 ft/sec. Therefore, with a nozzle throat area of  $0.449 \text{ in.}^2$  and the minimum flow rate of  $N_2H_4$  (0.955 lb/sec at  $X = 0.45$  with pure  $N_2H_4$ ), the pressure at the entrance to the turbine nozzles will be  $4350 \times 0.955/32.2 \times 0.449$  or 287 psia.<sup>a</sup>

Equation (58) is based on a pressure drop across the catalyst bed of 25 psi. However, the maximum variation of  $\Delta P_c$  around the value used in Equation (58) will be  $\pm 20\%$  or  $\pm 5$  psi. As a result, the maximum value of  $\Delta P_c$  which must be anticipated is 30 psi. The maximum pressure upstream from the catalyst bed  $P_{c \max}$  will be  $300 + 5 + 30 = 335$  psia. If an injector pressure drop of 100 psia is used at the minimum

<sup>a</sup> The minimum flow rate of 0.955 lb/sec represents a first approximation based on  $P_c/P_e = 20.0$ . Since at the minimum hydrazine flow rate  $P_c/P_e$  will be somewhat less than 20.0, the minimum hydrazine flow rate will be somewhat greater than 0.955 lb/sec. A trial-and-error solution for  $\dot{w}_{\min}$  gives a value of 0.964 lb/sec, and  $P_{c \min} = 290$  psia.

flow rate ( $\dot{\omega}_{\min} = 0.955$  lb/sec), the maximum injector pressure drop that is obtained at  $\dot{\omega} = 1.05$  lb/sec will be  $100 (1.05/0.955)^2 = 121$  psi. The maximum injection pressure will be  $335 + 121 = 456$  psi. The minimum injection pressure (assuming that the pressure drop between the catalyst bed and turbine nozzles is proportional to  $\omega^2$  and that  $\Delta P_c$  is 80 % of that given by Eq. (56) will be  $\left(\frac{0.955^2}{1.05^2}\right) (5 + 20) + 287 + 5 + 100 = 413$  psia. The hydrazine feed system, in order to compensate for variations in X and in hydrazine purity, must be capable of regulating the hydrazine injection pressure between 410 and 460 psia. Additional regulation of the hydrazine injection pressure will be required if variations in the efficiency of the turbine or pump occur.

B. Mixture of 74 wt %  $N_2H_4$ , 16 wt %  $HNO_3$ , and 10 wt %  $H_2O$

This mixture might be used for this purpose in place of concentrated hydrazine because of its lower ( $-38^\circ F$ ) freezing point.

In order to insure a gas temperature of  $1900^\circ F$  or less with this mixture, it will be necessary (Cf. Table V) to design the reaction chamber in such a manner as to dissociate 70 % of the ammonia. The values of X obtained with this reaction chamber should be in the range  $0.63 < X < 0.77$ , and  $T_c$  should be between  $1750$  and  $1900^\circ F$ .

C. Minimum Performance ( $X = 0.77$ )

1. First Approximation. Assume  $T_e = 800^\circ F$ . Then, by interpolation in Table V,  $\Delta H_{T_e}^{T_c} = 549.9 + \frac{3}{20} \times (670.6 - 549.9) = 568$  Btu/lb. Also,  $M_g = 13.88 + \frac{3}{20} (14.99 - 13.88) = 15.55$  lb/mol, and  $\bar{c}_p$  (avg isobaric specific heat) =  $\frac{568 \times 15.55}{1750 - 800} = 9.3$  Btu/mol  $^\circ F$ ; and  $T_e = T_c \left(\frac{P_e}{P_c}\right)^{\frac{R}{\bar{c}_p}} = 2210 \left(\frac{1}{20}\right)^{\frac{1.987}{9.3}} = 705^\circ F$ .

2. Second Approximation. Assume  $T_e = 700^\circ F$ . For the temperature interval  $700$  to  $1750$ ,  $\Delta H_{T_e}^{T_c}$  (interpolating in Table V) =  $623.5$  Btu/lb,  $\bar{c}_p = 9.24$  Btu/mol  $^\circ F$ , and  $T_e = 2210 \left(\frac{1}{20}\right)^{\frac{1.987}{9.24}} = 700^\circ F$ . The value of  $\Delta H_{T_e}^{T_c}$  with this mixture at  $X = 0.77$  and  $P_c/P_e = 20.0$  is, therefore,  $623.5$  Btu/lb; hence  $\dot{\omega}_{\max} = 1.133$  lb/sec.

By the same method of calculation,  $T_e$ ,  $\Delta H_{T_e}^{T_c}$ , and  $\dot{\omega}$  at  $X = 0.63$  were found to be  $730^\circ F$ ,  $669$  Btu/lb, and  $1.056$  lb/sec, respectively.

Since X is greater than 0.55, the H-A-3 catalyst must be used for this application. It is assumed that this catalyst will be used in the form of  $1/4$ -inch spheres.

Assuming a ratio of  $G/a_v$  greater than  $11 \times 10^{-4} \frac{lb}{in \cdot sec}$ , Equation (60) may be used to determine  $G_{\max}$ . However, Equation (60) is based on a value of  $(T_c/M_g)$  of  $165 \frac{mol}{lb \cdot R}$  (the value of the ratio obtained with pure  $N_2H_4$  at  $X = 0.50$ ). Therefore, in order to compute  $G_{\max}$  for the mixture, it is necessary to correct for the value of  $T_c/M_g$  which will be obtained with the mixture. It is assumed that the average value of  $T_c/M_g$  in the bed will be equal to that obtained at  $X = 0.50$ . From Table V at  $X = 0.50$ ,  $M_g = 15.63$  lb/mol,  $T_c = 2490^\circ R$ , and  $T_c/M_g = 159 \frac{mol}{lb \cdot R}$ . The values of  $G_{\max}$  given by Equation (60) should therefore be multiplied by the ratio  $159/165 = 0.965$ , as follows:

$$G_{\max} = \frac{4 \times 1.133}{D_c^2} = \frac{1.444}{D_c^2} = 0.965 \times 0.062 \left( \frac{F_v^{1.7} F_c}{a_v L_c} \right)^{0.5} = 0.06 \left( \frac{F_v^{1.7} F_c}{a_v L_c} \right)^{0.5} \quad (65)$$

Equation (60) is based on pressure drop across the catalyst bed of 15 psi. Using and assuming a pressure loss of 5 psi between the catalyst bed and turbine nozzles,  $\bar{P}_c$ . Substituting this value of  $\bar{P}_c$  in Equation (65) and solving for  $L_c$  yields

$$L_c = \frac{0.536 F^{1.7} D^4}{a_v c} \quad (67)$$

In this mixture, the ratio of the hydrazine nitrate concentration to that of water is greater than 1.7. Consequently, Equation (41) may be used to estimate  $L_c$ . From Figure 26, it can be seen that at a pressure of 312.5 psia an effective residence time  $\theta_e$  of  $4.3 \times 10^4$  in. sec is required to dissociate 70 % of the ammonia. Substituting this value in Equation (41),

$$L_c = \frac{\theta_e G}{\bar{P}_c (1-F_v)} = \frac{4.3 \times 10^4 \times 1.444}{312.5 D_c^2 (1-F_v)} = \frac{198.6}{D_c^2 (1-F_v)} \quad (68)$$

Eliminating  $L_c$  between Equations (67) and (68) and solving for  $D_c$ ,

$$D_c = 2.68 \left[ \frac{a_v}{F_v^{1.7} (1-F_v)} \right]^{1/6} \quad (69)$$

Using values of  $a_v$  and  $F_v$  from Figure 18, a trial-and-error solution of Equation (69) gave  $D_c = 6.1$  in.,  $a_v = 15.6 \frac{\text{in.}^2}{3}$  and  $F_v = 0.362$ . Substituting these values in Equation (68),  $L_c$  was found to be 8.5 inches. The value of  $G/a_v$  is  $25.7 \times 10^{-4}$  lb/in. sec.

The minimum injection pressure drop ( $\dot{m} = 1.06$  lb/sec) is 394 psia, and the maximum injection pressure ( $\dot{m} = 1.133$ ) is 441 psia.

A chamber of smaller diameter but greater length could be used if larger catalyst particles were substituted for the 1/4-inch-diameter spheres. For example, with 3/8-inch-diameter spheres (values of  $a_v$  and  $F_v$  obtained from Ref. 16),  $D_c$  would be 5.75 inches,  $L_c$  would be 9.3 inches,  $a_v$  would be  $10.5 \text{ in.}^2/\text{in.}^3$ , and  $F_v$  would be 0.35.